

UC San Diego

Research Theses and Dissertations

Title

Late Holocene Stratigraphy, Humboldt Bay, California: Evidence for Late Holocene Paleoseismicity of the Southern Cascadia Subduction Zone

Permalink

<https://escholarship.org/uc/item/7328g533>

Author

Valentine, David Wade

Publication Date

1992-08-01

LATE HOLOCENE STRATIGRAPHY , HUMBOLDT BAY, CALIFORNIA:
EVIDENCE FOR LATE HOLOCENE PALEOSEISMICITY OF THE SOUTHERN
CASCADIA SUBDUCTION ZONE

By

David Wade Valentine

A Thesis

Presented to

The Faculty of Humboldt State University

In Partial Fulfillment
of the Requirements for the Degree
Master of Science

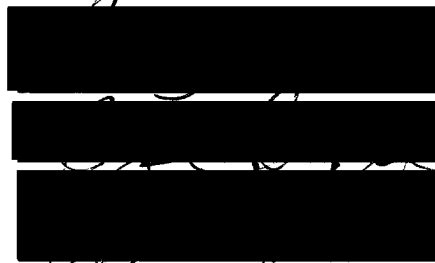
August, 1992

Late Holocene Stratigraphy , Humboldt Bay, California:
Evidence for Late Holocene Paleoseismicity of the Southern Cascadia
Subduction Zone

By

David Wade Valentine

We certify that we have read this study and that it conforms to acceptable standards of scholarly presentations and is acceptable, in scope and quality, as a thesis for the degree of Master of Sciences



Major Professor

Approved by the Graduate Dean



Late Holocene Stratigraphy , Humboldt Bay, California: Evidence for Late
Holocene Paleoseismicity of the Southern Cascadia Subduction Zone

By
David Wade Valentine

ABSTRACT

Late Holocene stratigraphy representing rapid episodic subsidence is found in synclines of Humboldt Bay, California. These synclines are associated with the Cascadia subduction zone fold and thrust belt, which bends eastward in Northern California. In the axes of the synclines, repeated sequences of intertidal muds overlying saltmarsh to lowland peat deposits represent episodes of rapid submergence followed by gradual emergence. Observations of the contacts between the peats and overlying muds are abrupt (<1 cm). The rapid submergence most likely represents coseismic subsidence associated with large magnitude earthquakes. The evidence for these submergence events is found within both the northern Freshwater syncline and the southern South Bay syncline.

Radiocarbon dating indicates at least eight rapid episodic subsidence events during the past 3500 years. Rapid episodic events have occurred for the following age ranges: 0-300, 500-800, 1050-1350 (2 events), 1600-1900, 2450-2600, 2800-3300, 3200-3400. There are indications of additional events back to about 4300 years, with ages of 3700-3900 and 4000-4300. The age ranges of the subsidence events are similar to ages for paleoseismic events from the Little Salmon fault. The Humboldt Bay paleoseismic events may be a record of great earthquakes occurring on the megathrust of the underlying Cascadia subduction zone.

To the late Edward Lee Valentine

Acknowledgments

I gratefully acknowledge the one person who made this project challenging, enjoyable, and possible, Gary Carver. I would like to thank my thesis committee for putting up with the delays in the production schedule; Raymond "Bud" Burke, for the multiple discussions, and helpful comments given; and Greg Vick for excellent study on Mad River slough which made this project possible.

Big thanks and congratulations to Christine Shivelle Manhart, assistant, micropaleontologist, and oceanographer, who always make field work entertaining. I wish I had a video camera, several times.

I would like to thank the many people who helped in the mud: Laura Kadlikluk, Kevin Leche, Kathy Moley, Wen-Hoa Li, Ralph Johnson, and David Arnold. Thanks to the many people who made Humboldt entertaining: Jen, Carol and everyone else.

Emotional and financial support was provided by my parents, and grandparents. Thanks to many friends who never made it to Humboldt (or couldn't find me) but still wrote; Brett, Kathy, Jane, Marie, and Jill, thanks for listening, and I owe you my sanity.

Financial support for this project was provided by the California Sea Grant Program, RCZ-86, and RCZ-88, and Humboldt State University through the Telonicher Marine Laboratory Summer Marine Science Program. Land access was provided by the US Fish and Wildlife Service, Humboldt Bay reserve.

"Keep Subduction Safe and Legal"

Contents

Abstract	i
Dedication	ii
Acknowledgments	iii
Contents	iv
List of Figures	v
List of Tables	vi
Introduction	1
Regional Geology	4
Modern Marsh Characteristics	9
Eustatic Sea-level Changes	14
Geomorphology of Humboldt Bay	15
Methods	20
Recording of Stratigraphic Details	21
Site Descriptions	22
Jacoby Slough/Arcata	22
Freshwater Slough	24
Eureka Slough	26
Bay Islands	28
South Bay	29
Discussion	32
Stratigraphy	32
Mad River Slough—Type Section	32
Formation of Buried Salt-Marsh Horizons	34
Correlation	40
Late Holocene Paleoseismicity in Humboldt Bay	42
Regression of all data	42
Regression of data by site	45
Recurrence interval	51
Proposed cycle	51
Summary of Humboldt Bay Paleoseismicity and Comparison to the Regional Paleoseismicity	55
Conclusions	58
References	59
Appendix 1: Radiocarbon Dating	64
Appendix 2: Statistical Data Analysis Summary	74

List of Figures

Figure 1. General patterns of coseismic uplift and subsidence accompanying the 1964 Alaskan Earthquake, and the 1960 Chilean Earthquake, with Cascadia subduction zone for comparison	2
Figure 2. Map showing generalized structure of the Cascadia subduction zone, and location of estuaries containing multiple buried lowland surfaces.....	3
Figure 3. Tectonic map of northwestern California showing the extent of contractual and translational zones.	5
Figure 4. Map of Quaternary tectonic structures and generalized vertical tectonic curve for the northern California coast.	7
Figure 5. Map of southern end of the Cascadia subduction zone fold and thrust belt.	8
Figure 6. Isopach map of Holocene sediment overlain on a structural geologic map of the northern California shelf.	10
Figure 7. Diagram depicting the position of the low, middle, and high salt marsh zones for Humboldt Bay, California.	11
Figure 8. Development of a typical rising salt marsh with rising sea level and continued sedimentation.	13
Figure 9. Worldwide eustatic sea-level curves showing a non-uniform Holocene transgression.	16
Figure 10. Worldwide eustatic sea-level curves showing the uniform Holocene transgression.	17
Figure 11. Holocene sea-level curves for the five predicted global zones.	18
Figure 12. Map of Humboldt Bay, showing subdivisions, present salt marsh locations and study sites.	19
Figure 13. Stratigraphic columns and map of Jacoby Creek.	23
Figures 14. Stratigraphic columns and map of Freshwater Slough, Eureka Slough, and bay islands.....	25
Figure 15. Stratigraphic Columns from First Slough, Eureka, California.....	27
Figure 16. Stratigraphic columns and map of South Bay.	30
Figure 17. Generalized stratigraphic sections of the upper Holocene sediments of Mad River Slough.....	33
Figure 18. Schematic curves illustrating the upwards growth of mudflat-salt marsh for various conditions of sedimentation, sea-level change, and compaction.	35
Figure 19. Proposed courses for the Mad River.	37
Figure 20. Calibrated age vs. depth for all samples.....	44
Figure 21. Calibrated age vs. depth, and least squares regression lines for selected regions.	46
Figure 22. Calibrated radiocarbon ages grouped by age and by region.....	48
Figure 23. Scenarios for the formation of the stratigraphy found in Humboldt Bay.	54
Figure 24. Histogram of calibrated ages.	57
Figure A1. Map of Humboldt Bay showing sample locations.....	66

List of Tables

Table 1. Stepwise regression analyses results.	43
Table 2. Regression analyses by site.	47
Table 3. Recurrence interval calculation.....	52
Table A1. Radiocarbon ages from all localities near Humboldt Bay.....	67

Introduction

The scarcity of seismicity has created a debate on the seismic potential of the Cascadia subduction zone. There is no historic records of a great earthquake occurring along the Cascadia subduction zone since the first permanent European settlements around 1810 AD (Heaton and Kanamori, 1984). Two hypotheses have been debated: a locked subduction zone capable of producing great earthquakes (Heaton and Kanamori, 1984; Heaton and Snavely, 1985; Adams, 1984), and aseismic subduction with little or no seismicity (Acharya, 1985; Ando, and Balazs 1979; Reilinger and Adams, 1982; Savage, Lisowski, and Prescott, 1981; West and McCrumb, 1988).

Regional zones of subsidence and uplift have been documented for several great earthquakes (Figure 1; Fitch and Scholtz, 1971; Plafker and Savage, 1970; Plafker, 1972). Within the zone of subsidence, estuarine sediments bury the low-lying land such as salt marshes and coastal forests. Multiple lowland horizons covered by estuarine sediments may represent repeated tectonic events. Recent studies of late Holocene marsh stratigraphy in bays and estuaries of the Pacific Northwest have found physical stratigraphy that suggests the Cascadia subduction zone is active and has previously produced great earthquakes (Atwater, 1987; Darienzo and Peterson, 1990; Nelson and Personius, in press; Shivel, and others, 1991; Vick, 1988; Clarke and Carver, 1992).

Along the coast of Oregon, Washington, and northern California, estuaries contain repeated cycles of submerged lowland and salt-marsh horizons covered by estuarine sediments (Figure 2). Humboldt Bay contains stratigraphic sequences similar to those described along the Pacific Northwest coast (Vick, 1988; Clarke and Carver, 1992). This thesis uses stratigraphic sequences as evidence for paleoseismic events.

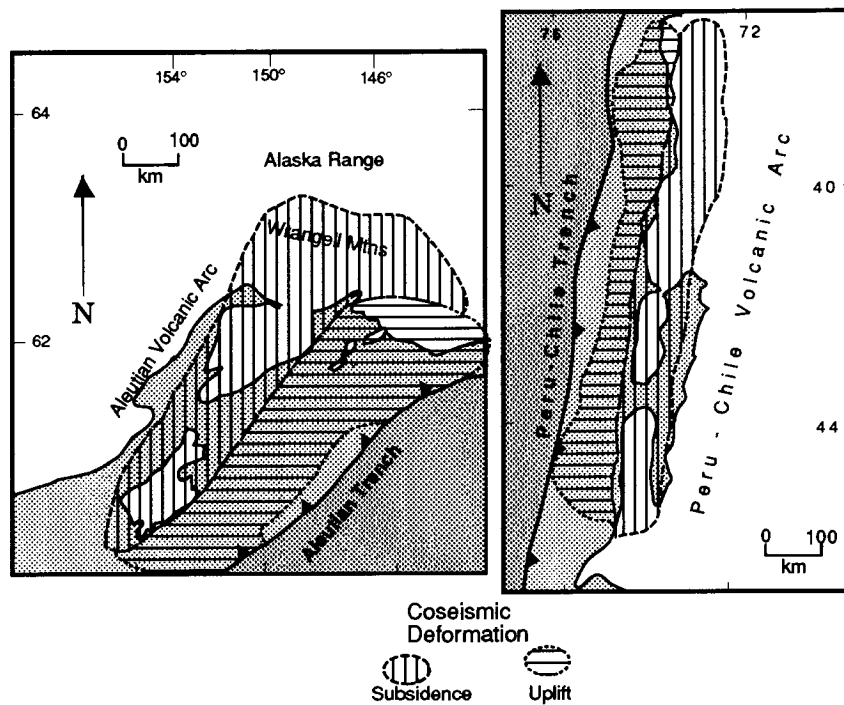
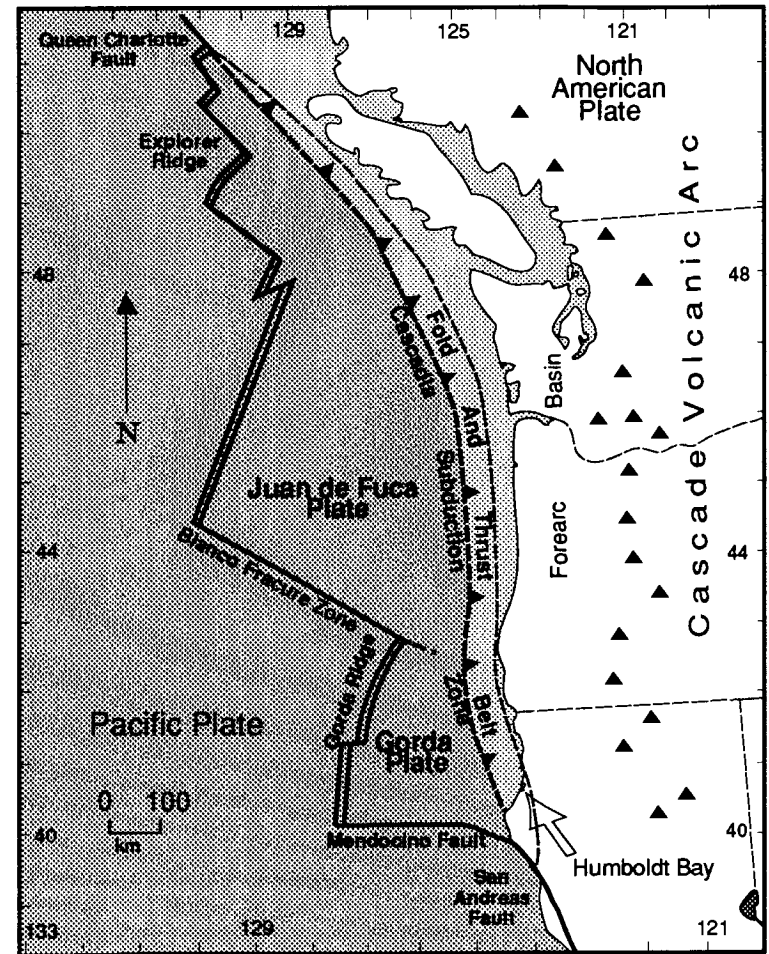


Figure 1. Map of uplift and subsidence from the 1964 Alaskan, the 1960 Chilean earthquakes, with the Cascadia subduction zone for comparison. The uplift and subsidence zones show the approximate lengths of the ruptures for the events. A major event along the Cascadia subduction zone might be expected to rupture segments of approximately the same size. (after Vick, 1988; and Plafker, 1970)



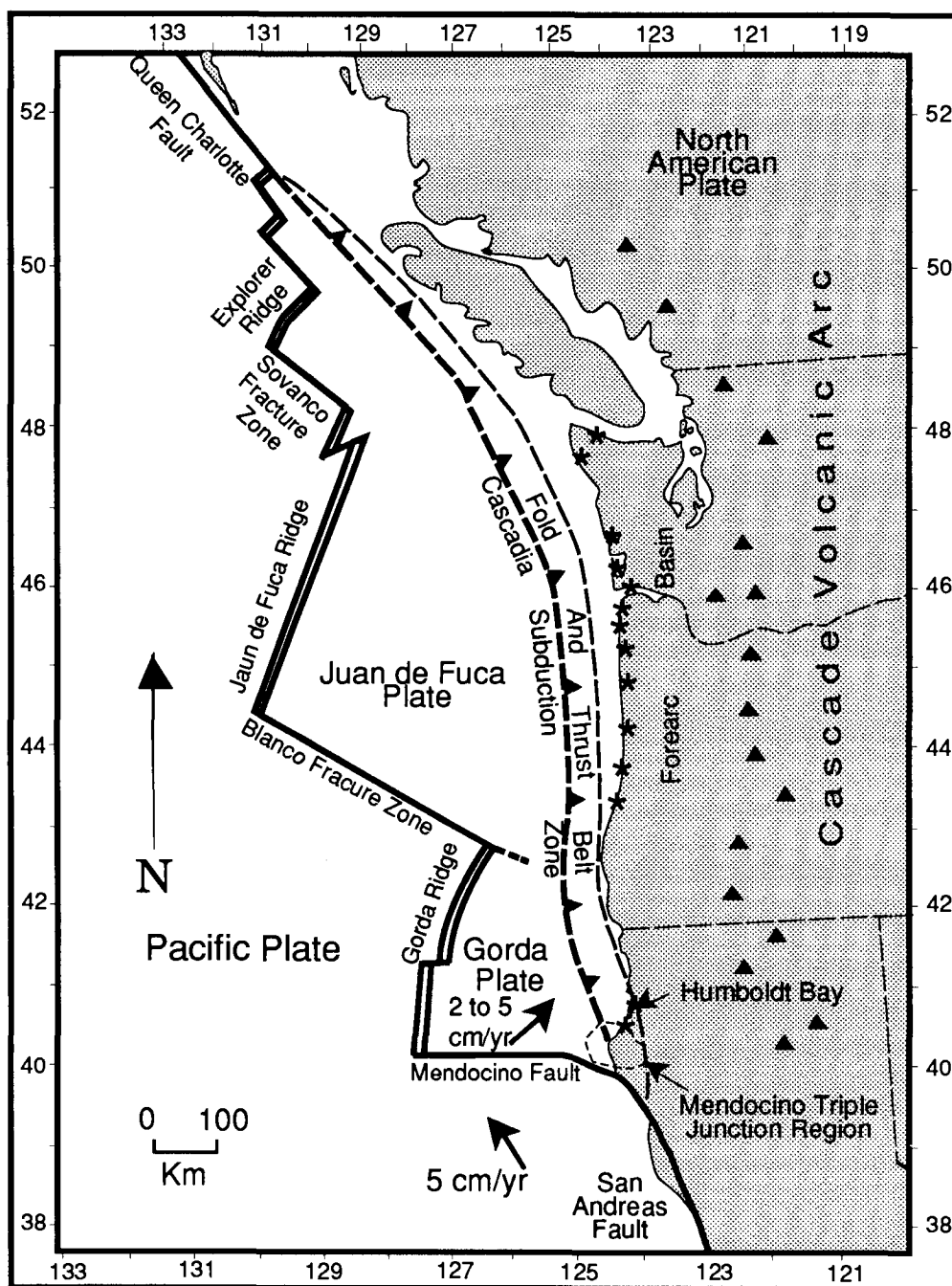


Figure 2 . Map showing the generalized structure of the Cascadia subduction zone, and location of estuaries containing multiple buried surfaces.

* Locations with evidence for coseismic subsidence (Atwater, 1987; Darienzo and Peterson, 1990; Nelson and Personius, 1992; Grant and others, 1990)

▲ Active Volcanoes

↖ Plate Motions, North American plate is held fixed

Regional Geology

The 1200 km Cascadia subduction zone parallels the Pacific Northwest Coast (Figure 2). Seafloor magnetic anomalies indicate that 10 million year old crust from the Juan de Fuca and Gorda plates is subducting at a rate of 3 to 4 cm a year (Figure 2; Riddihough, 1984; Nishimura, Wilson, and Hey, 1984). These plates offshore of the Cascadia subduction zone may represent the segment boundaries of subduction zone (Nelson and Personius, in press), but the boundary for the southern segment of the zone is debatable. Several researchers use the Blanco fracture zone as the boundary of the Gorda plate (Silver, 1971; Riddihough, 1980; Riddihough, 1984; Stoddard, 1987). Wilson (1988) extends the Juan de Fuca plate South of the Blanco fracture zone, and proposes a Gorda deformation zone with a soft deformation boundary in the northern portion of the "so-called Gorda plate." The proposed boundary between deformed and undeformed plate segment projects onshore north of Humboldt Bay.

On the coast of northern California, three regions near the Mendocino triple junction show distinct zones of deformation (Figure 3; Lisowski, Savage and Prescott, 1991; Kelsey and Carver, 1988). The fold and thrust belt of the Cascadia subduction zone, which parallels the coast for most of the Cascadia subduction zone, turns eastward and comes onshore as this belt approaches the triple junction (Figure 3), due to the internal deformation of the underlying Gorda plate. The deformation seen in the Humboldt Bay region started about 700,000 years (Carver, 1987). This contractual deformation caused by the subducting Gorda plate and is distinctly different from the translational deformation of the San Andreas fault system. South of the Mendocino triple junction, the translational deformation overprints the older contractual deformation (Kelsey and Carver, 1988). The study area, Humboldt Bay, is within the contractual deformation zone, and is not presently

effected by the translation effects of the North American-Pacific plate boundary (Lisowski, Savage, and Prescott, 1991).

Along the coast of northern California north of the Mendocino triple junction, the deformation of the North American plate is seen as a series of deformed marine terraces offset by thrust faults. (Figure 4; Carver and others, 1985). This fold and thrust belt represents the upper plate deformation of the Cascadia subduction zone. Uplifted terraces increasingly offset with greater age indicate continued faulting throughout the late Quaternary (Carver, and others, 1985). Studies of the thrust faults indicate late Holocene activity. Displacement has occurred along the Little Salmon fault at least three times in the past 2000 years. Along the McKineleyville fault, an uplifted Holocene terrace located near Clam beach contains evidence for three events. Uplift of this terrace has occurred within the past 1100 years (Carver, and others, 1989; Carver, 1989; Clarke and Carver, 1992).

Mapped zones of deformation and structures from the offshore accretionary prism correlate with onshore structures (Figure 5; Clarke, and Carver, 1989; Clarke, 1992). Two regions of this deformation, the zone of broad open folding and the zone of *en echelon* faulting and folding, traverse Humboldt Bay. The zone of broad open folding (Zone C, Figure 5) parallels the subduction front becoming the Freshwater syncline on land. The Freshwater syncline is a shallow and broad feature, and can be followed offshore for 50 km. The syncline forms Arcata Bay and is bound to the north by the Fickle Hill anticline and to the south by the Eureka anticline. The zone of *en echelon* folds and thrusts (Zone D, Figure 5) becomes South Bay and the Little Salmon fault system onshore. The onshore structures include the Little Salmon fault system, the Humboldt Hill anticline, the Table Bluff anticline, and an unnamed syncline, informally called the South Bay syncline.

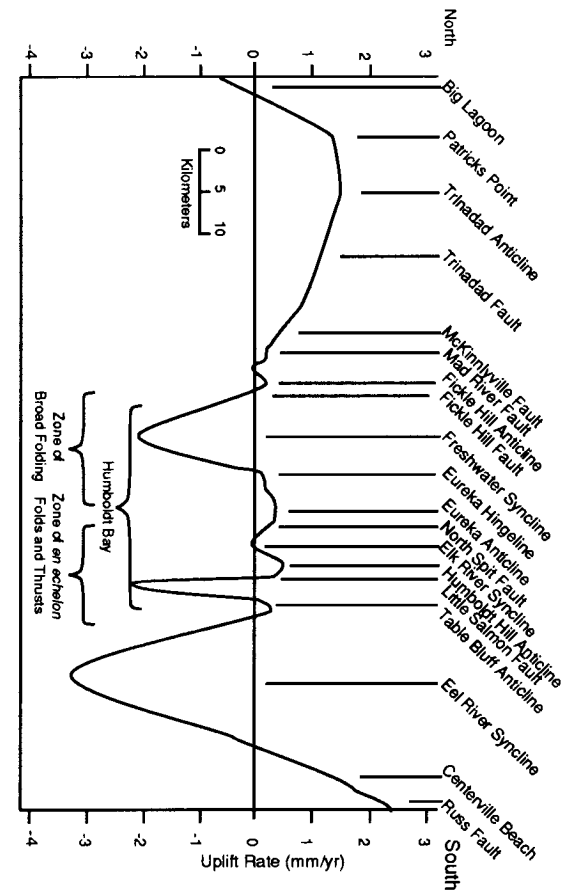
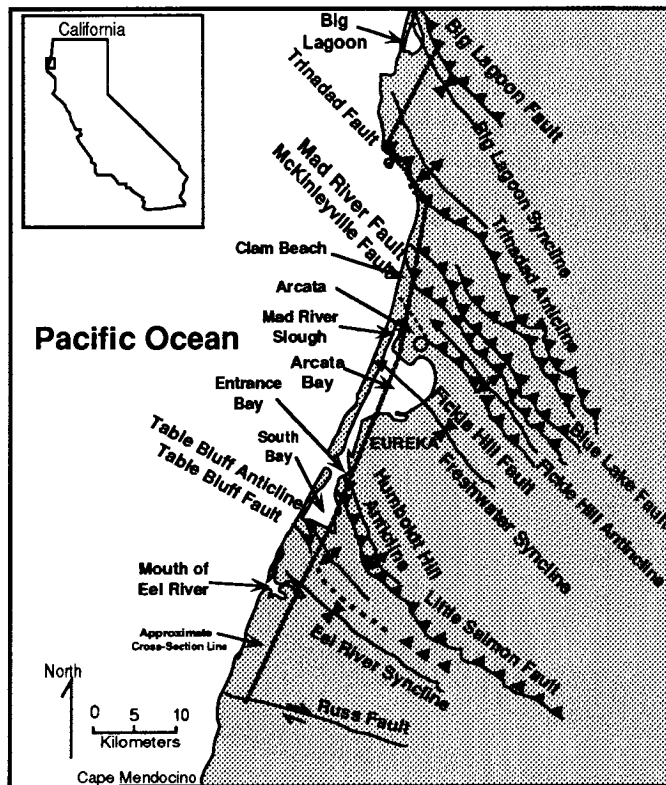


Figure 4. Map of Quaternary tectonic structures along the northern California coast and generalized vertical tectonic curve of the northern California Coast.

The two synclines forming Arcata and South Bays are separated by a zone of gradual uplift. The zones are inferred from offshore data in figure 7. Uplift data are from Carver and others, 1985, Eel River subsidence are after Vick, 1988, and are inferred from Borgeld, 1985. Humboldt Bay subsidence rates from Vick, 1988, and this study. (Modified from Vick, 1988; Map after Carver, and others, 1985).

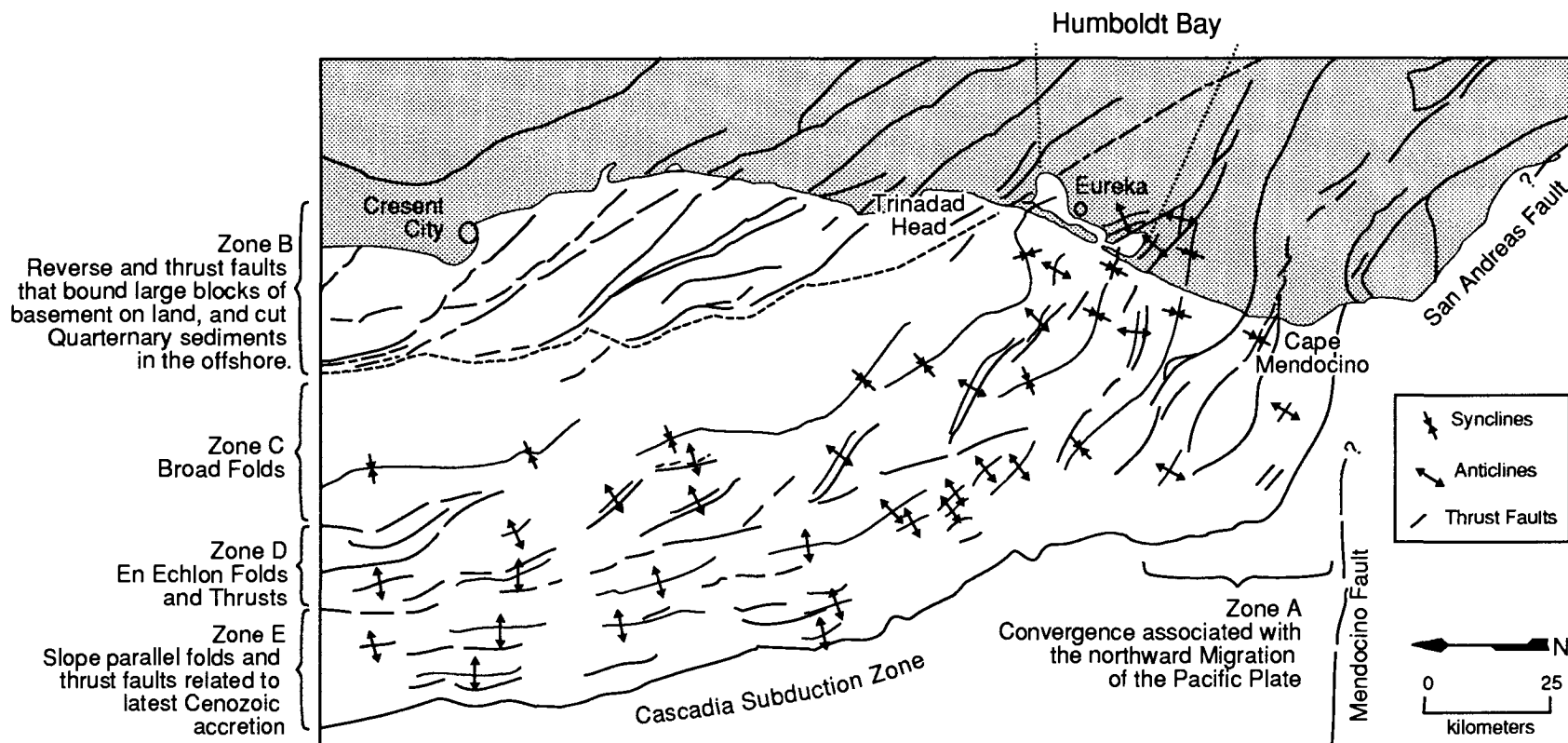


Figure 5. Map of southern end of the Cascadia subduction zone fold and thrust belt.

Humboldt Bay lies in zones C and D. Zone A, contractural deformation across west to northwest trending folds and associated reverse and thrust faults; Zone B, conspicuous north-northwest trending, east to northeast dipping reverse and thrust faults that bound large blocks of basement rock on land and cut Quaternary sediments offshore; Zone C, Broad Open Folds having north-northwest trends (axial part of basin); Zone D, right stepping en echelon folds and thrust faults that are oblique to the structural grain of adjacent zones C and E; Zone E, slope parallel folds and thrust faults that have north to northwest trends related to the latest Cenozoic accretion. Structural discontinuity between domains D and E is an east-dipping fault or narrow zone of faulting. (after Clarke, 1992).

One of the major structures traversing Humboldt Bay is the Little Salmon fault. It bounds the Humboldt Hill anticline, and vertically offsets mid-Pleistocene Rio Dell deposits by approximately 1700 meters (Woodward-Clyde Consultants, 1980). The Little Salmon fault is active, and has had several events during the past 2000 years (Carver and others, 1985; Clarke and Carver, 1992). The fault overthrusts the eastern end of the Table Bluff anticline (Ogle, 1953), which forms the southern boundary of Humboldt Bay.

Humboldt Bay consists of two regions of subsidence separated by a region of uplift (Figure 4). The Quaternary uplift on the Eureka and Humboldt Hill anticline that separates the synclines is about 0.3 mm/yr (G. Carver, personal communication, 1992). In the South Bay, an estimated subsidence rate of 2.3 mm/yr was calculated for the past 700,000 years based on the estimated age of top the Rio Dell formation, and the vertical offset across the Little Salmon fault (Woodward-Clyde Consultants, 1980). Because there is no leveling data available, the short term uplift and/or subsidence rates of the structures crossing Humboldt Bay are unknown. But, Holocene isopach maps of the northern California shelf sediments show that synclines are accumulating at a rate greater than average shelf rate (Figure 6; Borgeld, 1985; Vick, 1988).

Modern Marsh Characteristics

The stratigraphy found in Humboldt Bay contains repeated salt marsh peat horizons separated by horizons containing estuarine sediments. The occurrence of marsh deposits provides a datum for interpreting sea-level changes. Modern marsh plants grow, and salt marsh peat horizons form, in narrow elevation ranges relative to mean high water (MHW) (Figure 7; Bloom, 1964). Below MHW few plants grow,

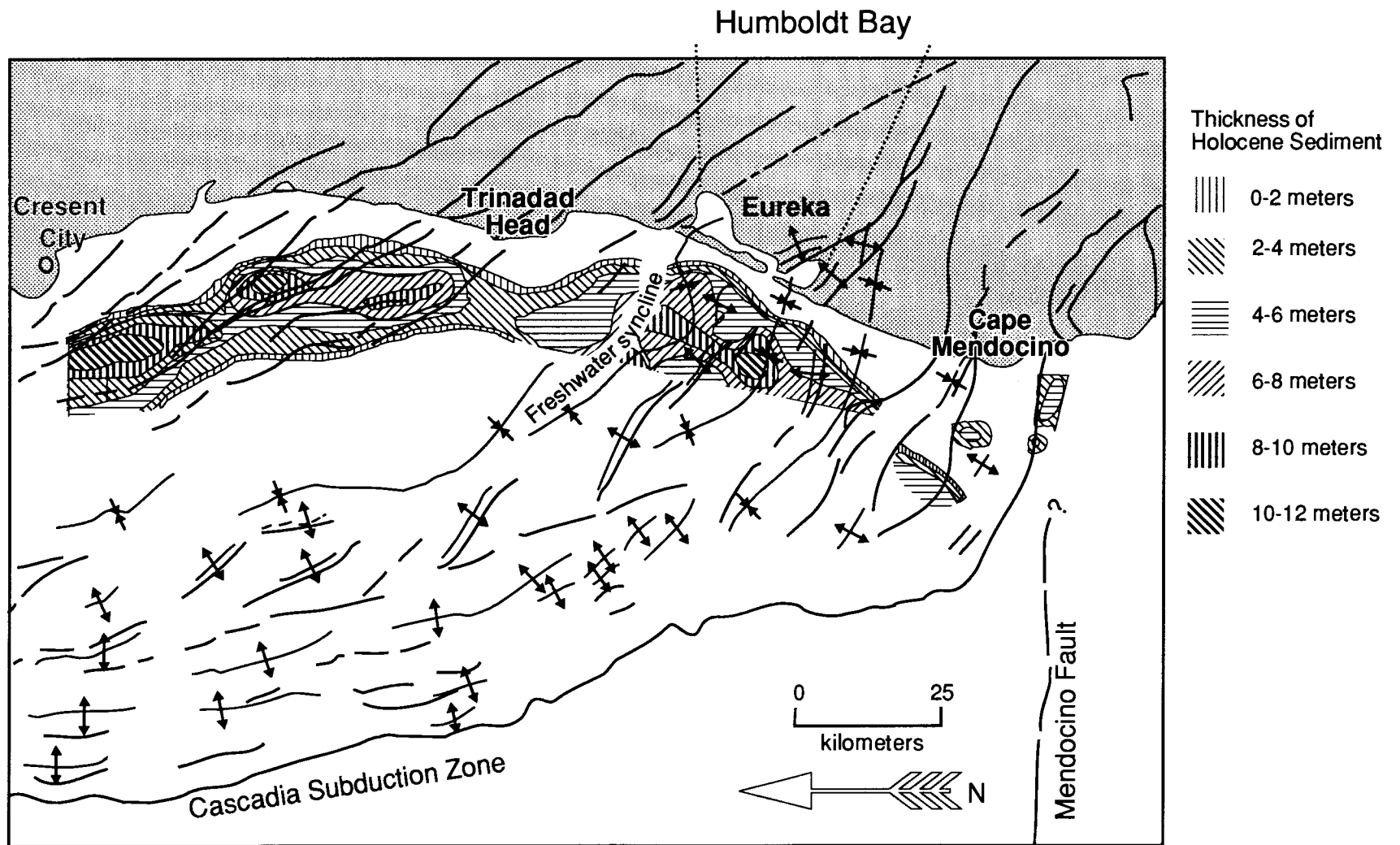


Figure 6. Isopach map of Holocene sediments overlain on a structural geologic map of the northern California shelf. Depositional pockets correlate with the offshore structures suggesting active subsidence (after Vick, 1988; isopach data from Borgeld 1985; structure from Clarke, 1992)

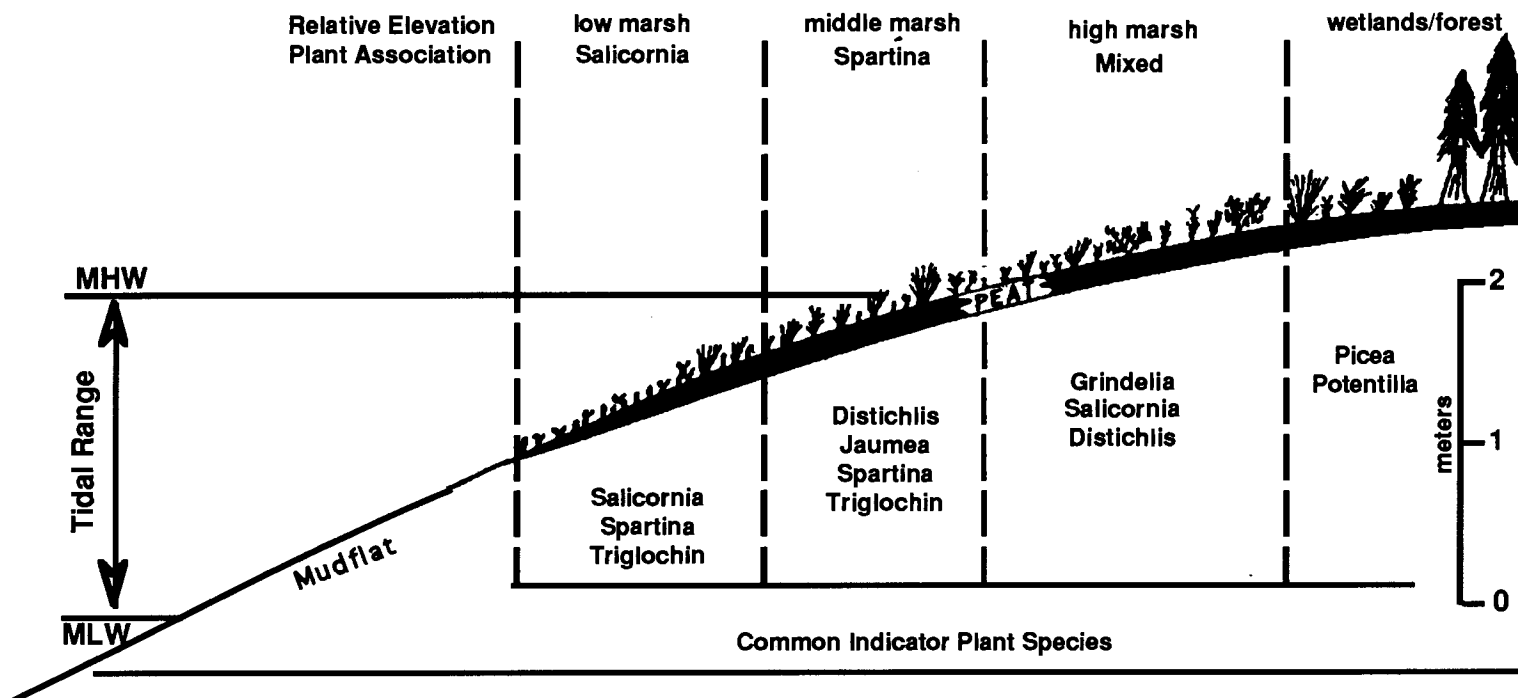


Figure 7. Schematic diagram depicting the position of the low, middle and high salt marsh zones for Humboldt Bay, California. Also shown are the plant association, and species common to each zone. (after Vick, 1988; based on Eicher, 1987)

and above this level there is a succession of plants occurring at differing elevations (Behre, 1986).

Salt marsh peats require a specific environment and do not form where the tidal range is large (Behre, 1986). Freshwater peats form in a variety of environments, including at the mouths of streams and rivers. During rapid sea-level rise, the environment is not favorable to the growth of saltwater marshes, and estuarine deposits overlie the freshwater marsh deposits. As sea-level rise slows, the environment becomes favorable for the formation of salt water marshes, and salt marsh peats overlie the freshwater marsh deposits (Bloom, 1964). Burial by estuarine mud occurs during a rapid rise in sea-level because the sediment influx is not great enough to stabilize the intertidal deposits and allow for the colonization of the intertidal flats by halophyte (salt tolerant) species. When conditions are favorable, thick accumulations of peat can occur (Figure 8; Bloom, 1964; Redfield, 1967; Atwater, and others, 1977).

In the Sacramento-San Joaquin delta, rates of upward building of the marsh surfaces have probably averaged 1 to 2 mm/year for the past 6000 years (Atwater and Belknap, 1980). Thick peat accumulations have occurred in the Sacramento delta because there is sufficient sediment input, and the rate of accretion exceeded the rate of compaction of the peat, and the rate of sea-level rise (Atwater, and others, 1977).

Salt marsh plants grow within a limited range, and plant associations can be related to the elevation above mean sea-level (MSL). This elevation is important because marsh surfaces have a limited local relief of only a few centimeters. In Humboldt Bay, peat horizons form within a limited tidal range, approximately 1.5 meters above MSL to Higher High Water (HHW). Three elevations zones, high, middle, and low marsh, are based on plant associations. These associations are the

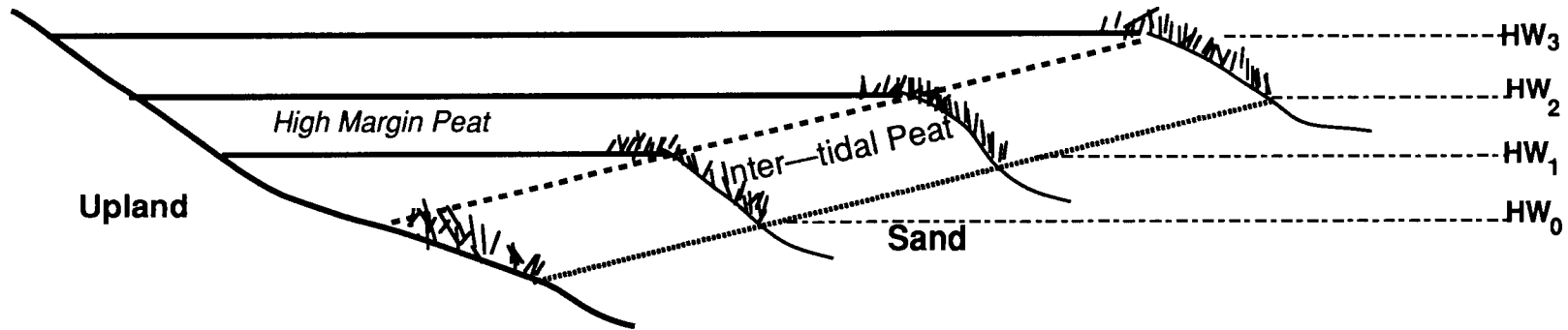


Figure 8. Development of a typical saltmarsh formed during the late Holocene sea-level rise with constant sedimentation. HW_0 represents mean high water (MHW) at time zero, while HW_1 , HW_2 , and HW_3 represent MHW at each successive interval. The peat horizon thickens with gradual sea-level rise. This creates a peat horizon which thickens towards the upland edge of the marsh. (After Redfield, 1967).

salicornia association for the low marsh zone, the spartina association for the middle marsh zone, and the mixed marsh association for the high marsh zone (Figure 7; Eicher, 1987). The macrofossil plant community is used to estimate and constrain the elevation of the marsh horizon by identifying the plant macrofossils in the peat.

Of these three zones, the easiest to recognize in the field is the high or mixed marsh. The high marsh surface has an abundance of an easily identifiable species, *Grindelia stricta*. *Grindelia stricta* is important because it grows within a limited range, is a woody plant, which preserves well and easily identifiable in buried peat horizons. An estimate of the paleoelevation of the peat horizon can be done using plant macrofossils, but most species readily decompose and are not easily identified. Another important plant is *Triglochin maritima*. It is an important pioneer in the mud flats. The presence of its rhizomes indicates that the mudflat is nearing or is above MHW, the elevation accepted as the beginning of marsh growth, and peat accumulation. *Triglochin maritima* is not an accurate indicator of elevation because it has been recorded at elevations well above MHW (B. Atwater, written communication, 1989). The initial locations of growth of *Triglochin maritima* in the intertidal flat are far spaced and sporadic, therefore, its absence is also not an indicator that the mudflat has not reached MHW.

Eustatic Sea-level Changes

Because Eustatic Sea-level change and salt marsh formation are intertwined, Holocene eustatic sea-level changes could be a hypothesis for the formation of multiple submerged horizons. The following review of Holocene sea-level research summarizes the information available on sea-level changes.

Attempts to define global sea-level curves for the Quaternary have met with difficulties. Researchers have realized that one curve could not predict global

eustatic sea-level rise. Local tectonics, isostatic adjustments and sea-level fluctuations due to the distribution of the ice cause local or regional fluctuations which cannot be resolved on a global scale.

Some eustatic sea-level curves, "non-uniform" curves, show fluctuations of up to 8 meters during the early Holocene, and fluctuations of 1 to 2 meters during the late Holocene (Figure 9; Belknap and Kraft, 1977). Other eustatic curves, "uniform" curves, show a rapidly rising sea-level during the early Holocene, with gradual rise during the late Holocene (Figure 10; Belknap and Kraft, 1977). Both types of curves show a relative stability or a slow rise for the past 5000 years. The location of a site relative to the late Pleistocene ice sheets, as well as local tectonics and isostatic subsidence, can cause the variability in sea-level curves. Submergence and emergence can occur simultaneously at different locations (Figure 11; Clark and others, 1978). With respect to the Clark, and others (1978) model of forebulge and glacial isostatic effects, Humboldt Bay lies between two regions, and should not have experienced any subsidence (Figure 11; Vick, 1988).

Geomorphology of Humboldt Bay

Humboldt Bay has three subdivisions: Arcata Bay, Entrance Bay, and South Bay (Figure 12). The three bays are essentially three coastal estuaries linked by the growth of a barrier spit to form a continuous bay (Thompson, 1971). The relatively narrow channels connecting the bays are constrained by uplands on the east and barrier spits on the west. Each of the three subdivisions occupies a former stream valley filled with fluvial and estuarine sediments.

The bay has been surveyed several times; the first survey was in 1853. These surveys show little natural change between the surveys of 1853 and 1870. Between 1870 and 1910, most of the wetlands were diked and reclaimed for agricultural

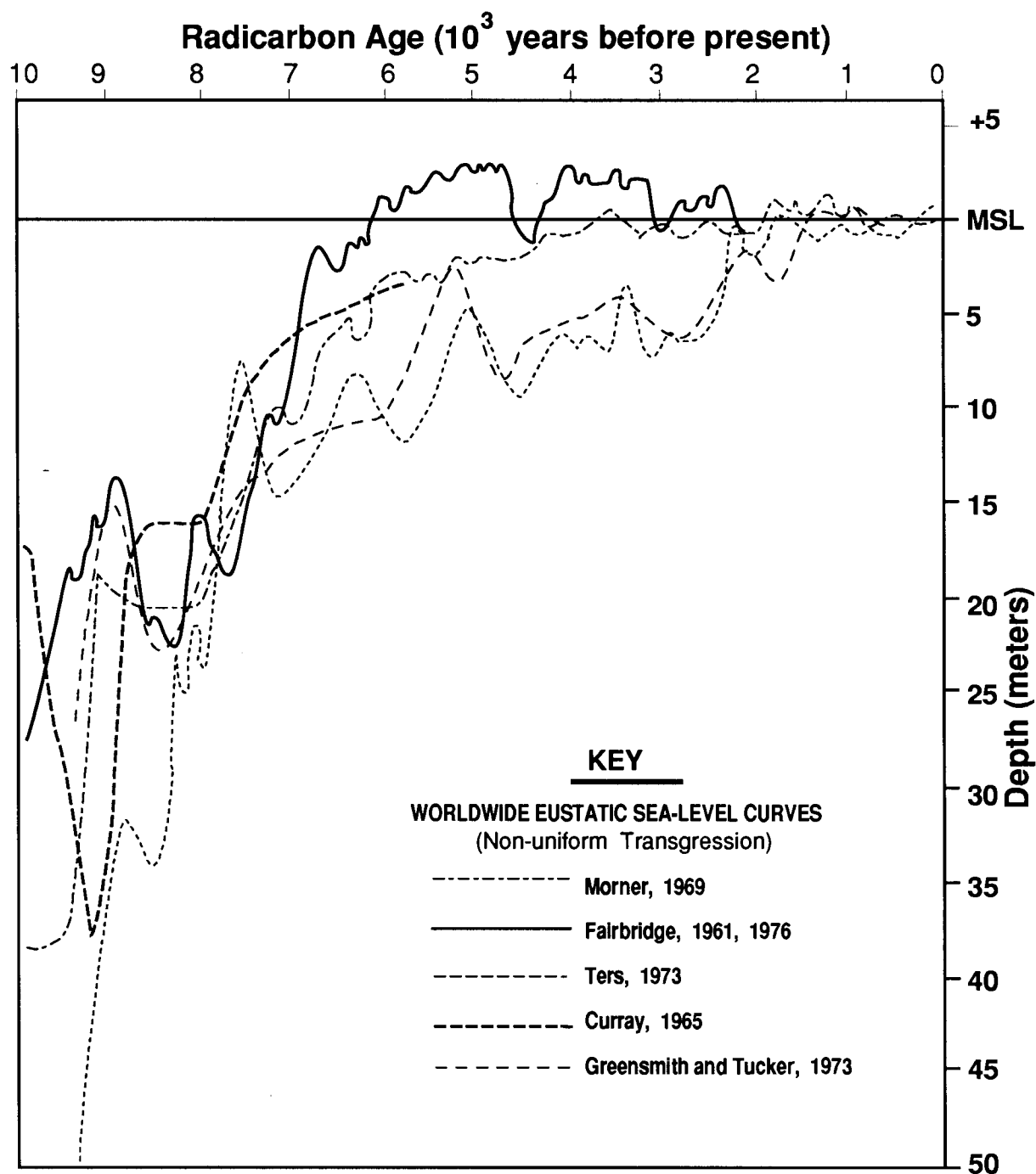


Figure 9. Worldwide eustatic sea-level curves showing a non-uniform Holocene transgression. Note the curves show only minor differences after about 600 years BP, and become similar to the uniform curves on figure 10 (after Belknap and Kraft, 1977).

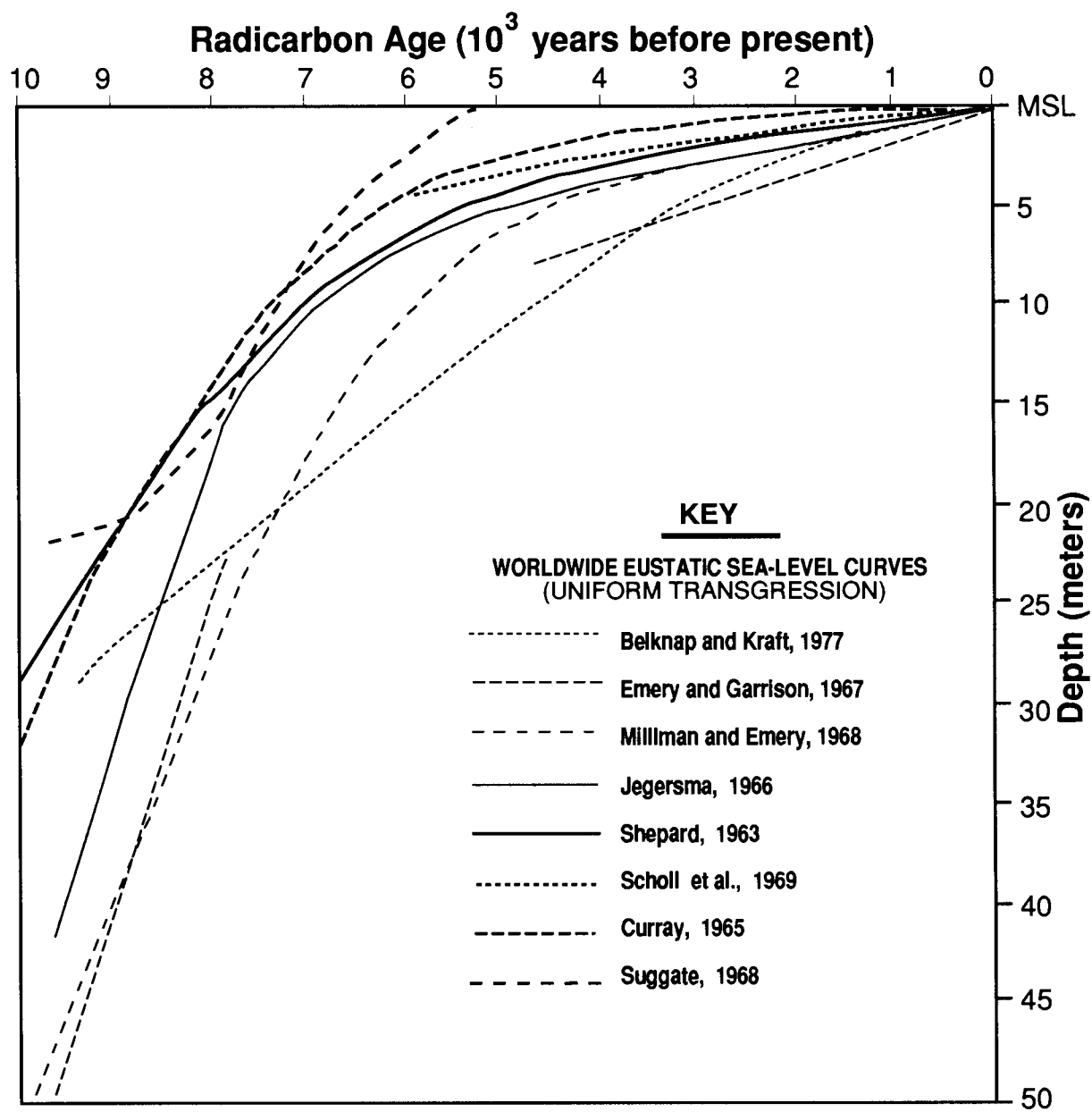


Figure 10. Worldwide eustatic sea-level curves showing the uniform Holocene transgression. The inflection about 6000 year BP signifies the decline the rate of sea level rise (after Belknap and Kraft 1977)

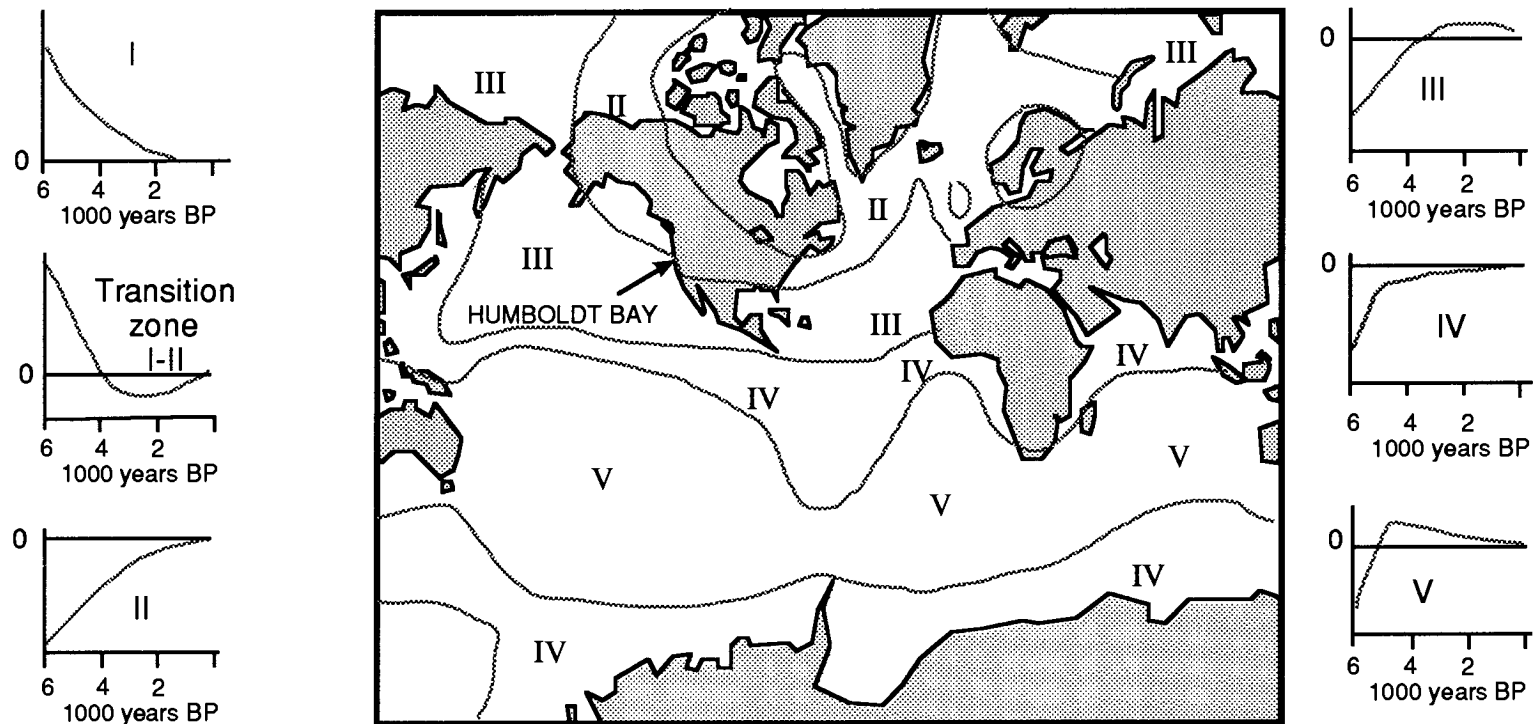


Figure 11. Holocene sea-level curves for the five predicted global zones.

Prediction based on mathematical analysis of glacial unloading and ocean floor loading by meltwater and the related geoidal and gravitational responses of a layered viscoelastic earth. Humboldt Bay is located along the line of transition between zones II and III. Averaging the two curves closely matches the empirical eustatic sea-level curves (Vick, 1988, figure from Clark, 1978)

Humboldt Bay, California

Large Marsh areas,
and Islands

Mud Flats

10 m contour,
shown only in some
locations

Sites

△ No Buried Surface

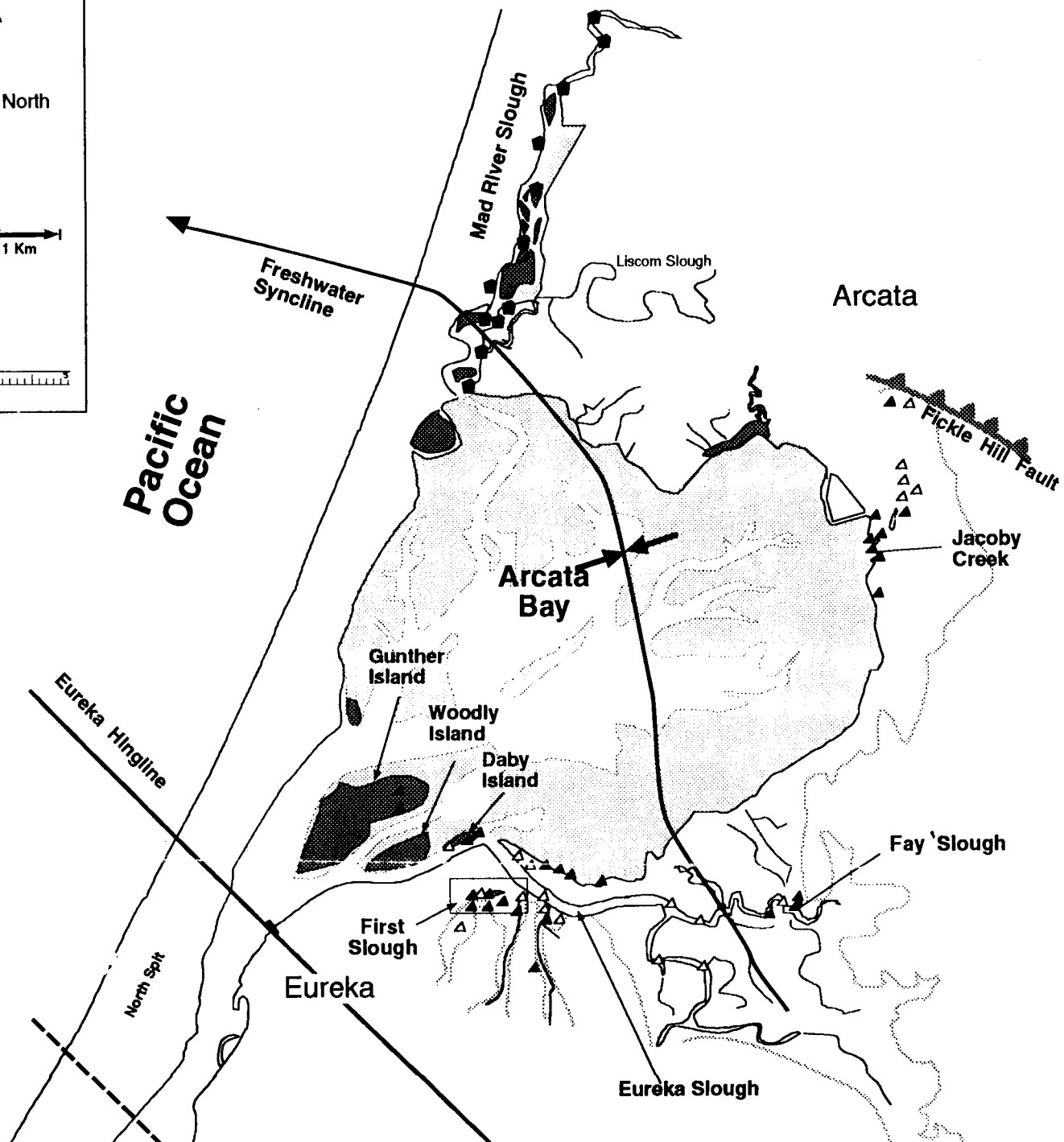
▲ One or more
Buried Surfaces

■ One or more
Buried Surfaces
From Vick, 1988

North

1 Km

Kilometers



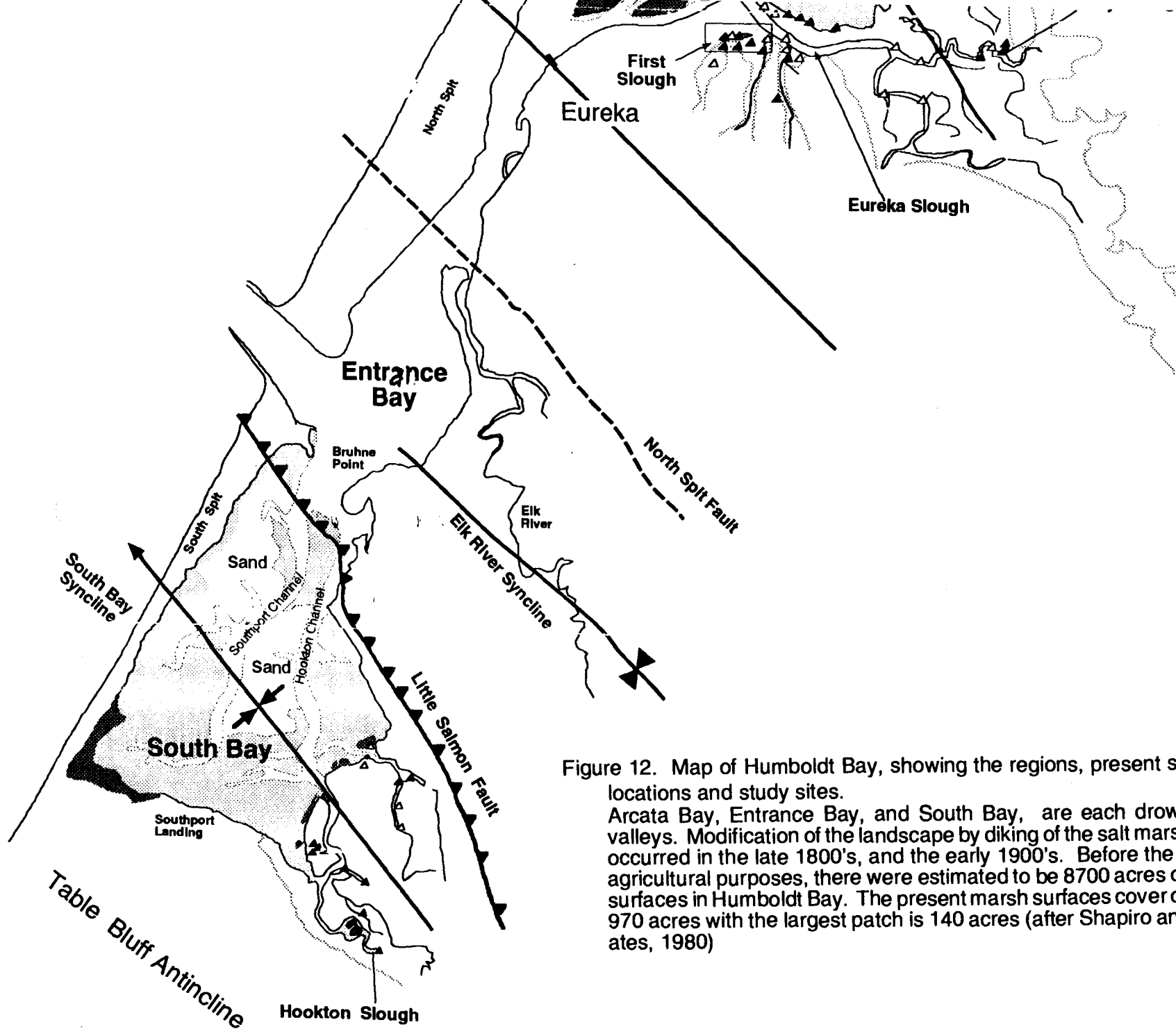


Figure 12. Map of Humboldt Bay, showing the regions, present salt marsh locations and study sites.

Arcata Bay, Entrance Bay, and South Bay, are each drowned river valleys. Modification of the landscape by diking of the salt marsh regions occurred in the late 1800's, and the early 1900's. Before the diking for agricultural purposes, there were estimated to be 8700 acres of wetland surfaces in Humboldt Bay. The present marsh surfaces cover only about 970 acres with the largest patch is 140 acres (after Shapiro and Associates, 1980)

purposes. Before the diking of the wetlands, there was approximately 8700 acres of wetlands in Humboldt Bay. The present marsh covers only about 970 acres with the largest patch being 140 acres (Shapiro and Associates, 1980). Recently, several of the previously diked areas have been opened to tidal action, in an effort to restore them to wetlands. Freshwater marshes persist during the wet season (September to April) in old tidal channels in the diked agricultural land (Shapiro and Associates, 1980).

There is no long term tidal gauge history for Humboldt Bay. The tides in Humboldt Bay are diurnal with a maximum range of about 3 meters between MHHW, and MLLW. The characteristics of several tide stations occupied in the late 1970's does not vary greatly, agreeing to within 0.1 feet (NOAA, 1985).

The long tidal history of nearby sites is inconclusive. Since 1940, San Francisco shows submergence of about 1.5 mm/yr, and Crescent City shows an emergence of about 1.5 mm/yr (Hicks, 1978). Because of the tectonic instability of the northern California region, comparisons with these two stations are likely to be erroneous. A general assumption that the local sea-level has been stable or slowly rising over the past 3000 years has been made for this study.

There are several recognizable intertidal and sub-tidal environments in Humboldt Bay: tidal channels; low and high tidal flat; and three salt-marsh zones. Each of these has different sedimentologic characteristics (Thompson, 1971). Tidal zones are identifiable in the field and are helpful in constraining tidal elevations in the bay. The low tide flats form near MLW and the salt marshes form above MHW.

Methods

Modern marsh sites were examined using a 2 cm gouge corer. Samples were logged in the field for sediment types, apparent structures, contacts, and buried peat

horizons. If the presence of peat horizons could be established at the site in cores, then tidal channel exposures were examined at low tides. Notes of horizon depth, plant fossils, and sediment type were noted for both cores and tidal channel bank exposures. Sites were located on Humboldt Bay mid-scale (1":500') maps. Sites were reoccupied to collect samples for radiocarbon dating. Samples for radiocarbon (^{14}C) dating were taken by combining samples of the same horizon from several closely spaced cores. Although a sample from multiple cores is not ideal because of the possibility of contamination, it was the only method which could extract enough material required for conventional radiocarbon analysis.

Recording of Stratigraphic Details

The accuracy of the stratigraphic log depends upon the type of measurement and the type of sediment. Data from tidal channel exposures have greater accuracy than data from cores. The data from cores are less reliable for several reasons: 1) depth estimates vary when using cores; 2) details of the stratigraphy are not seen because the cores only have a 2 cm diameter; and 3) the corer cannot penetrate thick($\approx >30$ cm) layers of sand.

Without closely spaced cores, and/or tidal channel exposure, direct correlation of the horizons over large distances between sites is questionable. The stratigraphy shown in this thesis is based on depths for local site correlations. Radiocarbon dating for sites at Mad River slough indicate that the horizons are laterally continuous, except for the expected breaks due to the pools and small tidal channels (Vick, 1988).

Past and present marsh islands should be the best locations for coring. The interiors of the islands have not been affected by tidal channel migration, and the undiked islands have not been effected by oxidation. Although there may be erosion

and deposition near the edges of these islands, the interiors appear to preserve the sequences of peats in several locations.

In land which has been diked, groundwater fluctuations, and freshwater flushing of the land has caused concretions to form. These concretions obscure the stratigraphy, which makes identification of the buried horizons difficult down to about 1.5 meters. The freshwater flushing is oxidizing the organic layers, compacting the sediments, and helping develop an iron stain from the oxidation, which can obscure the buried horizons. Concretions which commonly form in the first two meters cause difficulty in core penetration. Most diked areas were avoided, and the results for lands behind the dikes are unreliable for about the first 1.5 meters.

Site Descriptions

The horizon numbers of this study do not directly correlate between the areas; i.e., peat horizons 1-3 at South Bay do not necessarily correlate with peat horizons 1-3 at Eureka. This numbering simplifies site descriptions. The paleoseismicity section uses the radiocarbon ages to correlate the sites, and discusses the implications.

Jacoby slough/Arcata

Jacoby slough is located on the northern flank on the Freshwater syncline (Figure 13). This region is affected by the presence of Jacoby creek, and may have been affected by the migration of the ancestral Mad River when it flowed through McDaniel slough. Only two peat horizons are fully documented as continuous layers at this site.

Horizon 1 can be found in tidal exposure, and in cores at several sites (Figure 13). This horizon contains *Grindelia stricta* remnants at JC-A and JC-D, and begins between 86 cm and 115 cm below the present marsh surface. A 25 meter tidal

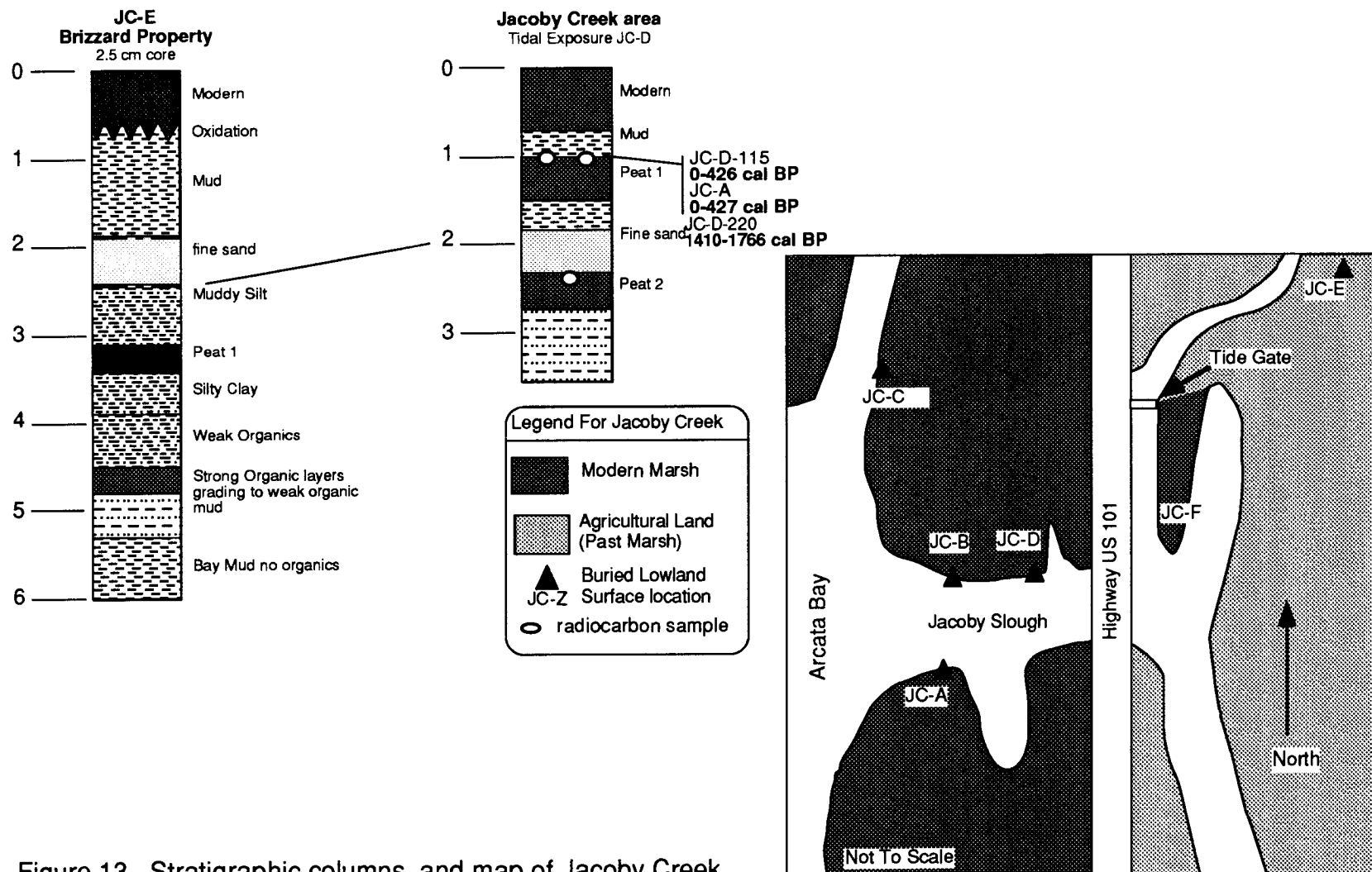


Figure 13. Stratigraphic columns, and map of Jacoby Creek. Extensive sand layers hamper the correlating of the layers in this area. Horizontal Bars represent meters below present

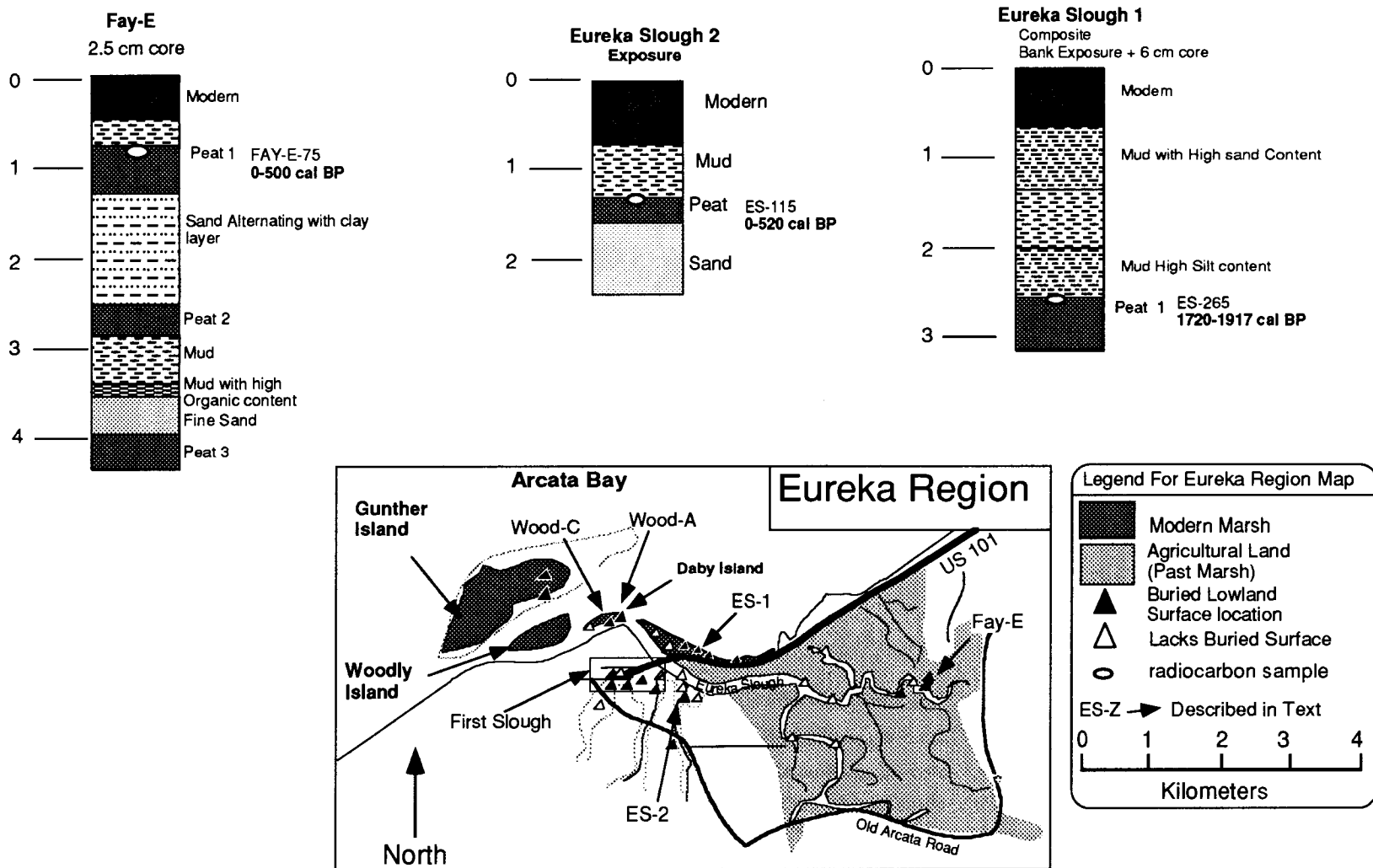
exposure of horizon 2 is found at JC-D. At JC-C, a thin layer of black oxidized sand can be found in cores about 30 cm below the base of horizon 1, with two cores having a 2 cm peat layer. This oxidized layer has not been found in the tidal channel exposure. This oxidized layer at JC-C may correlate with horizon 2. At location JC-F, no buried peat horizons are found, but black sand layers similar to those at JC-C are found at elevations which may correlate with the peat horizons at the other locations. Sedimentologic evidence from site JC-F indicates that the area underwent a rapid change in depositional environment across these boundaries. This change itself is not indicative of sea-level changes, but sea-level changes could be the cause of the changes in the depositional environment.

Extensive sand layers formed by Jacoby creek make the investigating and tracing of peat horizons difficult. A third horizon located at 6 meters is found at JC-E. Horizon 3 is probably more extensive, but all sites except one are difficult to investigate to this depth due to these extensive sand layers.

To the west of Jacoby creek, in Arcata Bay, a layer of river or stream gravels underlie the modern bay sediments. They are found within the transitional mudflat zone, and are oxidized, indicating subareal exposure. Because there was no dateable material found, it is unknown whether their submergence into the intertidal zone is due to the rise in sea-level, and/or subsidence of the syncline.

Freshwater slough

Two peat horizons are found at Freshwater slough (Figure 14). The oxidation within the diked areas has eliminated horizon 1 in all but the tidal channels. The first peat horizon is a tidal channel exposure, but it is found only at one site. I believe that this horizon is a remnant of a more extensive pre-agricultural land horizon, as indicated by an age of 300 ± 30 RCYBP (FAY-E-75). Heavy silting within the tidal channel makes it difficult to find deeper horizons in tidal channel exposures.



Figures 14. Stratigraphic columns and map of Freshwater Slough, Eureka Slough and bay islands. Horizontal bars represent meters below modern surface. See figure 15 for detail on First Slough area.

Horizon 2 is found in cores near the bay margin. This horizon is not extensive, and is not found in any tidal exposures. The activity of Freshwater creek probably eroded much of the horizon. More evidence for peat horizons in the Freshwater slough region might be found within the diked agricultural lands.

Eureka slough

Eureka slough is a stratigraphically complex area near a hingeline of the Eureka anticline. Freshwater Creek empties into Eureka slough, providing a large sediment supply (Figures 14 and 15). Coring implements have difficulty penetrating the sand layers deposited by the migrating Eureka slough and/or storm flows from nearby creeks. The main slough channel contained no buried peat horizon exposures. Small infilled drainages off the main channel and on the flanks of the Eureka anticline contain small pocket marshes. These marshes contain evidence for several buried peat horizons. One site, First slough (Figure 15), proved to be especially valuable to the study of coseismic subsidence.

First slough is artificially split by U.S. Highway 101 (Figure 14). The area to the east of the roadway contains a small pocket marsh, which has a drainage channel cut through it. At its northern end, this channel exposes a buried peat, horizon 1, for a distance of 70 meters. At one point, horizon 1 directly overlies a soil horizon (column bridge, Figure 15). Underlying the Holocene sediments in First slough appears to be a ridge which has been buried by rapid rise in sea-level, and tectonic subsidence. Ages from the southern end of First slough are older than the ages of horizons at Mad River slough. The lowest horizon is a freshwater peat, which is overlain by estuarine sediments and saltwater peat. This indicates that these horizons were protected from erosion by Eureka slough, and have been slowly uplifted to their present elevations by slow uplift on the flanks of the Eureka anticline.

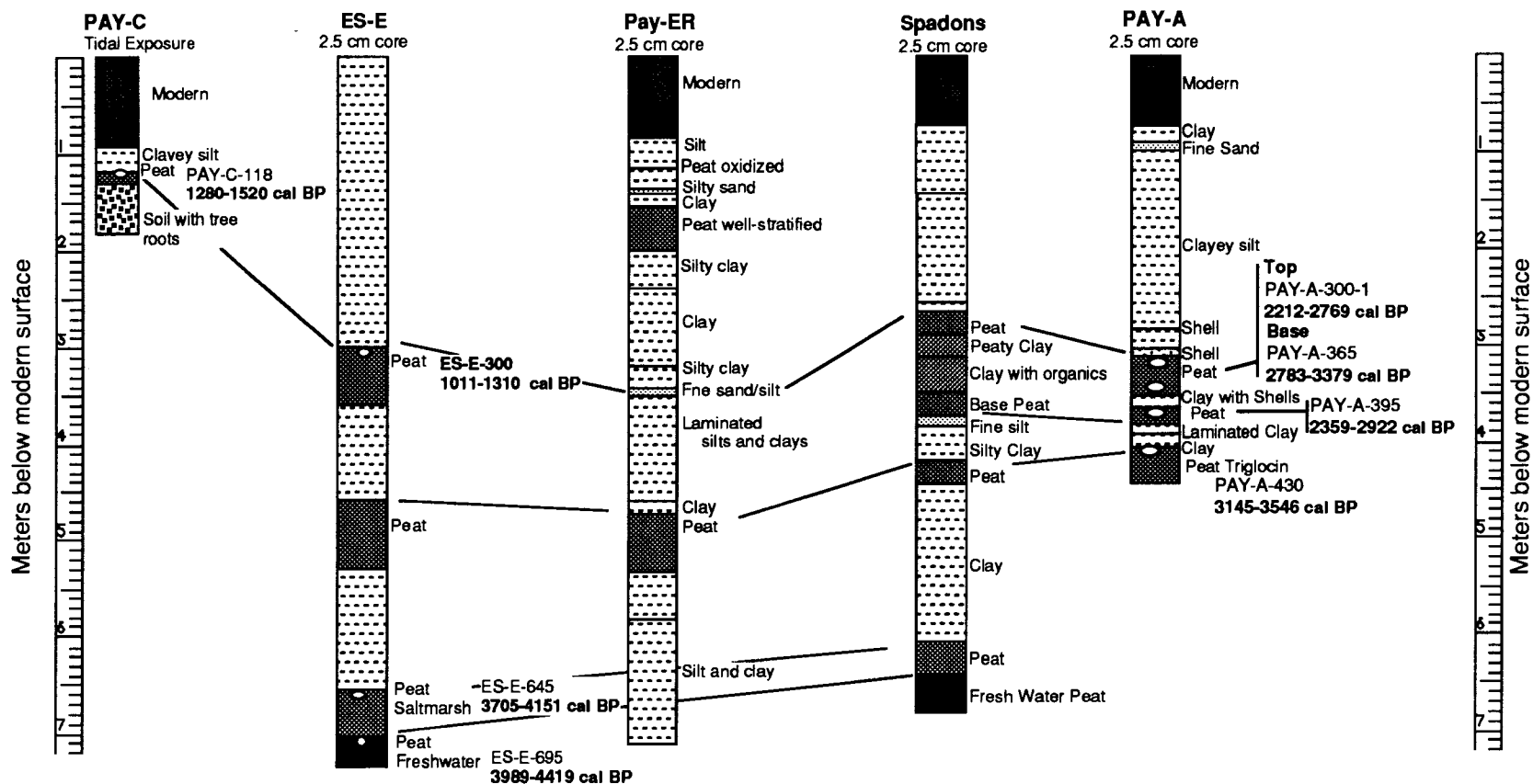


Figure 15. Stratigraphy of First Slough, Eureka, California.
This is the only location where a fresh water peat is found.
vertical scale is meters, no horizontal scale.

At least three other places in the Eureka area had extensive buried peat horizons. The first, ES-1, is located to the north of Eureka slough (Figure 14). Horizon 1 overlies an extensive sand layer, and is buried by 100-120 cm of estuarine sediment. Horizon 1 is extensive, and contains *Grindelia stricta* remnants in some cores indicating elevations above MHHW. Third slough (ES-2; Figure 14), a small infilled creek to the south of Eureka slough contains evidence for two buried horizons. The first horizon is under an extensive sand layer, can be penetrated the tidal channel the creek. In another channel, to the east, clam shells (*saxiomus nuttalli*) are found in sediments in growth position at approximately 70 cm. Their present is above their growth range, and they are buried by intertidal and marsh sediments. Horizon 2 is found underlying the creek bed at 265 cm.

Bay Islands

One buried peat horizon is found on the northern extents of islands in Arcata Bay (Figure 14). Horizon 1 dies out to the south, and may reflect the presence of the Eureka hingeline (Figure 12), or local erosion by tidal action in the Eureka slough. To the west, at Gunther island, horizon 1 also disappears to the south. The disappearance of the buried peat horizon 1 along approximately the same East-West line supports the positioning of the Eureka hingeline through the islands.

Because the tidal channels of Humboldt Bay have been extensively dredged, it might be argued that the buried peat horizon on the islands is caused by the dumping of dredge spoils. Woody island was a site for the dumping of dredge spoils for many years, and it is not used in this study. It is not believed that dredge spoils were dumped on Northern Gunther island, but, it was diked for a short period in the early 1900's. There is no record of diking or the dumping of dredge spoils on Daby island (Shapiro and Associates, 1980). The buried peat horizon is found on both islands. The presence of a horizon on both islands, and the horizons age from Daby island

(580±40 RCYBP Wood-C-70-1) indicates that horizon is not due to the dumping of dredge spoils on the islands.

South Bay

The South Bay contains multiple buried peat horizons some at depths of greater than 6 meters (Figure 16). Only one tidal exposure containing one buried horizon is found in South Bay. Up to five other buried horizons have been found from cores at various locations. The South Bay salt marshes were converted to agricultural land in the early 1900's, almost no pristine salt marsh remains. Several areas have been returned to tidal action.

The large island (Figure 16) was diked for a short period from the late 1920's to early 1940's. Although no definite horizons are found on the island, the stratigraphy indicates that this was the location of the outlet of Little Salmon creek, or a large tidal channel, the Hookton slough. The marsh at this island has not reestablished itself after more than 40 years of tidal exposure, indicating either too little sediment is arriving through the breaks in the dike, large amounts of consolidation occurred, or that the region is interseismically subsiding. Any of the three processes would hinder the recolonization of the mudflats by salt-marsh vegetation.

Hookton slough has a high rate of silting. Near the two marsh islands has the infilling has proceeded at a rapid pace. The channels were navigable at low tide until the 1940's, but are now silted up. The silt is accumulating around the borders of marsh islands. The interior of these islands preserves two buried horizons.

A thick peaty mud horizon near the Little Salmon fault, at the outlet of Little Salmon Creek, is puzzling. The peat/peaty mud extends from the present marsh surface to a depth of 150 cm. This is the only location where a thick (>1 meter) accumulation of salt marsh has been found in Humboldt Bay. Rapid sedimentation in an abandoned tidal channel is believed to have caused this deposit.

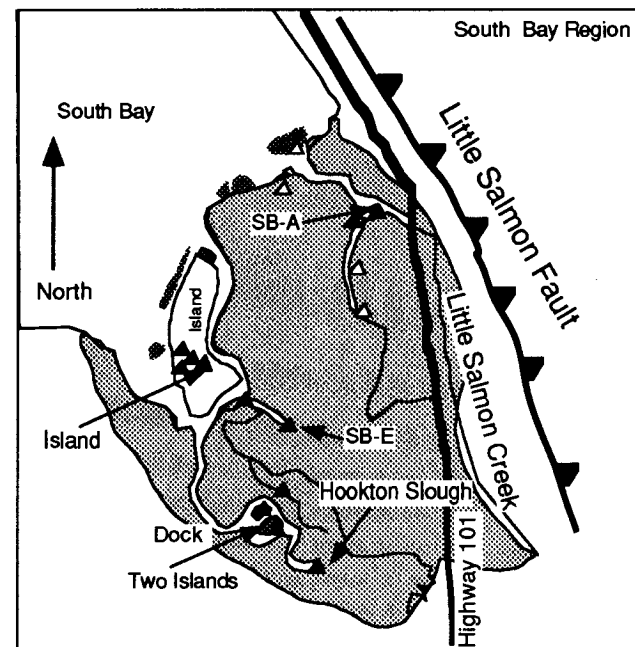
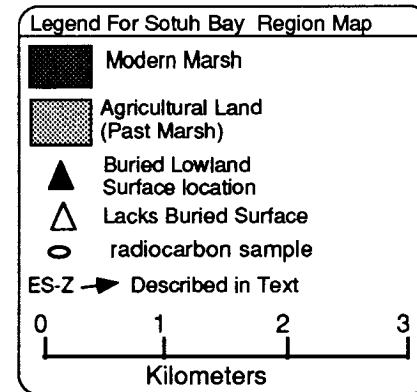
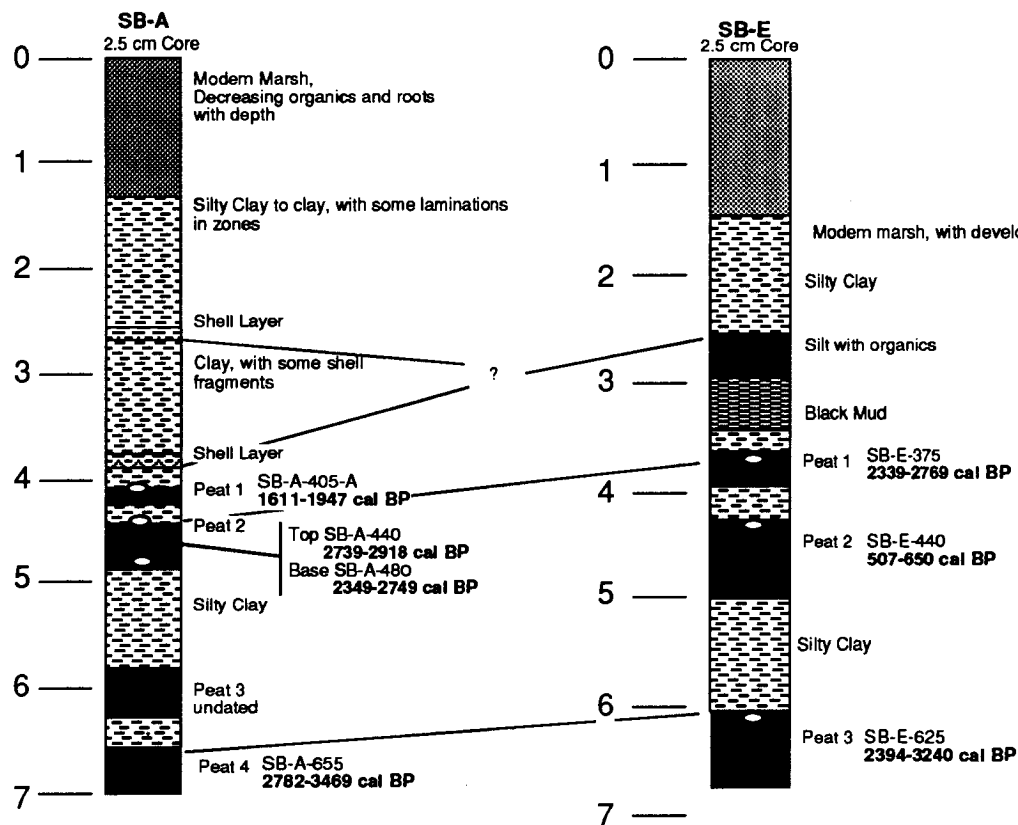


Figure 16. Stratigraphic columns and map of South Bay. Only one tidal exposure is found in this region. Numbered horizontal bars represent meters below modern surface.

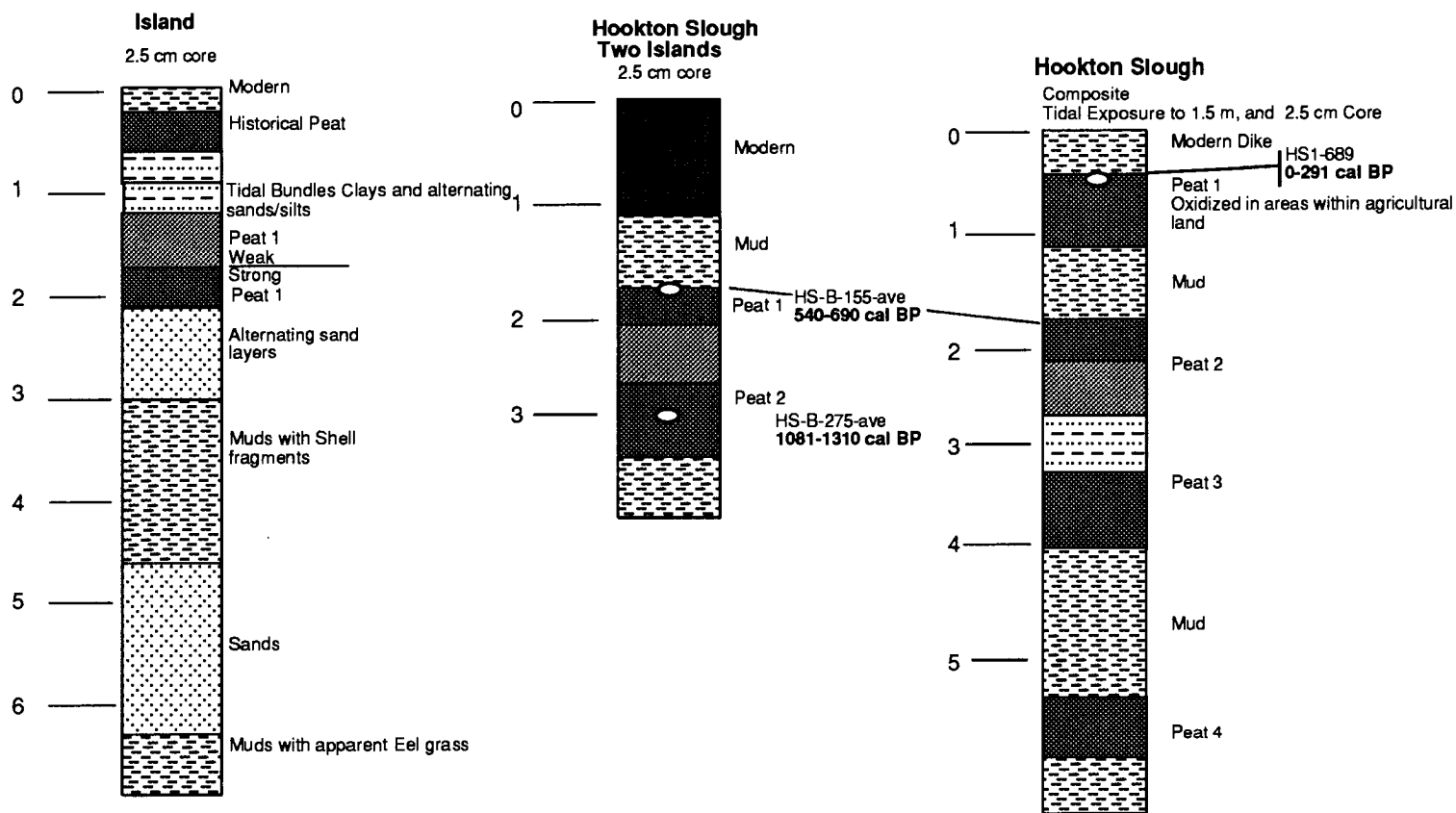


Figure 16 (cont). Stratigraphic columns and map of South Bay. Only one tidal exposure is found in this region. Horizontal bars represent meters below modern surface.

On the eastern edge of South Bay, horizon 1 is found in tidal exposure, and in exposures in drainage ditches in the agricultural lands. Horizon 2 is found in cores at the two marsh islands, and in a bank exposure in a large drainage ditch. Horizon 2 may be represented by a thick black mud horizon at SB-A, near Little Salmon Creek. At SB-A, horizon 3 is found only in core, but the horizon is found in cores throughout South Bay. Correlating horizons below horizon 3 are difficult to correlate because of their depth and the inconsistent number of horizons at each site, but up to five horizons are found at depths to 6 meters.

Discussion

Stratigraphy

Mad River Slough—Type Section

Mad River slough was studied by Vick (1988), whose work laid the basis for undertaking of this study of the late Holocene stratigraphy of Humboldt Bay. The stratigraphy of the sites investigated in this study are similar to those described by Vick. Mad River slough, site MRS-3, is the type section for the buried stratigraphy in Humboldt Bay.

Up to four buried horizons are found in the tidal channel bank exposures in the Mad River slough region, to depths of 3.2 meters below the modern horizon. These horizons can be followed for several tens of meters at each exposure, and are believed to laterally continuous for several kilometers. (Figure 17; Vick, 1988). Most sites are tidal bank exposures. At core locations, buried peat horizons can be seen exposed in the tidal channel slopes at low tide. Most Mad River slough sites have been surveyed for elevation control, and additional radiocarbon dating done on this are for the present study (Figure 17; Appendix 1).

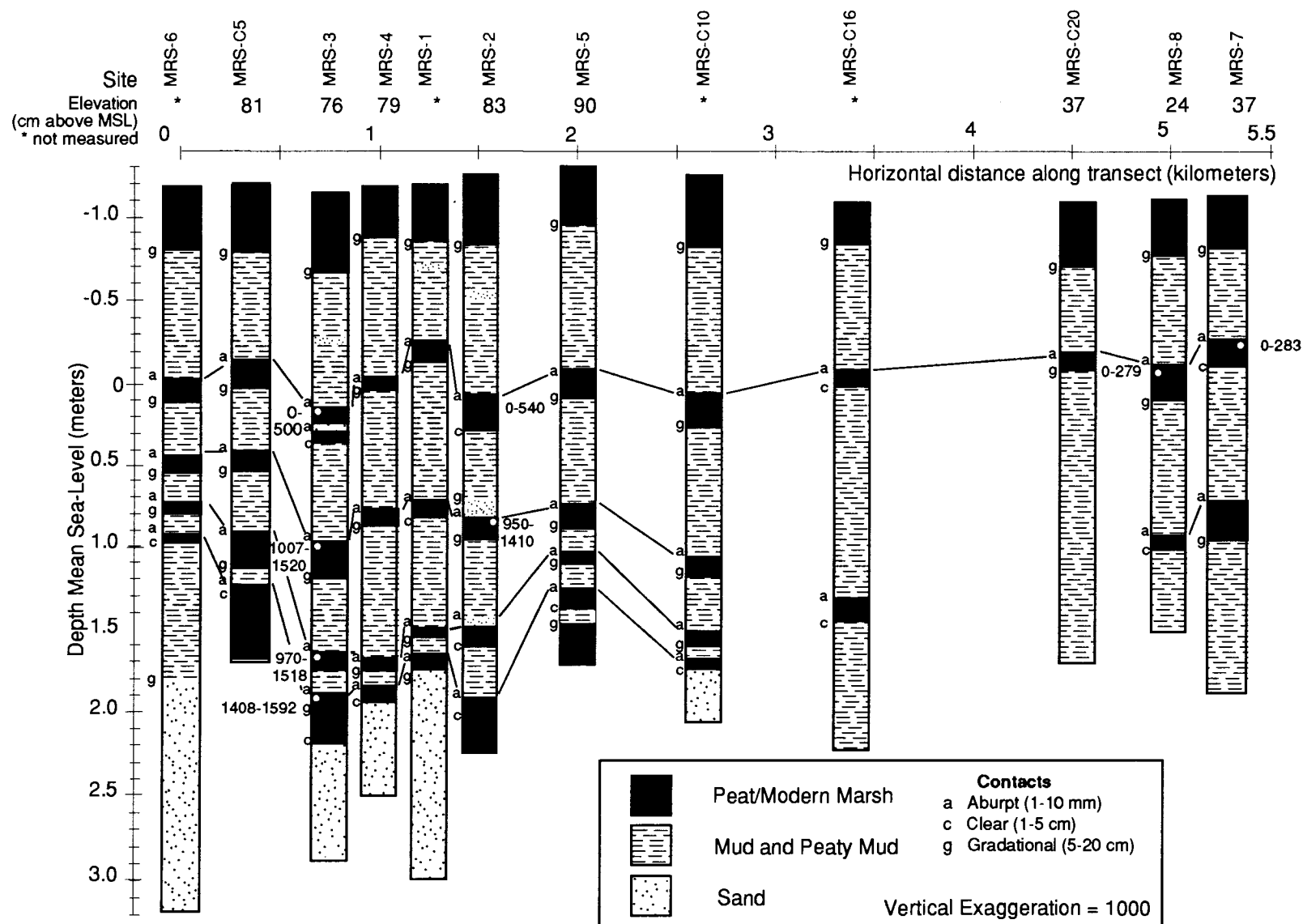


Figure 17. Generalized stratigraphic sections of the upper Holocene sediments of Mad River Slough. All ages reported as calibrated years before present (modified from Vick, 1988)

Formation of Buried Salt-Marsh Horizons

Within the stratigraphy of Humboldt Bay, there are several buried salt-marsh horizons below the elevation at which they formed. These horizons underlie extensive areas of the bay. The localities examined in this investigation contain from none to seven buried horizons. Marsh surfaces develop at elevations above mean high water. Once these surfaces form, they act to sustain an elevation above mean high water. There are several possible explanations for the existence of the horizons. Changes in the rate of upward growth of the salt-marsh surface are due to changes in organic growth of the marsh surface, the lack of accumulation of sediment, compaction, and/or rapid sea-level changes (Figure 18; Allen, 1990).

During rising sea-levels, sediment influx determines whether or not salt-marsh surfaces maintain an elevation above mean high water (MHW). A constant sediment influx during a rising sea-level should produce gradational contacts marsh changes into a estuarine environment. During periods of stable or slowly rising sea-level, reduced or increased sedimentation rates are accommodated at the salt-marsh/tidal-flat margin. Reduced sediment influx may cause erosion at the seaward edge of the marsh surface. Increased sediment influx may cause a seaward progradation of the marsh margin. There are abrupt contacts that are not erosional between the lowland horizons and the overlying estuarine sediments. One can see evidence for rapid sediment accumulation in the estuarine sediments overlying the buried peat horizons. Across the boundary, a rapid fluctuation in the water depth relative to the land surface occurred. The possibility of one or more of the phenomenon causing these fluctuations, and being accountable for the formation of the stratigraphy of Humboldt Bay is discussed below.

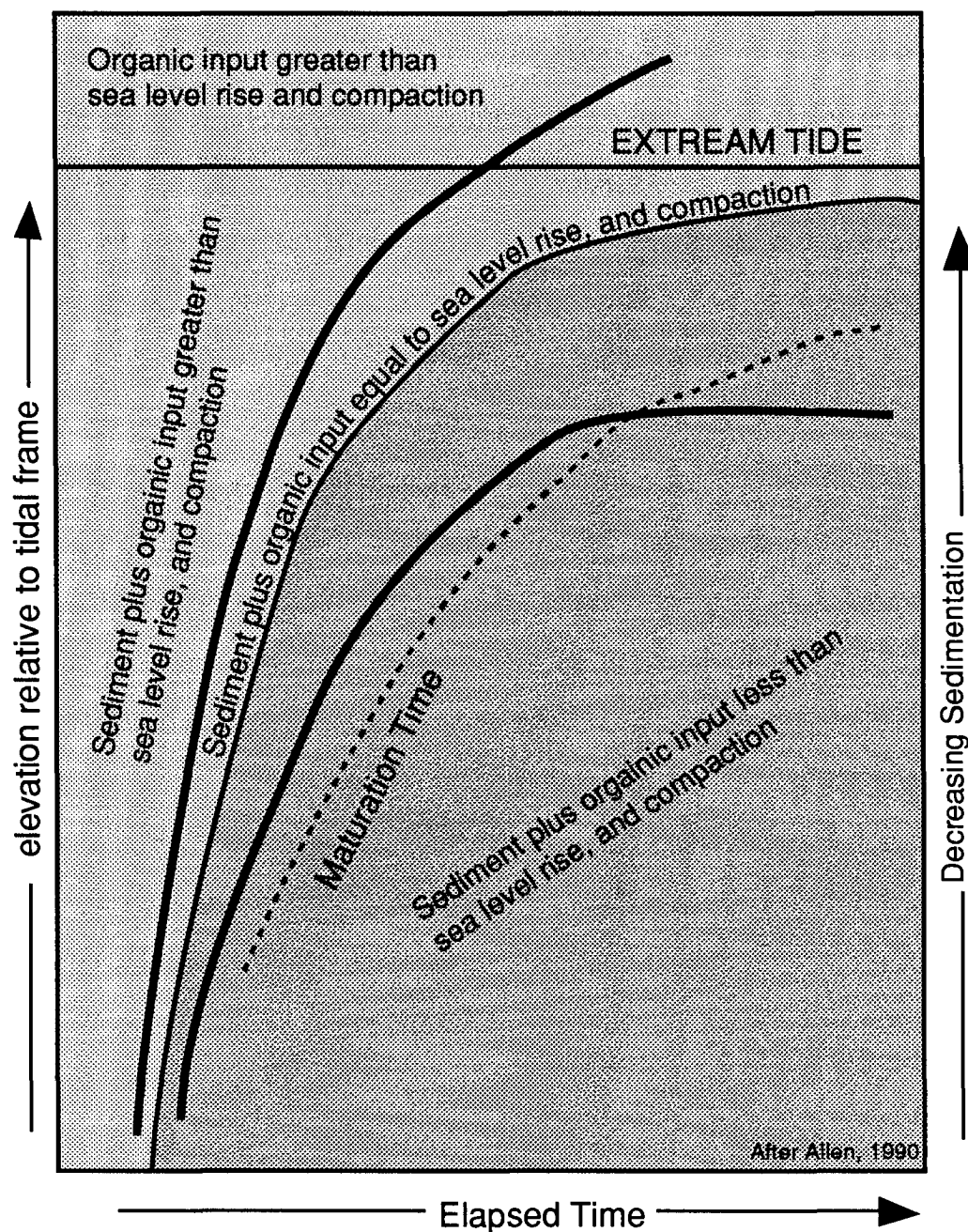


Figure 18. Schematic curves illustrating the upward growth of a mudflat-saltmarsh (elevation of surface relative to tidal frame) for various conditions of sedimentation, sea-level change, and compaction. After Allen, 1990.

Changes in the Bay Entrance

Sequences of buried marsh horizons are documented in areas where berms have broken in shallow estuaries in Europe (Behre, 1986). Presently, there are no berms blocking Humboldt Bay, and there is no record of a blockage occurring historically. If the bay entrance did become blocked it would only be for a short period, at most a summer. This would cause a freshwater influx, and the lack of tidal fluctuations would reduce the sedimentation on marsh and mudflat horizons. I believe that periodic blockage of the bay entrance did not play a role in the formation of the buried marsh horizons.

Although there is no evidence that the bay entrance has been blocked, the bay entrance did migrate several kilometers before the placement of the jetties. The entrance would migrate south, and then break north, with a cycle of about five years (Thompson, 1971). A migrating bay entrance could locally effect salt-marsh horizons by increasing the local tidal range of an area. The present mean tidal fluctuation varies by less than 10 cm, over the 20 km length of the bay (NOAA, 1985). It is hard to argue that the migration of the bay mouth would cause tidal fluctuations greater than this measurement. Changes in the bay entrance would not effect the extensive salt-marsh surfaces shown on the early maps (U.S. Army Corps of Engineers, 1911) because most surfaces are several km from the bay entrance. The migration of the bay entrance apparently had no effect on the surfaces shown on several maps, but the stabilization of the entrance by the jetties caused erosion in Entrance bay (Thompson, 1971). If bay mouth migration occurs, it would not have affected the stratigraphy from Arcata to Eureka.

Changes in the Mad River Course

The one source for an increased sediment supply would be the Mad River. Presently, the Mad River does not flow into Humboldt Bay. Changes in the course

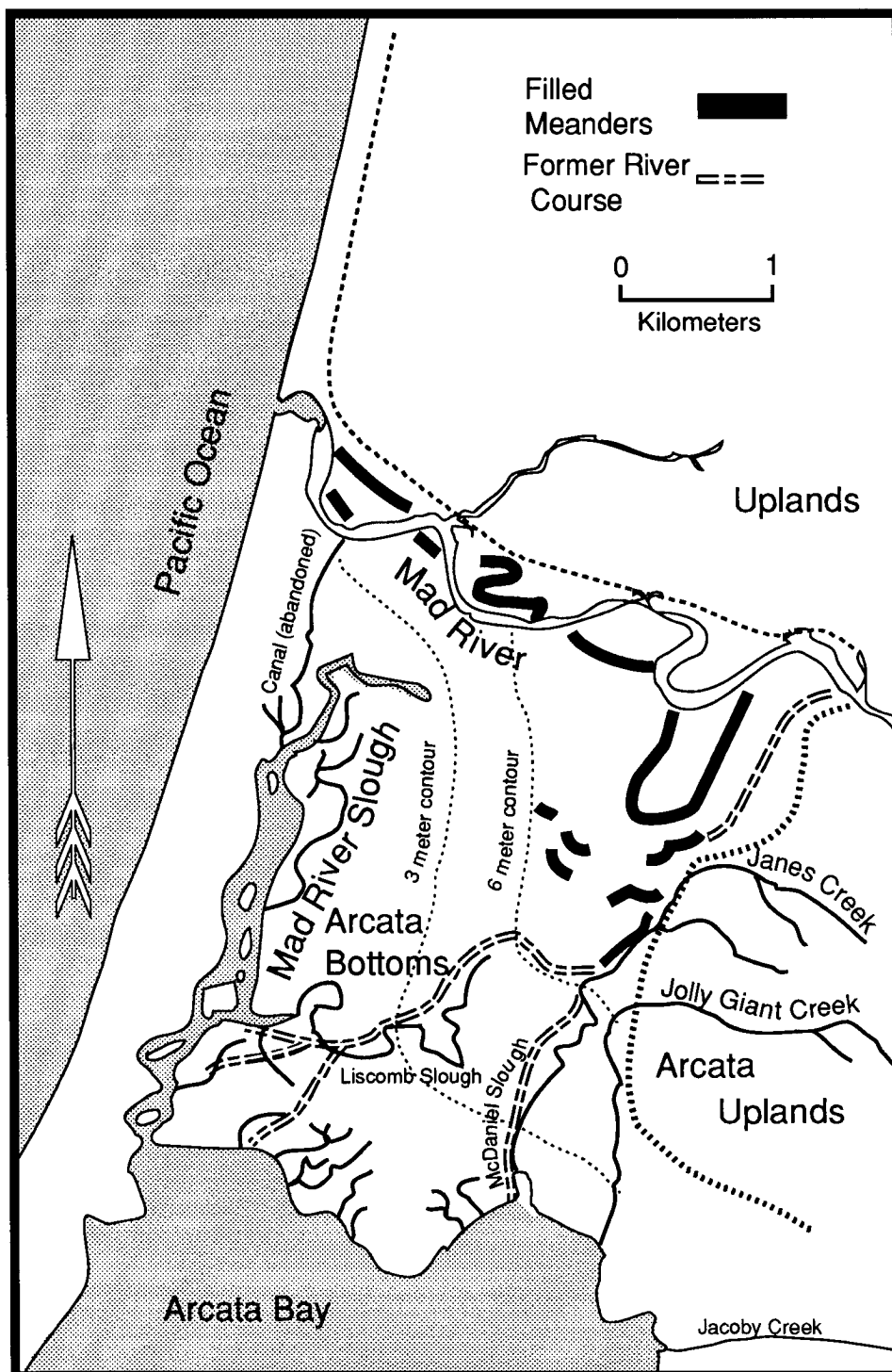


Figure 19. Proposed courses for Mad River. There is no geomorphic evidence that Mad River used the Mad River slough as a direct entrance to Humboldt Bay (after Thompson, 1971).

of the river may effect the sediment supply in the Arcata Bay area, but whether this sediment would effect Eureka and South Bay is questionable. From the geomorphology, it appears that the Mad River entered Arcata Bay through several different courses such as McDaniel and Liscomb Sloughs. There is no evidence that the Mad River slough was a direct pathway to the bay (Figure 19; Thompson, 1971).

The Mad River emptying into Humboldt Bay would cause several changes which separately or in combination may cause a local change. A drop in the salinity, increased sediment influx, and changes in the plant communities might occur. If this occurred, a progression of buried horizons grading into a thick peat horizon should be found in Mad River slough. There are no indications of a thick peat horizon forming in the Mad River slough, or anywhere else in Humboldt Bay, and the buried horizons are laterally continuous for several kilometers. These horizons were not caused by the changing of the course of the Mad River. The sediment carried by flood events may have caused some of the laminations found within of the buried salt marshes.

Compaction

No evidence for large amounts of compaction have been found in studies undertaken in other estuaries along the Pacific Northwest. During the formation of the peat, the effect of compaction is small in magnitude relative to the effects of sediment input, and sea-level change (Allen, 1990). The stratigraphy indicates the events occur episodically, and compaction is not an episodic phenomenon. Episodic compaction might occur during large magnitude earthquakes, but this compaction cannot be separated from coseismic subsidence.

Change of Environment due to Sea-Level Changes

Sequences of salt-marsh peat horizons overlain by estuarine muds represent a rapid sea-level change, but might be attributed to other effects. Other examples

of rapid sea-level changes occur along the eastern North America coast. Many estuaries along the Atlantic coast contain sequences of freshwater peat overlain by estuarine muds which are used as indicators of rapid sea-level change. In these areas, such as the Connecticut coast, modern saltwater peats overlie freshwater peats, but in the early Holocene stratigraphic record, estuarine muds overlie the freshwater peats (Bloom, 1964). During the early Holocene, rapid sea-level rise (>0.18 m/100 year) did not allow sediments to accumulate rapidly enough for the marsh plants to colonize the intertidal mud flats (Bloom, 1964). Since about 6000 years before present when eustatic sea-level rise slowed, a thick sequence of peat accumulated.

The eustatic sea-level has been stable or slowly rising for the past 6000 years (Figure 10), there is no reason to believe that there have been any rapid eustatic sea-level fluctuations over the period of the dated horizons. One would expect to find thick peat deposits towards the edges of the bay, with thinning towards the interior, similar to those found by Redfield (1967; Figure 8). In Humboldt Bay, the stratigraphy indicates that extensive regions have been repeatedly submerged, and have reemerged after the accretion and/or uplifting of these areas to MHW. These events have occurred repeatedly during a period when sea-level is assumed to be relatively stable, and the slow sea-level rise should be represented by a thick accumulation of peat,. But there are no indications of thick peat accumulations occurring along the edges of the bay, therefore, the relative sea-level changes which caused these buried peat horizons are related to local land level changes. Rapid episodic subsidence in the syncline axes crossing Humboldt Bay is the best explanation for a rapid local sea-level change.

Subsidence

The preferred explanation for the formation of the extensive buried peat horizons is rapid submergence due to coseismic subsidence. Such rapid submergence and burial have occurred as a consequence of the great 1960 Chilean earthquake (Atwater and others, in press), and the 1837 event (Muir-Wood, 1989). Presently, Chile is the only locality where historic earthquake subsidence is correlated with multiple submerged lowland horizons (Atwater and others, in press; Muir-Wood, 1989).

The Humboldt Bay region the preservation of buried peat horizons is due to local tectonics. The long recurrence interval, the slow uplift rate, and slow sea-level rise creates an environment which preserves the submerged deposits. The preservation of four extensive, closely-spaced, buried horizons within 1700 years of one another in Mad River slough is unexplainable without movement of the local and regional structures.

Correlation

The dynamic nature of an estuarine environment can make correlation between cores difficult. Creeks flowing into the bay and tidal channels in the bay may erode previously preserved stratigraphy., and salt-marsh surfaces may not form at all sites. The Mad River slough has a stratigraphy documented from both cores and tidal exposures (Vick, 1988). But, Mad River slough correlations are not without problems due to erosion and deposition. The problems in an area with excellent tidal channel exposures, indicate how difficult it is to correlate when using cores.

The correlation of the horizons is important because the late Holocene stratigraphy of Humboldt Bay is formed by periodic subsidence events. The change from lowland/salt-marsh to intertidal sediments is not itself an indicator of rapid submer-

gence, but several lines of evidence indicate that these horizons are the result of rapid submergence, and that they can be correlated.

These sequences are usually a salt marsh peat, covered by an estuarine mud, which grades into another salt-marsh horizon, but some horizons are lowland forests covered by estuarine mud. The lowland forest horizons have *in situ* plant remnants entombed in estuarine muds. The upper reaches of Mad River slough have stumps in growth position, and layers of forest litter. Terminal growth rings from the stumps indicate that they were not stressed until their submergence into the intertidal zone (Vick and Carver, 1988). Salt-marsh horizons have plants which are entombed by estuarine mud. The lower boundary of the horizons is gradational (<2 cm) to clear (0.5 cm to 2 cm). The upper boundary is usually abrupt (<0.5 cm). The buried peat horizons vary in thickness from 10 cm to 50 cm. These horizons were formed above MHW, and are presently below MHW. Many of the horizons contain entombed plant remains with an abrupt upper contact, this indicates a rapid submergence into the intertidal zone.

The estuarine muds separating the buried lowland layers indicate rapid deposition (Vick, 1988). Trees and salt marsh plants are preserved by the rapid deposition of the estuarine muds. If the plants had not been buried by rapid sediment deposition, decomposition and incorporation into a gradational contact should have occurred. To be preserved, the salt marsh plants must have been covered within a few months. The trees would take longer to decompose, but the presence of bark layers on the lower sections indicates that the sediments were accumulating rapidly. In some sites, the sediment layers are from 2 to 10 cm, and do not contain evidence of bioturbation. The lack of bioturbation indicates rapid deposition. In other areas, the estuarine mud contains shells, which could indicate depths below MHW. Occasional sand layers containing detrital material indicate storm events. The estuarine muds

found indicate accretion within the intertidal zone. When surface reaches approximately MHW, salt-tolerant plants colonize intertidal mud flats, and begin the formation of new salt-marsh horizons. The estuarine muds grade upward into the buried peat horizons.

Stratigraphic correlations are limited to small regions of the bay, because surfaces cannot be correlated over long distances. Additionally, the correlations of the horizons are limited by the accuracy of radiocarbon dating. Because of the limited number of dates and the precision of the analyses, inaccurate correlations may still exist.

Late Holocene Paleoseismicity in Humboldt Bay

The Holocene paleoseismic record consists of buried peat horizons with 38 radiocarbon dates, and 10 radiocarbon dates from other paleoseismic investigations. Statistical relations in this data set were investigated using graphical methods described by Montgomery and Peck (1982). The variables investigated by regression analysis were *calibrated radiocarbon age (calibrated age)*, *depth*, *number of buried horizon at site (horizon number)*, and *thickness of sediment between horizons (thickness)*. Although a recurrence interval, and age ranges of the events can be determined from this data set, one cannot claim a high statistical confidence for the age ranges for each event because of the overlap of the calibrated radiocarbon ages.

Regression of all data

There is a high correlation between *depth* and *calibrated age*, and between *depth* and *horizon number*. Regressions for both *depth* and *calibrated age* are presented in Table 1, and a plot of *calibrated age* vs. *depth* is shown in figure 20. The rate of subsidence from the regressions of *depth* vs. *calibrated age*, and *calibrated age* vs. *depth* (Figure 20) is 1.4 mm/yr and 1.7 mm/yr, respectively. Multiple regression analysis using the *calibrated age* and *depth* as the dependent variables,

Dependent Variable: Depth

Adjusted R ²	F-ratio	Variables	Variable Coefficient	Standard Error of the Coefficient	T-Ratio
77.3	137	Constant	0.7270	0.213	3.41
		Calibrated age	0.001425	0.0001	11.7
77.6	70.3	Constant	0.5419	0.2584	2.10
		Calibrated age	0.001228	0.0002	6.18
		Horizon	0.2316	0.1853	1.25
84.3	100	Constant	0.7823	0.2453	3.19
		Calibrated age	0.001501	0.0001	14.1
		Sed Thickness	-0.2209	0.16989	-1.30
83.9	65.3	Constant	0.6930	0.3347	2.07
		Calibrated age	0.001434	0.0002	7.16
		Horizon	0.7030	0.1837	0.398
		Sed Thickness	-0.1868	0.1920	-0.973
81.9	46.3	Constant	0.7142	0.4106	1.74
		Calibrated age	0.001440	0.0001	12.3
		is ES	-0.5686	0.4344	-1.31
		is MRS	0.007453	0.4351	0.017
		is SB	0.5366	0.4337	1.24

Dependent Variable: Calibrated age

Adjusted R ²	F-ratio	Variables	Variable Coefficient	Standard Error of the Coefficient	T-Ratio
77.3	137	Constant	-91.7	149.6	-0.613
		Depth	546.2	46.7	11.7
80.6	84	Constant	262.1	151.4	-1.73
		Depth	408.0	66.1	6.18
		Horizon	274.8	99.4	2.76
84.7	104	Constant	-278.6	164.5	-1.69
		Depth	566.2	40.2	14.1
		Sed thickness	171.1	102.7	1.67
87.9	90.4	Constant	-540.0	168.2	-3.21
		Depth	419.1	58.5	7.16
		Sed thickness	257.6	95.5	2.7
		Horizon	277.5	87.4	3.17
81.1	35.3	Constant	-89.5	598.2	-0.15
		Depth	559.7	52.3	10.7
		is ES	342.2	543.7	0.629
		is MRS	-158.1	559.7	-0.283
		is SB	-291.4	524.2	-0.556

Table 1. Stepwise regression analysis results.

Variable coefficient for Depth as dependent variable is meters/year.

Variable coefficient for Calibrated age as dependent variable is

years/meter. Depth- depth below modern surface. Calibrated age-

Calibrated radiocarbon age. Horizon- number of buried horizon at site.

Sed Thickness- cycle thickness, top of lower layer to top of layer. is ES,

is MRS, is SB- site variables for Eureka Slough (ES), Mad River Slough (MRS), and South Bay (SB).

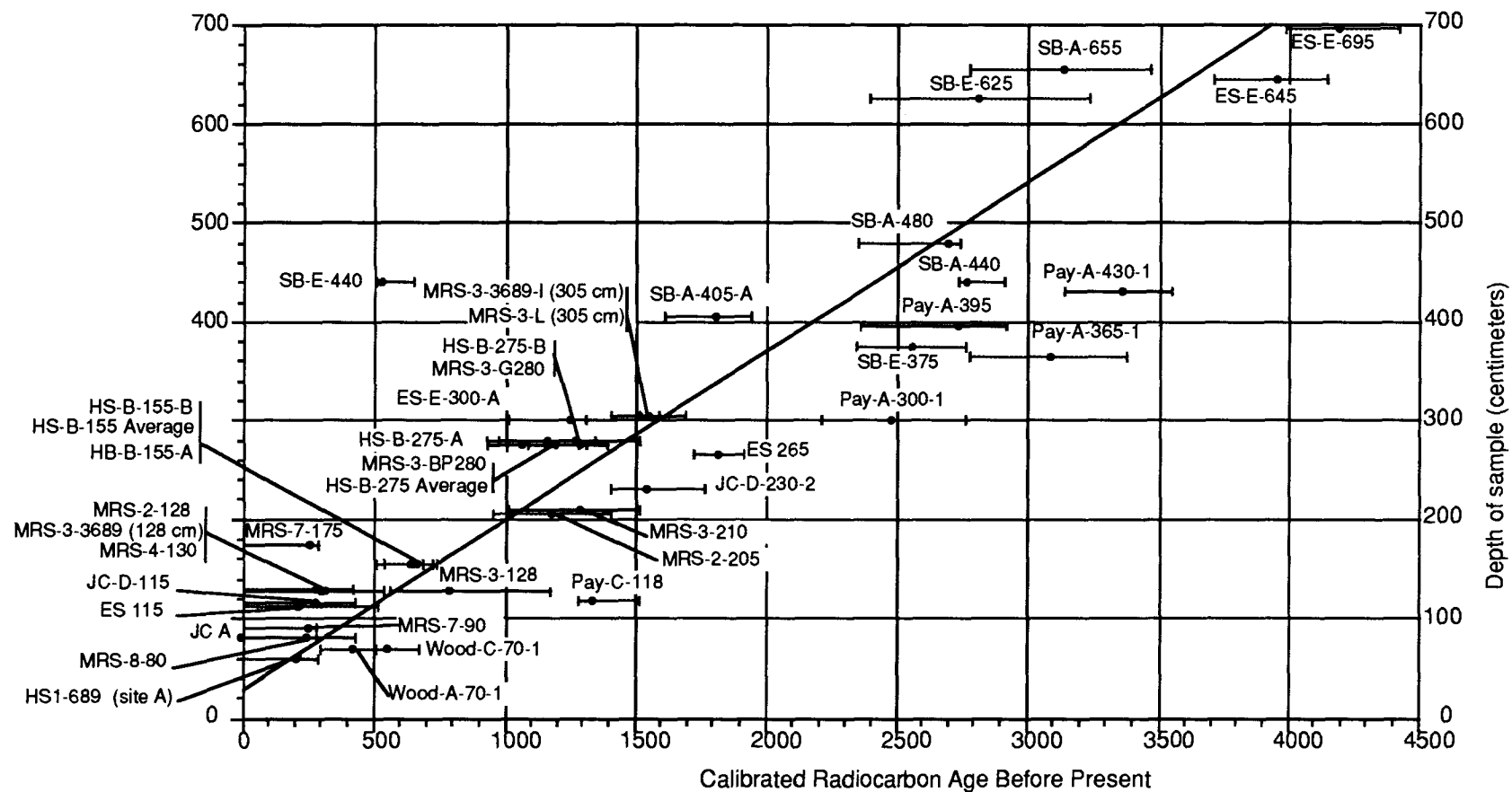


Figure 20. Calibrated age vs. depth for all samples. Error bars are two standard deviations for the calibrated age ranges. The regression line is for calibrated age as the dependent variable. See Table 1 for the regression coefficients

and *depth*, *calibrated age*, *thickness*, and the *horizon number* as independent variables show an equivalent range of 1.2 to 1.5 mm/yr for *depth* as the independent variable, and 1.6 to 2.4 mm/yr for *calibrated age* as the independent variable. The calculated rate may be explained by either eustatic submergence due to sea-level rise and/or tectonic subsidence and compaction.

Regression of data by site

All ages from the Humboldt Bay stratigraphy in one regression do not represent all the diversity of the individual sites. In order to investigate this, the data was further broken into groups by site (Table 2). Multiple linear regressions for each site are not applicable because the number of degrees of freedom falls below one for most sites. Simple linear regression of *calibrated age* vs. *depth*, was done for the four sites with the most dates. Two have confidence intervals for the intercept which includes zero at the 95% confidence interval.

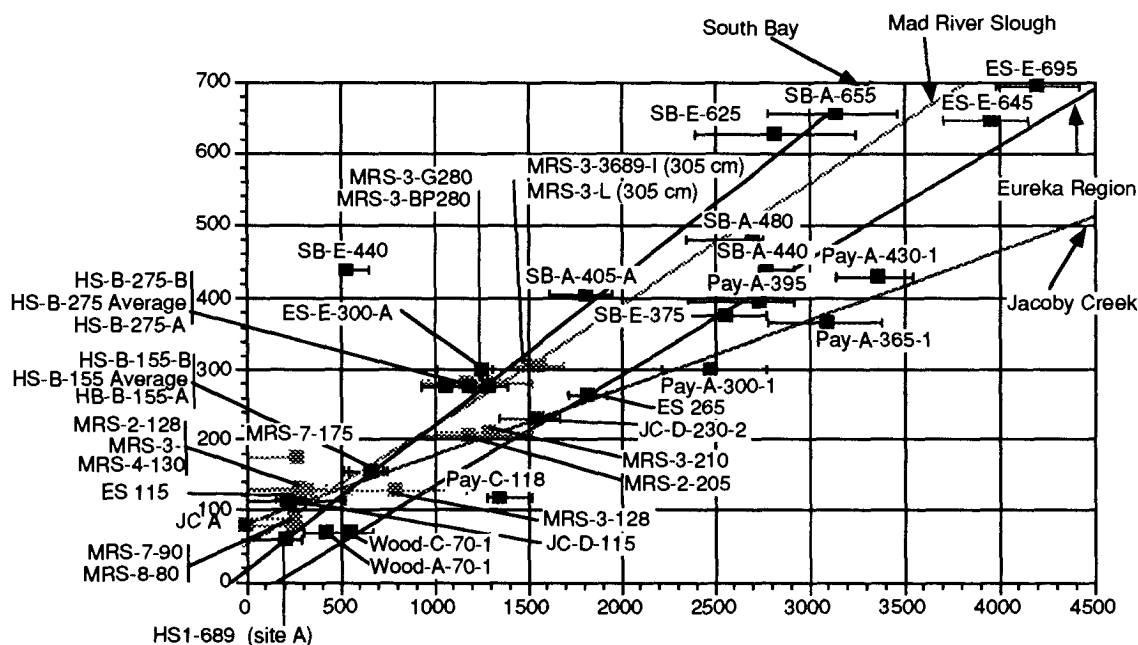
The individual site regressions have different characteristics depending upon which independent variable is used (Figure 21). If *calibrated age* is used, then the coefficients of *depth* are highly variable. If *depth* is used, then the coefficients of *calibrated age* are all approximately equal for Mad River Slough, Eureka Slough, and South Bay. This indicates that the *depth* is the dependent variable, and that the intercepts might be related to variations in the site elevations.

The South Bay sedimentation rate is between 1.4 and 2.2 mm/yr (Table 2, Figure 21 A). This rate is less than the long term rate subsidence rate of 2.4 from the borehole stratigraphy (Woodward-Clyde Consultants, 1980).

Paleoseismic Ranges

The stratigraphy and radiocarbon ages suggest up to eight events over the past 3000 years for the Humboldt Bay region, and up to ten for the past 4300 years (Figure 22). The number of events is comparable with the estimate of 13 events since

A)



B)

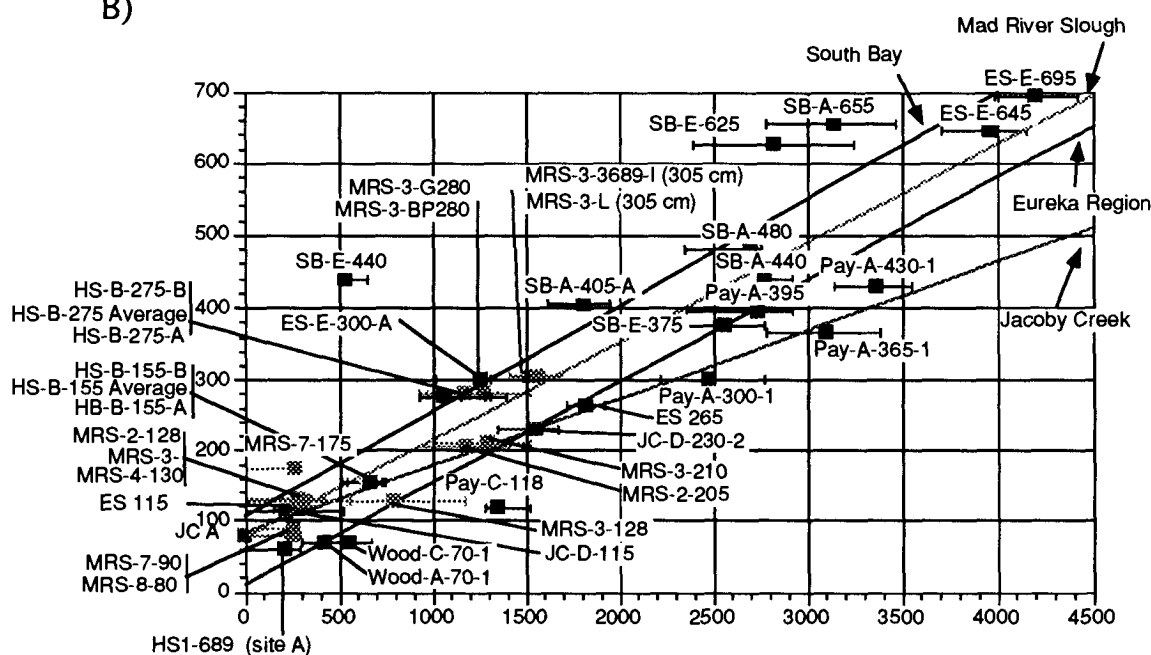


Figure 21. Least squares regression lines for selected regions.

A) regressions for calibrated age vs depth. B) regressions for depth vs calibrated age. Error bars represent the two standard deviation range for the sample. See Table 2 for regression coefficients

Dependent Variable: Depth Independent Variable: Calibrated Age

Site	Adjusted R ²	Number of Cases	Variable	Variable Coefficient	Standard Error of the Coefficient	T-Ratio
All sites	77.3	41	Constant Calibrated age	0.727 0.001425	0.001 0.213	11.7 3.41
ES	85.9	13	Constant Calibrated age	0.129 0.001503	0.3942 0.0002	0.328 8.62
MRS	74.9	13	Constant Calibrated age	0.937 0.001172	0.1925 0.0002	4.87 6.07
SB	66.9	12	Constant Calibrated age	1.096 0.001534	0.6059 0.0003	1.81 4.82
JC	95.9	3	Constant Calibrated age	0.8612 0.000814	0.1138 0.0001	7.57 6.91

Dependent Variable: Calibrated age Independent Variable: Depth

Site	Adjusted R ²	Number of Cases	Variable	Variable Coefficient	Standard Error of the Coefficient	T-Ratio
All sites	77.3	41	Constant Depth	-91.7 546.2	149.6 46.7	-0.61 11.7
ES	85.9	13	Constant Depth	167.6 579.5	240.7 67.24	0.70 8.62
MRS	72.5	13	Constant Depth	-289.0 617.5	276.2 124.2	-1.05 4.97
SB	66.9	12	Constant Depth	-5.854 455.9	380.6 94.5	-0.015 4.82
JC	95.9	3	Constant Depth	1023.6 1203.8	262.2 174.2	-3.90 6.91

Table 2. Regression analyses for individual sites

Depth- depth below modern surface.

Calibrated age- Calibrated radiocarbon age.

ES, iMRS, SB, JC - site variables for Eureka Slough (ES), Mad River Slough (MRS), South Bay (SB), and Jacoby Creek (JC).

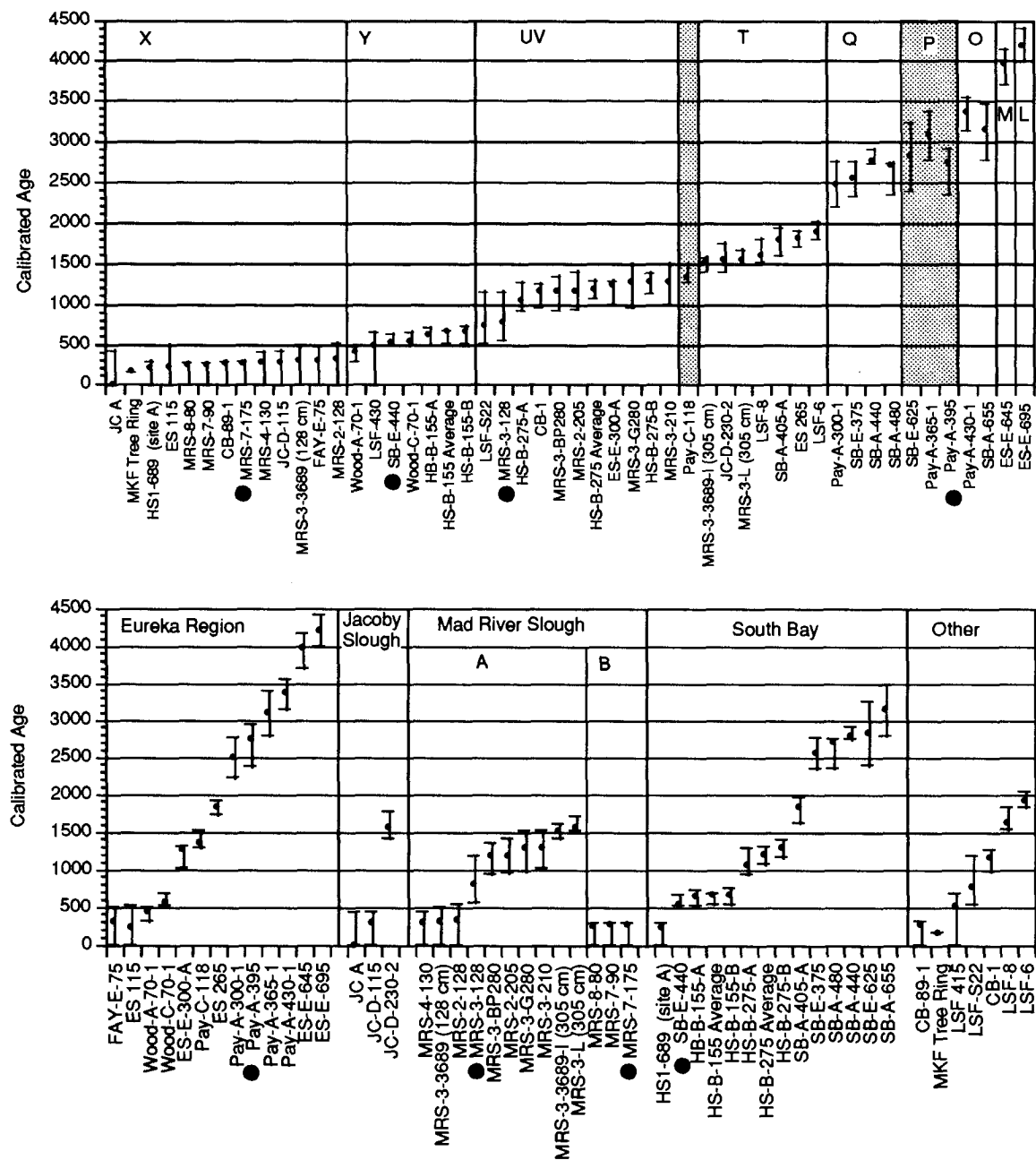


Figure 22. Calibrated radiocarbon ages grouped by age and by region. Events labeled on upper plot are chosen based on the stratigraphic evidence. They can also be distinguished by the distinct jumps in the trend of the individual groups of ages. UV is an event pair which cannot be distinguished using radiocarbon ages. Bullets (●) indicate problem ages. See text and appendix 1 for descriptions.

the Mazama ash (6340 YBP) from the turbidites in the Cascadia channel (Adams, 1990). The following is description of possible paleoseismic events for the southern end of the Cascadia Subduction zone.

Event Y

Event Y, which is prevalent in the stratigraphic record, has limiting ages of 1810 AD and the last event on the Little Salmon Fault (415 RCYBP; Carver and others, 1989). The preferred age is 1742 AD from a tree buried by a landslide along the Little Salmon Fault (Jacoby and others, 1989). Event Y is regional in nature, being found in all areas covered by this study.

Event X

Event X is constrained by events on the Little Salmon fault. There have been two events on the Little Salmon fault in the last 1000 years: one at less than 415 RCYBP, and one at 815 RCYBP (Carver, and others, 1989). At present, no physical stratigraphic evidence for event X has been found at Mad River slough. This event can be identified in the stratigraphy of South Bay. The age and stratigraphic separation of three horizons, one at 60 cm (HS1-689, 140 RCYBP), a second at 155 cm (HS-A-155-Ave, 660 RCYBP), the third at 275 cm (HS-B-275, 1160 RCYBP), are an indication that the ages that fall into this zone are not an artifact of the calibration from 450 RCYBP to 800 RCYBP. Daby island contains one horizon with ages that fall in this range. A second dune soil from Clam beach must also fall between 200 RCYBP and 1070 RCYBP (Carver, and others, 1989). Although this event is not widely preserved as a salt-marsh or lowland horizon, it can be supported by other evidence.

Event U and Event V

Events U and V can be distinguish by the stratigraphy of Mad River slough, but are not distinct events based on radiocarbon ages. Ages from other areas correlate

with this time frame, but they cannot be properly placed into either event category. This tightly space group of distinct events is bracketed by movement on the Little Salmon fault (LSF 860; Carver, 1989), and the stratigraphy at MRS-3 (MRS-3-210 is stratigraphically above MRS-3-G285).

Event T

Event T is separated stratigraphically from event U in Mad River slough. This is the lowest horizon found in the slough, and yields ages around 1700 RCYBP. Evidence for event T is found in the Eureka slough and South bay regions as well. Fault slip dated at 1970 RCYBP on the Little Salmon Fault is the lower age limit of this event , while 1730 RCYBP is the upper age limit (Clarke and Carver, 1992). The upper limit includes the data in Mad River slough, while the lower limit includes the ages in Eureka slough, and South Bay. The ages in Eureka slough and South Bay are shifted by about 150 years, but there is no strong evidence to suggest that they represent a separate event.

Event Q

Event Q is represented South Bay, and horizons in First slough. In South Bay, a horizon dated at 1850 RCYBP overlies the horizon dated at 2480 to 2670 RCYBP. The age constraints of these horizons are poor. The presence of the horizon in First slough, helps support event Q. The horizon representing Q is found between 360 and 425 cm is extensive, and is found at near every site.

Events P and O

Events P and O are supported by the stratigraphy in Eureka and South Bay. The deep stratigraphy of the South Bay is poorly documented, and has problems with age control, but it appears that there is a comparable number of horizons/events in both SB-E and SB-A. There is evidence for two events in South Bay and one event in First Slough following Event Q. For South Bay, an undated horizon lies between Event Q,

and the lower horizon dated at 2900 RCYBP. For First slough, inverted radiocarbon ages leads to inconclusive evidence. The upper horizon is PAY-300, and the base of this peat is PAY-365, but PAY-395 dated younger than this horizon. Stratigraphic evidence suggests that these are separate horizons. Pay-395 is a clean horizon, and is separate from PAY-365 (Figure 15). PAY-430 may be separate from PAY-395, but if the date on PAY-A-365 is correct, then PAY-395 and PAY-430 could be the same horizon, or could be horizons relating to event P and event O.

Event M and L

These are the oldest horizons in First slough. The lowest horizon is a fresh water peat, which is covered by a saltwater peat. This could represent sea-level rise, the breaking of a berm, or coseismic subsidence. This salt-marsh horizon has a clean upper horizon indicating rapid submergence. Two out of three cores to this depth penetrated this sequence. The third penetrated estuarine sediments. I interpret the freshwater-marsh/saltwater-marsh/estuarine sediments to represent two coseismic subsidence events.

Recurrence interval

The concept of a characteristic earthquake with an estimated recurrence interval and magnitude is not applicable to the southern end of the Cascadia Subduction Zone based on our record of paleoseismicity for the past 4300 years. The period between events ranges from 100 years to 900 years with an average of 426 years (Table 3). It would be difficult to develop a probability model for this region based on these ten events.

Proposed cycle

The repeated cycles of buried salt marsh deposits in Humboldt Bay are created by episodic coseismic subsidence. Repeated cycles of coseismic subsidence, post seismic rebound, sedimentation, and interseismic rebound formed the stratigraphy

Event	Estimated Age interval	Estimated Age	Estimated Years between events
Y	0-300	216	
X	500-800	650	434
V	900-1250	1100	450
U	1050-1350	1300	100
T	1600-1900	1600	300
Q	2450-2600	2500	900
P	2800-3400	2900	350
O	3200-3400	3300	400
M	3700-3900	3900	600
L	4000-4300	4200	300

Events	Reccurence Interval	Standard Deviation
X to T	321	162
X to O	419	243
X to L	426	224

Table 3. Recurrence interval calculation

found in much of Humboldt Bay. During an event, the land in the synclines subsided submerging the marsh horizons and some of the wetlands into the intertidal environment. Mud on the intertidal flat is suspended during the event, and some is deposited onto the submerged marsh horizons. During the interseismic period, intertidal muds are deposited onto the submerged horizons, and the horizons accrete sediments. Salt marsh plants colonize the intertidal sediments, as the intertidal flats reach MHW, and trap more sediment (Figure 23A). Salt-marsh horizons grow inward from the bay margins as the intertidal flats accrete. Peat deposits are formed near MHW, perhaps as soon as a few decades after the bay margins achieve stability as indicated from the stratigraphy of events U, and V in the Mad River slough. These two horizons are indistinguishable using radiocarbon dating, but are separated by 70 cm of sediment. Assuming a conservative 100 year time interval between events U and V, this stratigraphy suggests an initial sedimentation rate much greater than the average 7 mm/yr sedimentation rate. High rates of sedimentation in the initial stages of marsh development are consistent with modeling of marsh growth by Allen (1990). Because sediment accumulation rates are in part a function of water depth, this rapid rate may be a combination of sedimentation and interseismic uplift. Once the marsh horizons approach maturity, the sedimentation accumulation rate drops significantly (Allen, 1990). The time between events preserved the high rates of sedimentation. A flood event producing large amount of sediment may have expedited the recovery, however, there is no information in the stratigraphic record to support this contention. Apparently, the recovery of the marsh around the bay is possible within a few decades of an event.

During the interseismic period, some submerged areas emerge above the intertidal zone due to interseismic uplift and/or sediment accumulation. Such areas will contain both salt-marsh/estuarine and freshwater environments in the same

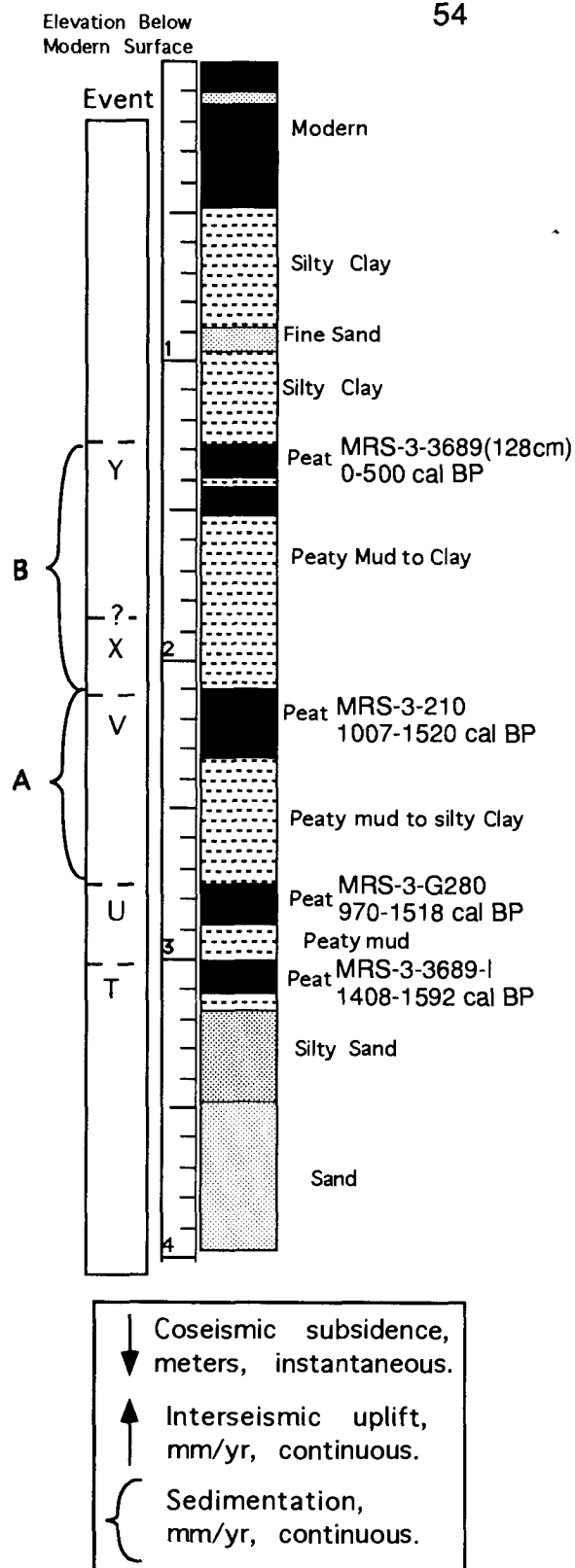
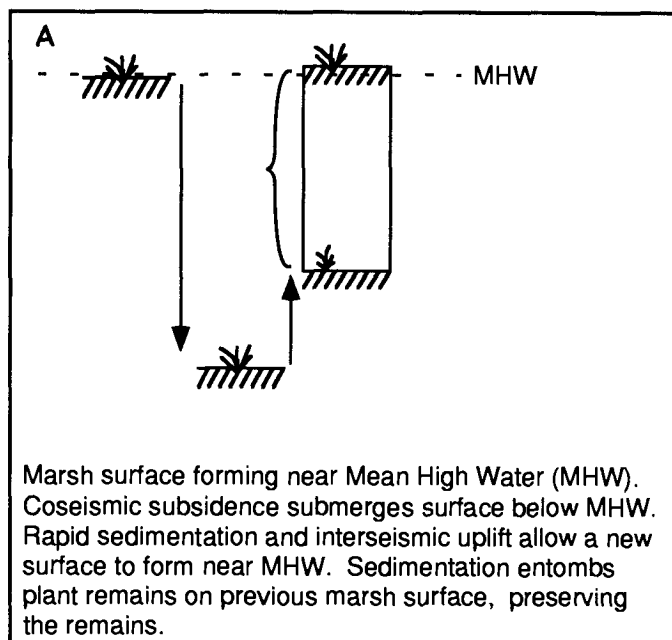
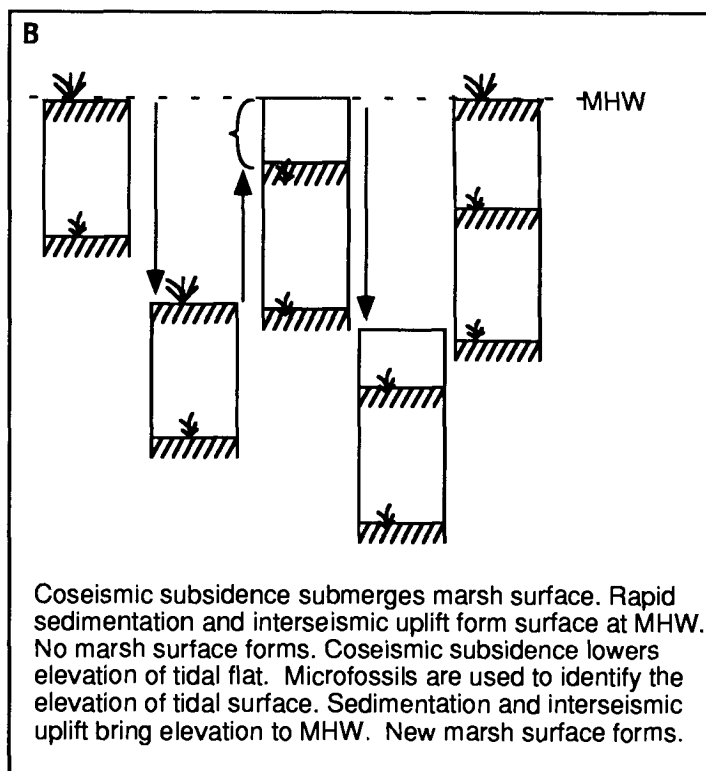


Figure 23. Scenarios for the formation of the Stratigraphy found in Humboldt Bay. Sequence A is the ideal occurrence. Occurrences are shown on a stratigraphic column from Mad River Slough (MRS-3).

sequence. Examples are the freshwater peat horizons in First slough, and spruce stumps in the Mad River slough. These sites have emerged from intertidal environments to environments above the tidal zone during the interseismic period. Because such sites require greater subsidence to submerge them into the intertidal zone during an event, they may not record smaller subsidence events.

The pattern of subsidence is not identical for every earthquake. Regions near Eureka slough may not have been submerged, and could have emerged, during the event Y, but were submerged during the event T. The Mad River slough may not record event X. These data may indicate that there is no characteristic location of the transition between probable coseismic uplift occurring on the regional marine terraces and coseismic subsidence for the Humboldt Bay region. This is probably due to the complex structure of the fold and thrust belt along the coast.

Salt-marsh morphology can determine the presence or absence of a horizon. If a salt-marsh never formed over the site, then no record of this event would be preserved in the stratigraphy (Figure 23B). Other reasons for missing horizons include stream/tidal channels which erode the previous stratigraphy. Either would explain the lack of some horizons in the some sections. All the above explanations are plausible, and probably do occur within the stratigraphy of Humboldt Bay.

Summary of Humboldt Bay Paleoseismicity and Comparison to the Regional Paleoseismicity

The paleoseismic evidence documented in Humboldt Bay is seen as several distinct age groupings when the ages are plotted on a histogram (Figure 24). It is important to note that it is hard to distinguish radiocarbon age for the period from 0 to 300 years BP, and that the period around 1100 to 1300 years RCYBP contains an event pair, U and V (referred herein as U-V), that cannot be separated using

radiocarbon dating. Because of the lack of ability to distinguish these buried peat horizons using radiocarbon dating, these events are grouped as one event in any analysis of the ages. Using the stratigraphy and the radiocarbon dating, ten events (Y, X, U-V, T, Q, O, P, M, and L) are identified. Not all events are identified at every Humboldt Bay site.

The record from the stratigraphy is longer than the paleoseismic record from the Little Salmon fault. Five events for the past 2000 years are supported by the stratigraphy, and three events documented by the paleoseismic investigations along the Little Salmon fault (Carver and others, 1985). Dates from the Little Salmon fault studies are important because they help constrain the ages of events in the Southern end of the Cascadia subduction zone. The Little Salmon fault has events with limiting ages of 415, 860, and 1730 RCYBP correlate well with the Humboldt Bay stratigraphy (Figure 21; Carver and others, 1985).

The separation of the events Y, X, and U-V are difficult without proper exposures. The separation and Y from X, and X from U-V occurs only in the South Bay stratigraphy. Additional support for Event X is from the stratigraphy of an uplifted terrace at Clam Beach which provides two events which bracket a third event. A sequence of two soils in a dune sequence overlying a raised beach terrace represents three distinct events (Carver, and others, 1989). A piece of driftwood in the terrace has an age of 1070 ± 30 RCYBP (MK Terr Drift). The latest soil has a tree buried in the dune with an age of 140 ± 30 RCYBP (MK Tree in Dune). If the scenario on the dune formation is correct, then evidence for event X is present, in at least two locations, one within Humboldt Bay, and one along the Mad River fault zone.

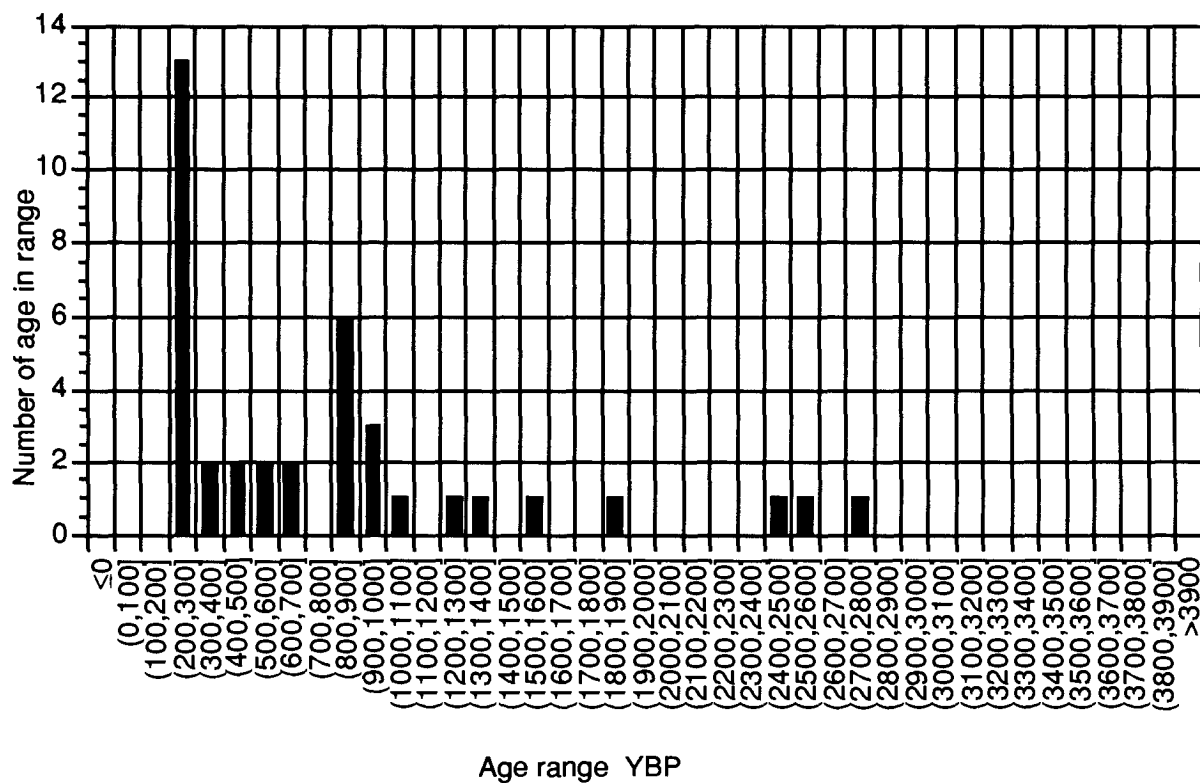


Figure 24. Histogram of calibrated ages.

Note the several apparent groupings which correlate with the paleoseismic events.

Conclusions

- 1) The stratigraphy of Humboldt Bay indicates that the bay is subsiding in discrete submergence events. Each submergence event represents a subsidence due to a Cascadia subduction zone earthquake.
- 2) The late Holocene stratigraphy preserves sequences that represent eight events during the past 3500 years, and ten events during the past 4500 years. The most recent event occurred about 300 years ago.
- 3) Long term subsidence within the synclines helps preserve the stratigraphy. The recent subsidence rates are not significantly different from the rates during the past 700,000 years.
- 4) Similar subsidence rates in different structures could indicate a regional subsidence. Further modeling of the structure of the region is needed.

References

- Acharya, H., 1985. Comment on "Seismic potential associated with subduction in the northwestern United States" By T.H. Heaton and H. Kanamori, *Bulletin of Seismological Society of America* 75(3): 889-890.
- Adams, J., 1984. Active deformation of the Pacific Northwest continental margin, *Tectonics* 3(4): 449-472.
- Adams, J., 1990. Paleoseismicity of the Cascadia subduction zone: evidence from turbidites off the Oregon-Washington margin, *Tectonics* 9: 569-583.
- Allen, J.R.L., 1990. Constraints on the measurement of sea-level movements from salt-marsh accretion rates, *Journal of Geologic Society of London* 147: 5-7.
- Ando, M., and Balazs, E.I., 1979. Geodetic evidence for aseismic subduction of the Juan de Fuca plate, *Journal of Geophysical Research* 84(B6): 3023-3028.
- Atwater, B.F., 1987. Evidence for great Holocene earthquakes along the outer coast of Washington State, *Science* 236: 942-944.
- Atwater, B.F. 1992. Geologic evidence for earthquakes during the past 2000 years along the Copalis river, southern coastal Washington, *Journal of Geophysical Research* 97:1901-1919.
- Atwater, B.F., Hedel, C.W. and Helley, E.J., 1977. Late Quaternary depositional history, Holocene sea level changes and vertical crustal movement, Southern San Francisco Bay, California, USGS professional paper 1014, 15 pp.
- Atwater, B.F., and Belknap, D.F., 1980. Tidal-wetland deposits of the Sacramento-San Joaquin delta, California. *in* Quaternary Depositional Environments of the Pacific Coast. Pacific Coast Paleogeography Symposium 4, Field and others, eds., p. 89-103.
- Atwater, B.F., West, D.O. and McCrumb, D.R., 1988. Coastline uplift in Oregon and Washington and the nature of Cascadia subduction-zone tectonics discussion and reply, *Geology* 16(10): 952-953.
- Atwater, B.F., Jimenez Nunez, Hector, and Vitta-Finzi, Claudio, in press. Net late Holocene emergence despite earthquake induced submergence, south central Chile, submitted to *Quaternary International*.
- Bartasch-Winkler, S., Ovenshine, A.T. and Kachadoorian, R., 1983. Holocene history of the estuarine area surrounding Portage, Alaska as recorded in a 93 m core, *Canadian Journal of Earth Sciences* 20: 802-820.

- Behre, K. E., 1986. Analysis of botanical macro remains *in* Sea-Level research: a manual for the collection and evaluation of data, van de Plassche, O., ed., Amsterdam, Netherlands, Free Univ. p. 413-433.
- Belnap, D.F. and Kraft, J.C., 1977. Holocene relative sea-level changes and coastal stratigraphic units on the northwest flank of the Baltimore Canyon Trough geosyncline, *Journal of Sedimentary Petrology* 34(3): 599-603.
- Bloom, A.L., 1964. Peat accumulation and compaction in a Connecticut coastal marsh, *Journal of Sedimentary Petrology* 34: 225-259.
- Borgeld, J., 1985. Holocene stratigraphy and sedimentation of the northern California continental shelf. PhD thesis University of Washington. 177 pp.
- Burke, R.M. and Carver, G.A., 1989. The Degree of Soil Development from Buried Soils Formed in Fault-Generated Colluviums Reflect Interseismic Time, Northern California, *Geological Society of America Abstracts with Programs* 21(5): 91.
- Carver, G.A. 1987. Late Cenozoic tectonics of the Eel river basin, coastal northern California. *in* Tectonics, Sedimentation and Evolution of the Eel River and Associated Coastal Basins of Northern California. San Joaquin Geologic Society Misc Pub No. 37, Schymiczek, H. and Suchsland, R., ed., Bakersfeild, California, p. 61-72
- Carver, G.A. 1989. Paleoseismicity of the southern part of the Cascadia subduction zone, *Seismological Research Letters* 60(1): 1.
- Carver, G.A., Burke, R.M., and Kelsey, H.M., 1985. Quaternary Deformation studies in the region of the Mendocino Triple Junction, *in* National Earthquake Hazards Reduction Program, Summaries of Technical reports XXI. p. 58-62.
- Carver, G.A., Vick, G.S., and Burke, R.M., 1989. Holocene Paleoseismicity of the Gorda Segment of the Cascadia Subduction Zone, *Geological Society of America Abstracts with Programs* 21(5): 64.
- Clark, J., Farrel, W.E. and Peltier, W.R., 1978. Global changes in postglacial sea level: A numerical calculation, *Quaternary Research* 9: 265-287.
- Clarke, S.H. 1992. Geology of the Eel River basin, and adjacent region—implications for late Cenozoic tectonics of the northwestern California continental margin and Mendocino triple junction, *American Association of Petroleum Geologists Bulletin* 76(2): 199-224.

- Clarke, S.H. and Carver, G.A., 1989. Onshore-Offshore Characteristics and Seismic Potential of Structures along the Gorda Segment of the Cascadia Subduction Zone, Geological Society of America Abstracts with Programs 21(5): 66.
- Clarke, S.H. and Carver, G.A., 1992. Late Holocene tectonics and paleoseismicity, southern Cascadia Subduction Zone, Science 255: 188-192.
- Darienzo, M.E. and Peterson, C.D., 1990. Episodic tectonic subsidence of late Holocene Salt Marshes, northern Oregon coast, U.S.A, Tectonics 9(1): 1-22.
- Eicher, A.L., 1987. Salt marsh vascular plant distribution in relation to tidal elevation, Humboldt Bay, California. Masters thesis Humboldt State University, Arcata, California. 78 p.
- Fitch, T.J. and Scholtz, C.H., 1971. Mechanisms of underthrusting in southwest Japan: a model of convergent plate interactions, Journal of Geophysical Research 76: 7260-7292.
- Heaton, T.H. and Kanamori, H., 1984. Seismic Potential associated with subduction earthquakes in the northwestern United States, Bulletin of Seismological Society of America 74(3): 933-941.
- Heaton, T.H. and Snavely, P.D.J., 1985. Possible Tsunami along the Northwestern coast of the United States inferred from Indian traditions, Bulletin of Seismological Society of America 75(5): 1455-1460.
- Hicks, S.D., 1978. An average geopotential sea level series for the United States, Journal of Geophysical Research 83(3): 1377-1379.
- Jacoby, G.C., Sheppard, P.R. and Carver, G.A. 1989. Dating of earthquake -induced landslides using tree-ring analysis, Geological Society of America Abstracts with Programs 21(5): 97.
- Kelsey, H.M. and Carver, G.A., 1988. Late Neogene and Quaternary tectonics associated with the northward growth of the San Andreas transform fault, northern California, Journal of Geophysical Research 93: 4797-4819.
- Lisowski, M., Savage, J.C. and Prescott, W.H., 1991. The Velocity Field along the San Andreas Fault in California, Geological Society of America Abstracts with Programs 23(5): A313.
- Montgomery, D.C., and Peck, E.A. 1982, Introduction to Linear Regression Analysis: Wiley and Sons, New York, 504 p.
- Muir-Wood, R., 1989. The November 7th 1837 earthquake in southern Chile, Seismological Research Letters 60(1):8.

- Nelson, A.R. 1992. Discordant ^{14}C ages limit correlations of Holocene tidal-marsh soils in the Cascadia Subduction Zone, southern Oregon coast, Quaternary Research, July 1992: in press.
- Nelson, A.R. and Personius, S.F., in press. The potential for great earthquakes in Oregon and Washington—An Overview of recent geologic studies and their bearing on segmentation of Holocene ruptures, central Cascadia subduction zone. in *Assessing and reducing earthquake hazards in the Pacific Northwest*, Rogers, A.M. and others, eds. US Geological Survey Professional paper 1560.
- Nishimura, C., Wilson, D.S. and Hey, R.N., 1984. Pole of rotation analysis of present-day Juan de Fuca motion, Journal of Geophysical Research 89: 10,283-10,290.
- NOAA, 1985. National estuarine inventory data atlas, Humboldt Bay, California. Strategic Assessment Branch, Ocean Assessments Division, Office of Oceanography and Marine Assessment, National Ocean Service, National Oceanic and Atmospheric. Rockville, Md., United States. National Oceanic and Atmospheric Administration.
- Ogle, B.A., 1953. Geology of Eel River Valley area, Humboldt County, California, Calif. Div Mines Bulletin 164. 128 p.
- Plafker, G., 1972. Alaskan earthquake of 1964 and Chilean earthquake of 1960: implications for arc tectonics, Journal of Geophysical Research 77(5): 901-925.
- Plafker, G.P. and Savage, J.C., 1970. Mechanism of the Chilean earthquakes of May 21 and 22, 1960, Geological Society of America Bulletin 81: 1001-1030.
- Redfield, A.C., 1967. The ontogeny of a salt marsh estuary. in *Estuaries*, Luaff, G.H., ed., Am. Assoc. Adv. Sci. Pub. p.108-114.
- Reilinger, R. and Adams, J., 1982. Geodetic evidence for active landward tilting of the Oregon and Washington costal ranges, Geophysical Research Letters 9(4): 401-403.
- Riddihough, R.P., 1980. Recent motions of the Jaun de Fuca plate system, Earth and Planetary Science Letters 51: 163-170.
- Riddihough, R.R., 1984. Recent movements of the Juan de Fuca plate system, Journal of Geophysical Research 89: 6980-6994.
- Rogers, G.C., 1988. An assessment of the megathrust earthquake potential of the Cascadia subduction zone, Canadian Journal of Earth Sciences 25(6): 844-852.

- Savage, J.C., Lisowski, M. and Prescott, W.H., 1981. Geodetic strain measurements in Washington, *Journal of Geophysical Research* 86: 4929-4940.
- Shapiro and Associates, 1980. Final Humboldt Bay wetland review and baylands analysis, Submitted to Army Corps of Engineers, San Francisco; Shapiro and Associates, Seattle, WA. 3 volumes.
- Shivelle, C., Carver, G.A. and Valentine, D.W., 1991. Foraminiferid stratigraphy as evidence for great earthquakes on the Cascadia Subduction zone in northern California, *GSA Abstracts With Programs* 23(2): A97.
- Stoddard, P.R., 1987. A kinematic model for the evolution of the Gorda plate, *Journal of Geophysical Research* 92(B11): 11524-11532.
- Stuvier, M. and Reimer, P.J., 1986. A computer program for radiocarbon age calibration, *Radiocarbon* 28: 1022-1030.
- Thompson, R.W., 1971. Recent sediments of Humboldt Bay, Eureka, California, *Petroleum Research Foundation* 789-82, 29 pp.
- U.S. Army Corps of Engineers, 1911. Humboldt Bay, California Survey 1911, Map 9 sheets. U.S. Army Corps of Engineers.
- U.S. Army Corps of Engineers, 1979. Reconnaissance Report: Humboldt Harbor and Bay, Review of Reports, Army Corps of Engineers, San Francisco.
- van de Plassche, O. 1980. Compaction and other sources of error in obtaining sea-level data—some results and consequences, *Eiszeitalter und Gegenwart* 30: 171-181.
- Vick, G., 1988. Late Holocene paleoseismicity and relative vertical crustal movements, Mad River Slough, Humboldt Bay, California. Humboldt State University. 88 p.
- Vick, G. and Carver, G.A., 1988. Late Holocene Paleoseismicity, northern Humboldt Bay, California, *Geological Society of America Abstracts with Programs* 20(7): A232.
- West, D.O. and McCrumb, D.R., 1988. Coastline uplift in Oregon and Washington and the nature of Cascadia subduction-zone tectonics, *Geology* 16(2): 169-172.
- Wilson, D., 1989. Deformation of the so-called Gorda plate, *Journal of Geophysical Research* 94(B5): 3065-3075.
- Woodward-Clyde Consultants, 1980. Evaluation of the potential for resolving the geologic and seismic issues at the Humboldt Bay Power Plant Unit No. 3, Woodward-Clyde Consultants, Walnut Creek, California.

Appendix 1: Radiocarbon Dating

The samples were collected from tidal exposures and multiple cores. They were cleaned of apparent modern roots, and macro-organic debris by hand. The samples were then wet sieved through a 0.5 mm (34) or 0.005 mm (265) mesh screens using distilled water. All organic remains were either air dried or dried in an oven at $\approx 40^{\circ}$ C.

Hand picking of the sample worked best for samples containing little sediment. If there was sediment, wet sieving was used to improve the recovery of organic material from the sample. Hand picking and the wet sieving left little sediment in the sample sent to the laboratory for radiocarbon analysis. This sediment is not believed to contribute to any error in the dating.

The primary lab used during this study was the Quaternary Research Laboratory University of Washington. This lab uses proportional gas counting. Several samples were run at Beta Analytic, which uses liquid scintillation counting. Samples from this and other studies are presented in Table A2.

The Sample ages may vary for a variety of reasons. Most marsh samples would be expected to date older than the actual age because incorporates carbon from materials of different ages (van de Plassche, 1980; Nelson, 1992). Dates from woody marsh remains, such as *Grindellia stricta* is expected to provide a more accurate date because it incorporates ^{14}C only when it is alive. Marsh samples may also vary if carbon from the marine source is incorporated into the plant. It is assumed that the marsh plants accumulated carbon only from the atmosphere, and therefore no calibration with the marine record is needed. ^{13}C ratios and corrections were done on the samples run at University of Washington.

Calibration of radiocarbon dates was done using a calibration program from the Quaternary Research Center laboratory (Stuvier and Reimer, 1986). Calibrated

ages are reported a one and two standard deviations from the laboratory date. No laboratory error is included in the calibrated ages. Several samples were averaged to estimate the mean age of a set of samples or a horizon. Averaged ages are excluded from the regression analysis of all samples and sites.

Table A1: Problem Dates

Sample	Problem
MRS-3 128	Older than ages from the same layer.
MRS-7-175	Same age as layer above. Probably a root from the above layer.
Pay-A-395-1	Inverted age in sequence. Probably contaminated during collection.
SB-A-440	Too Young, Contaminated during collection.

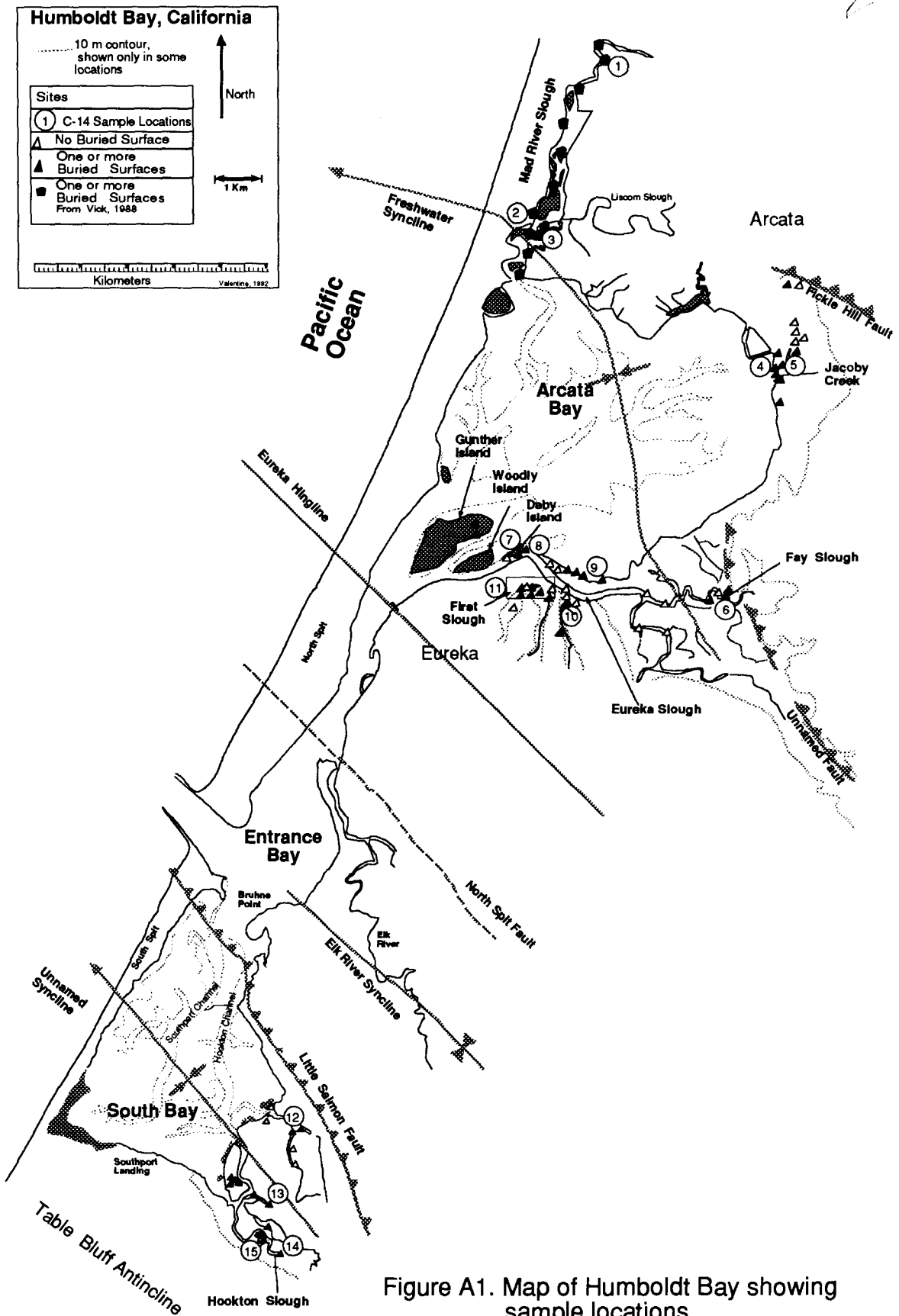


Figure A1. Map of Humboldt Bay showing sample locations

Radiocarbon Ages from All Localities Near Humboldt Bay.

QL-Quaternary Research Laboratory, University of Washington, B- Beta Analytic

Map Location	Sample Lab #	Age (RCYBP)	Calibrated age 1 s interval	Calibrated age 2 s interval	Material	Source
1	MRS-7-90 QL4261	124±19	cal AD 1678 (1692, 1723, 1811, 1923, 1955*) 1938 cal BP 272 (258, 227, 139, 27, 0*) 12	cal AD 1667 (1692, 1723, 1811, 1923, 1955*) 1955* cal BP 283 (258, 227, 139, 27, 0*) 0*	Tree Root	Vick, 1988
1	MRS-8-80 QL4263	114±19	cal AD 1682 (1701, 1720, 1813, 1834, 1840, 1847, 1876, 1918, 1955*) 1955* cal BP 268 (249, 230, 137, 116, 110, 103, 74, 32, 0*) 0*	cal AD 1671 (1701, 1720, 1813, 1834, 1840, 1847, 1876, 1918, 1955*) 1955* cal BP 279 (249, 230, 137, 116, 110, 103, 74, 32, 0*) 0*	Tree Root	Vick, 1988
1	MRS-7-175 QL4262	150±20	cal AD 1669 (1681, 1735, 1806, 1936, 1955*) 1946 cal BP 281 (269, 215, 144, 14, 0*) 4	cal AD 1658 (1681, 1735, 1806, 1936, 1955*) 1955* cal BP 292 (269, 215, 144, 14, 0*) 0*	Tree Root Probably from above layer	Vick, 1988
2	MRS-2-128 B25016	320±60	cal AD 1440 (1525, 1563, 1628) 1660 cal BP 510 (425, 387, 322) 290	cal AD 1410 (1525, 1563, 1628) 1955* cal BP 540 (425, 387, 322) 0*	Grindelia	Vick, 1988
2	MRS-4-130 QL4260	210±50	cal AD 1647 (1662) 1955* cal BP 303 (288) 0*	cal AD 1528 (1662) 1955* cal BP 422 (288) 0*	Grindelia	Clarke and Carver, 1990; This Study
2	MRS-2-205 B25017	1270±70	cal AD 640 (692, 699, 712, 748, 767) 890 cal BP 1310 (1258, 1251, 1238, 1202, 1183) 1060	cal AD 540 (692, 699, 712, 748, 767) 1000 cal BP 1410 (1258, 1251, 1238, 1202, 1183) 950	Peat	Vick, 1988

Table A1. Table of radiocarbon dates from the Humboldt Bay region

Map Location	Sample Lab #	Age (RCYBP)	Calibrated age 1 s interval	Calibrated age 2 s interval	Material	Source
3	MRS-3-128 B25016	910±90	cal AD 980 (1070, 1085, 1127, 1137, 1154) 1260 cal BP 970 (880, 865, 823, 813, 796) 690	cal AD 777 (1070, 1085, 1127, 1137, 1154) 1389 cal BP 1173 (880, 865, 823, 813, 796) 561	Peat	Vick, 1988
3	MRS-3-3689 (128 cm) QL4320	280±35	cal AD 1516 (1642) 1659 cal BP 434 (308) 291	cal AD 1450 (1642) 1955* cal BP 500 (308) 0*	Grindelia	Clarke and Carver, 1990; This Study
3	MRS-3-210 B25439	1360±70	cal AD 580 (657) 770 cal BP 1370 (1293) 1180	cal AD 430 (657) 943 cal BP 1520 (1293) 1007	Peat	Vick, 1988
3	MRS-3-BP280 B25440	1120±70	cal AD 660 (777, 793, 798) 977 cal BP 1290 (1173, 1157, 1152) 973	cal AD 600 (777, 793, 798) 1020 cal BP 1350 (1173, 1157, 1152) 930	Peat	Vick, 1988
3	MRS-3-G280 B25441	1330±70	cal AD 603 (668) 801 cal BP 1347 (1282) 1149	cal AD 432 (668) 980 cal BP 1518 (1282) 970	Grindelia	Vick, 1988
3	MRS-3-3689-I (305 cm) QL4321	1600±40	cal AD 411 (428) 532 cal BP 1539 (1522) 1418	cal AD 358 (428) 542 cal BP 1592 (1522) 1408	wood, probably root	Clarke and Carver, 1990; This Study
3	MRS-3-L (305 cm) QL4322	1670±20	cal AD 263 (364, 366, 388) 414 cal BP 1687 (1586, 1584, 1562) 1536	cal AD 257 (364, 366, 388) 429 cal BP 1693 (1586, 1584, 1562) 1521	wood, probably root	Clarke and Carver, 1990; This Study
4	JC A QL4323	45±80	cal AD 1670 (1955*) 1955* cal BP 280 (0*) 0*	cal AD 1523 (1955*) 1955* cal BP 427 (0*) 0*	Grindelia	This Study
5	JC-D-115 QL4416	220±30	cal AD 1644 (1659) 1955* cal BP 306 (291) 0*	cal AD 1524 (1659) 1955* cal BP 426 (291) 0*	Grindelia, Same as JC-A	This Study
6	FAY-E-75 QL4447	300±30	cal AD 1494 (1532, 1541, 1637) 1651 cal BP 456 (418, 409, 313) 299	cal AD 1450 (1532, 1541, 1637) 1952 cal BP 500 (418, 409, 313) 0*	Peat	This Study

Table A2 (cont). Table of radiocarbon dates from the Humboldt Bay region.

Map Location	Sample Lab #	Age (RCYBP)	Calibrated age 1 s interval	Calibrated age 2 s interval	Material	Source
5	JC-D-230-2 QL4449	1660±40	cal AD 260 (394) 526 cal BP 1690 (1556) 1424	cal AD 184 (394) 540 cal BP 1766 (1556) 1410	Grindelia	This Study
7	Wood-C-70-1 QL4417	580±40	cal AD 1296 (1330, 1347, 1393) 1419 cal BP 654 (620, 603, 557) 531	cal AD 1280 (1330, 1347, 1393) 1440 cal BP 670 (620, 603, 557) 510	Peat	This Study
8	Wood-A-70-1 QL4418	320±40	cal AD 1490 (1525, 1563, 1628) 1642 cal BP 460 (425, 387, 322) 308	cal AD 1450 (1525, 1563, 1628) 1653 cal BP 500 (425, 387, 322) 297	Peat	This Study
9	ES 115 QL4356	130±100	cal AD 1532 (1689, 1725, 1810, 1926, 1955*) 1955* cal BP 418 (261, 225, 140, 24, 0*) 0*	cal AD 1430 (1689, 1725, 1810, 1926, 1955*) 1955* cal BP 520 (261, 225, 140, 24, 0*) 0*	Peat	This Study
10	ES 265 QL4357	1870±20	cal AD 74 (129) 210 cal BP 1876 (1821) 1740	cal AD 33 (129) 230 cal BP 1917 (1821) 1720	Grindelia	This Study
11	Pay-A-430-1 QL4419	3130±40	cal BC 1492 (1430, 1420, 1415) 1321 cal BP 3441 (3379, 3369, 3364) 3270	cal BC 1597 (1430, 1420, 1415) 1196 cal BP 3546 (3379, 3369, 3364) 3145	Peat	This Study
11	ES-E-300-A QL4444	1270±40	cal AD 664 (692, 699, 712, 748, 767) 853 cal BP 1286 (1258, 1251, 1238, 1202, 1183) 1097	cal AD 640 (692, 699, 712, 748, 767) 939 cal BP 1310 (1258, 1251, 1238, 1202, 1183) 1011	Peat	This Study
11	ES-E-645 QL4445	3620±40	cal BC 2133 (2027, 2026, 2015, 1992, 1971) 1887 cal BP 4082 (3976, 3975, 3964, 3941, 3920) 3836	cal BC 2202 (2027, 2026, 2015, 1992, 1971) 1756 cal BP 4151 (3976, 3975, 3964, 3941, 3920) 3705	Peat	This Study

Table A2 (cont). Table of radiocarbon dates from the Humboldt Bay region.

Map Location	Sample Lab #	Age (RCYBP)	Calibrated age 1 s interval	Calibrated age 2 s interval	Material	Source
11	ES-E-695 QL4446	3800±30	cal BC 2391 (2274, 2252, 2231) 2142 cal BP 4340 (4223, 4201, 4180) 4091	cal BC 2470 (2274, 2252, 2231) 2040 cal BP 4419 (4223, 4201, 4180) 3989	Peat	This Study
11	Pay-C-118 QL4443	1460±40	cal AD 539 (600) 645 cal BP 1411 (1350) 1305	cal AD 430 (600) 670 cal BP 1520 (1350) 1280	Triglochin above soil	This Study
11	Pay-A-300-1 QL4422	2450±60	cal BC 790 (752, 720, 708, 695, 586, 585,538, 533, 521, 463, 447) 400 cal BP 2739 (2701, 2669, 2657, 2644, 2535, 2534, 2487, 2482, 2470, 2412, 2396) 2349	cal BC 820 (752, 720, 708, 695, 586, 585,538, 533, 521, 463, 447) 263 cal BP 2769 (2701, 2669, 2657, 2644, 2535, 2534, 2487, 2482, 2470, 2412, 2396) 2212	Peat	This Study
11	Pay-A-365-1 QL4421	2920±60	cal BC 1316 (1209, 1205, 1190, 1179, 1150, 1145,1129, 1122, 1110) 944 cal BP 3265 (3158, 3154, 3139, 3128, 3099, 3094,3078, 3071, 3059) 2893	cal BC 1430 (1209, 1205, 1190, 1179, 1150, 1145, 1129, 1122, 1110) 834 cal BP 3379 (3158, 3154, 3139, 3128, 3099, 3094, 3078, 3071, 3059) 2783	Peat. Base of peat Pay-A-300	This Study
11	Pay-A-395 QL4420	2600±60	cal BC 889 (797) 595 cal BP 2838 (2746) 2544	cal BC 973 (797) 410 cal BP 2922 (2746) 2359	Peat	This Study
12	SB-A-405-A QL4450	1850±40	cal AD 69 (132) 234 cal BP 1881 (1818) 1716	cal AD 3 (132) 339 cal BP 1947 (1818) 1611	Peat	This Study
12	SB-A-440 QL4451	2670±30	cal BC 894 (828) 800 cal BP 2843 (2777) 2749	cal BC 969 (828) 790 cal BP 2918 (2777) 2739	Peat	This Study

Table A2 (cont). Table of radiocarbon dates from the Humboldt Bay region.

Map Location	Sample Lab #	Age (RCYBP)	Calibrated age 1 s interval	Calibrated age 2 s interval	Material	Source
12	SB-A-480 QL4452	2480±40	cal BC 789 (759, 686, 657, 638, 616, 615, 592, 572, 558, 456, 455) 412 cal BP 2738 (2708, 2635, 2606, 2587, 2565, 2564, 2541, 2521, 2507, 2405, 2404) 2361	cal BC 800 (759, 686, 657, 638, 616, 615, 592, 572, 558, 456, 455) 400 cal BP 2749 (2708, 2635, 2606, 2587, 2565, 2564, 2541, 2521, 2507, 2405, 2404) 2349	Peat, Base of SB-A-440	This Study
12	SB-A-655 QL4457	2980±80	cal BC 1428 (1287, 1286, 1258, 1230, 1216, 1198, 1195, 1138, 1135) 1010 cal BP 3377 (3236, 3235, 3207, 3179, 3165, 3147, 3144, 3087, 3084) 2959	cal BC 1520 (1287, 1286, 1258, 1230, 1216, 1198, 1195, 1138, 1135) 833 cal BP 3469 (3236, 3235, 3207, 3179, 3165, 3147, 3144, 3087, 3084) 2782	Peat	This Study
13	SB-E-375 QL4455	2480±50	cal BC 792 (759, 686, 657, 638, 616, 615, 592, 572, 558, 456, 455) 410 cal BP 2741 (2708, 2635, 2606, 2587, 2565, 2564, 2541, 2521, 2507, 2405, 2404) 2359	cal BC 820 (759, 686, 657, 638, 616, 615, 592, 572, 558, 456, 455) 390 cal BP 2769 (2708, 2635, 2606, 2587, 2565, 2564, 2541, 2521, 2507, 2405, 2404) 2339	Peat	This Study
13	SB-E-440 QL4456	530±30	cal AD 1329 (1412) 1430 cal BP 621 (538) 520	cal AD 1300 (1412) 1443 cal BP 650 (538) 507	Peat	This Study
13	SB-E-625 QL4457	2720±80	cal BC 1048 (893, 878, 835) 790 cal BP 2997 (2842, 2827, 2784) 2739	cal BC 1291 (893, 878, 835) 445 cal BP 3240 (2842, 2827, 2784) 2394	Peat	This Study

Table A2 (cont). Table of radiocarbon dates from the Humboldt Bay region.

Map Location	Sample Lab #	Age (RCYBP)	Calibrated age 1 s interval	Calibrated age 2 s interval	Material	Source
14	HS1-689 (site A) QL4416	147±20	cal AD 1670 (1682, 1733, 1807, 1935, 1955*) 1945 cal BP 280 (268, 217, 143, 15, 0*) 5	cal AD 1659 (1682, 1733, 1807, 1935, 1955*) 1955* cal BP 291 (268, 217, 143, 15, 0*) 0*	Triglochin	This Study
15	HS-B-155-A QL4413	630±50	cal AD 1279 (1304, 1371, 1384) 1409 cal BP 671 (646, 579, 566) 541	cal AD 1227 (1304, 1371, 1384) 1440 cal BP 723 (646, 579, 566) 510	Peat	This Study
15	HS-B-155-B QL4412	690±40	cal AD 1262 (1281) 1386 cal BP 688 (669) 564	cal AD 1210 (1281) 1410 cal BP 740 (669) 540	Peat	This Study
15	HS-B-155 Average	666±31	cal AD 1278 (1284) 1388 cal BP 672 (666) 562	cal AD 1260 (1284) 1410 cal BP 690 (666) 540	Peat	This Study
15	HS-B-275-A QL4414	1180±50	cal AD 772 (886) 983 cal BP 1178 (1064) 967	cal AD 670 (886) 1020 cal BP 1280 (1064) 930	Peat	This Study
15	HS-B-275-B QL-4115	1360± 40	cal AD 639 (657) 759 cal BP 1311 (1293) 1191	cal AD 560 (657) 799 cal BP 1390 (1293) 1151	Peat	This Study
15	HS-B-275 Average	1289±31	cal AD 663 (686, 754, 757) 775 cal BP 1287 (1264, 1196, 1193) 1175	cal AD 640 (686, 754, 757) 869 cal BP 1310 (1264, 1196, 1193) 1081	Peat	This Study

Table A2 (cont). Table of radiocarbon dates from the Humboldt Bay region.

Site	Sample Lab #	Age (RCYBP)	Calibrated age 1 s interval	Calibrated age 2 s interval	Material	Source
Little Salmon Fault	LSF-430 QL4183	430±70	cal AD 1410 (1444) 1640 cal BP 540 (506) 310	cal AD 1280 (1444) 1660 cal BP 690 (506) 290		Carver, Burke, and Kelsey, 1985
Little Salmon Fault	LSF-S22 QL4182	870 ±105	cal AD 1000 (1191) 1280 cal BP 950 (759) 670	cal AD 777 (1191) 1420 cal BP 1173 (759) 530		Carver, Burke, and Kelsey, 1985
Little Salmon Fault	LSF-8 QL4119	1730 ±60	cal AD 233 (260, 281, 291, 298, 324) 386 cal BP 1717 (1690, 1669, 1659, 1652, 1626) 1564	cal AD 133 (260, 281, 291, 298, 324) 420 cal BP 1817 (1690, 1669, 1659, 1652, 1626) 1530		Carver, Burke, and Kelsey, 1985
Little Salmon Fault	LSF-6 QL4117	1970 ±30	cal BC 89 (cal AD 26, 42, 48) cal AD 70 cal BP 2038 (1924, 1908, 1902) 1880	cal BC 90 (cal AD 26, 42, 48) cal AD 130 cal BP 2039 (1924, 1908, 1902) 1820		Carver, Burke, and Kelsey, 1985
McKinnelyville Fault, Clam Beach	CB-1 QL4180	1160±30	cal AD 777 (784, 786, 874) 943 cal BP 1173 (1166, 1164, 1076) 1007	cal AD 690 (784, 786, 874) 980 cal BP 1260 (1166, 1164, 1076) 970	Driftwood in Uplifted Terrace	Carver, Vick, and Burke, 1989
McKinnelyville Fault, Clam Beach	CB-89-2 QL4316	120±35	cal AD 1667 (1685, 1730, 1808, 1931, 1955*) 1955* cal BP 283 (265, 220, 142, 19, 0*) 0*	cal AD 1650 (1685, 1730, 1808, 1931, 1955*) 1950 cal BP 300 (265, 220, 142, 19, 0*) 0	Tree in dunes	Carver, Vick, and Burke, 1989
McKinnelyville Fault	MKF Tree Ring	168 Dendrochronologic age converted to Radiocarbon Years	1742 AD Dendrochronologic age		Dendro-chronologic from tree buried by landslide	Jacoby and others, 1989

Table A2 (cont). Table of radiocarbon dates from the Humboldt Bay region.

Appendix 2: Statistical Data Analysis Summary

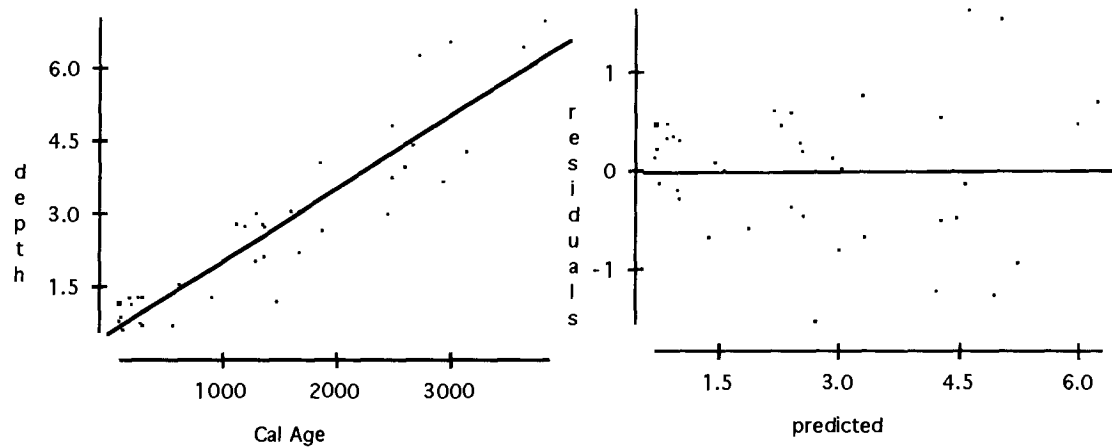
This section includes the data, and the summary printouts for the statistical analyses.

Dependent Variable Depth

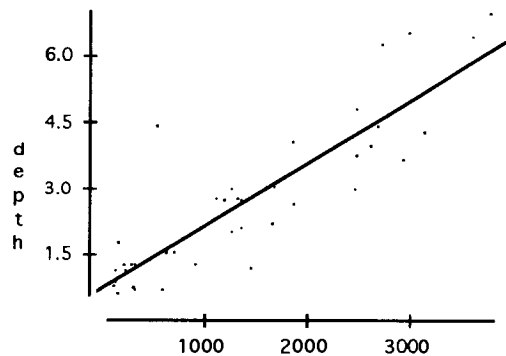
Dependent variable is: depth
 45 total cases of which 7 are missing
 $R^2 = 84.9\%$ $R^2(\text{adjusted}) = 84.5\%$
 $s = 0.7013$ with $38 - 2 = 36$ degrees of freedom

Source	Sum of Squares	df	Mean Square	F-ratio
Regression	99.3896	1	99.39	202
Residual	17.7076	36	0.491877	

Variable	Coefficient	s.e. of Coeff	t-ratio
Constant	0.499572	0.1934	2.58
CalAge	0.001513	0.0001	14.2



Regression analyses for depth as dependent variable



Dependent variable is: **depth**
 50 total cases of which 9 are missing
 $R^2 = 77.9\%$ $R^2(\text{adjusted}) = 77.3\%$
 $s = 0.8409$ with $41 - 2 = 39$ degrees of freedom

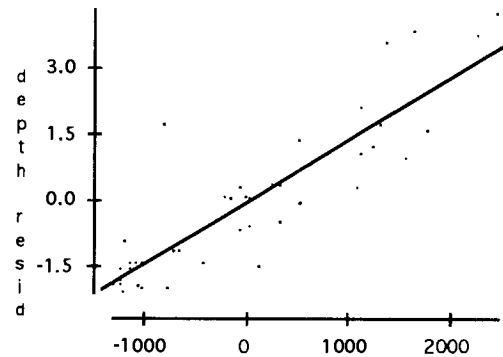
Source	Sum of Squares	df	Mean Square	F-ratio
Regression	96.9412	1	96.94	137
Residual	27.5765	39	0.707091	

Variable	Coefficient	s.e. of Coeff	t-ratio
Constant	0.727162	0.2132	3.41
Cal Age	0.001425	0.0001	11.7

Dependent variable is: **depth**
 50 total cases of which 12 are missing
 $R^2 = 85.2\%$ $R^2(\text{adjusted}) = 83.9\%$
 $s = 0.7157$ with $38 - 4 = 34$ degrees of freedom

Source	Sum of Squares	df	Mean Square	F-ratio
Regression	100.318	3	33.4	65.3
Residual	17.4164	34	0.512248	

Variable	Coefficient	s.e. of Coeff	t-ratio
Constant	0.693082	0.3347	2.07
Cal Age	0.001434	0.0002	7.16
Layer	0.073041	0.1837	0.398
Sed Thickness	-0.186798	0.1920	-0.973



Dependent variable is: **depth**
 50 total cases of which 9 are missing
 $R^2 = 83.7\%$ $R^2(\text{adjusted}) = 81.9\%$
 $s = 0.7500$ with $41 - 5 = 36$ degrees of freedom

Source	Sum of Squares	df	Mean Square	F-ratio
Regression	104.266	4	26.1	46.3
Residual	20.2518	36	0.562549	

Variable	Coefficient	s.e. of Coeff	t-ratio
Constant	0.714278	0.4106	1.74
Cal Age	0.001440	0.0001	12.3
is ES	-0.568610	0.4344	-1.31
is MRS	0.007453	0.4351	0.017
is SB	0.536668	0.4337	1.24

Regression analyses for depth as dependent variable

Dependent variable is: **depth**
 50 total cases of which 12 are missing
 R2 = 90.6% R2(adjusted) = 88.4%
 s = 0.6067 with 38 - 8 = 30 degrees of freedom

Source	Sum of Squares	df	Mean Square	F-ratio
Regression	106.692	7	15.2	41.4
Residual	11.0420	30	0.368067	

Variable	Coefficient	s.e. of Coeff	t-ratio
Constant	0.990068	0.7827	1.26
CalAge	0.001281	0.0002	6.13
Layer	0.224890	0.1787	1.26
SedThickness	-0.065078	0.1663	-0.391
is ES	-1.11464	0.6926	-1.61
is MRS	-0.499995	0.7198	-0.695
is SB	-0.006671	0.7073	-0.009
is JC	-0.663522	0.7966	-0.833

Dependent variable is: **depth**
 50 total cases of which 12 are missing
 R2 = 85.1% R2(adjusted) = 84.3%
 s = 0.7071 with 38 - 3 = 35 degrees of freedom

Source	Sum of Squares	df	Mean Square	F-ratio
Regression	100.237	2	50.1	100
Residual	17.4974	35	0.499926	

Variable	Coefficient	s.e. of Coeff	t-ratio
Constant	0.782289	0.2453	3.19
CalAge	0.001501	0.0001	14.1
SedThickness	-0.220893	0.1698	-1.30

Dependent variable is: **depth**
 50 total cases of which 9 are missing
 R2 = 77.9% R2(adjusted) = 76.7%
 s = 0.8516 with 41 - 3 = 38 degrees of freedom

Source	Sum of Squares	df	Mean Square	F-ratio
Regression	96.9566	2	48.48	66.8
Residual	27.5611	38	0.725292	

Variable	Coefficient	s.e. of Coeff	t-ratio
Constant	0.684462	0.3637	1.88
CalAge	0.001423	0.0001	11.5
error	0.000960	0.0066	0.146

Dependent variable is: **depth**
 50 total cases of which 9 are missing
 R2 = 78.7% R2(adjusted) = 77.6%
 s = 0.8349 with 41 - 3 = 38 degrees of freedom

Source	Sum of Squares	df	Mean Square	F-ratio
Regression	98.0303	2	49.02	70.3
Residual	26.4874	38	0.697037	

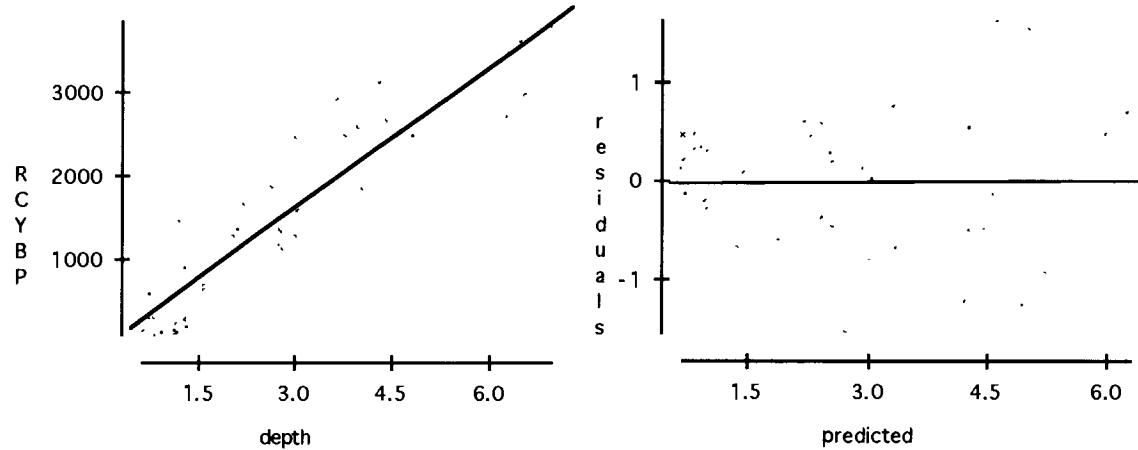
Variable	Coefficient	s.e. of Coeff	t-ratio
Constant	0.541917	0.2584	2.10
CalAge	0.001228	0.0002	6.18
Layer	0.231570	0.1853	1.25

Regression analyses for depth as dependent variable

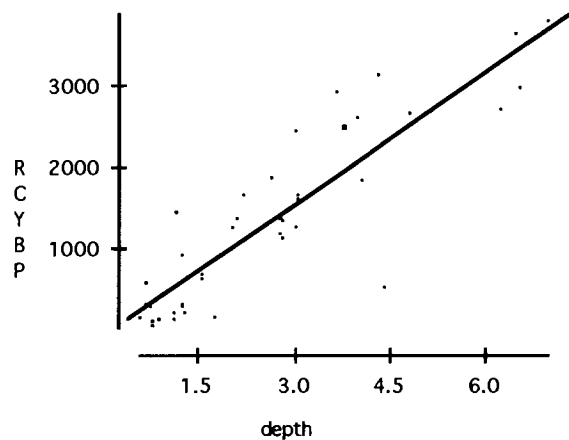
Dependent variable is: Cal Age
 45 total cases of which 7 are missing
 $R^2 = 84.9\%$ $R^2(\text{adjusted}) = 84.5\%$
 $s = 426.9$ with $38 - 2 = 36$ degrees of freedom

Source	Sum of Squares	df	Mean Square	F-ratio
Regression	36831607	1	4e+7	202
Residual	6562041	36	182279	

Variable	Coefficient	s.e. of Coeff	t-ratio
Constant	-58.0228	127.8	-0.454
depth	560.838	39.45	14.2



Regression analyses for calibrated age as dependent variable



Dependent variable is: **Cal Age**
 48 total cases of which 7 are missing
 $R^2 = 77.9\%$ $R^2(\text{adjusted}) = 77.3\%$
 $s = 520.5$ with $41 - 2 = 39$ degrees of freedom

Source	Sum of Squares	df	Mean Square	F-ratio
Regression	37145986	1	4e+7	137
Residual	10566798	39	270944	

Variable	Coefficient	s.e. of Coeff	t-ratio
Constant	-91.7034	149.6	-0.613
depth	546.186	46.65	11.7

Dependent variable is: **Cal Age**
 50 total cases of which 12 are missing
 $R^2 = 88.9\%$ $R^2(\text{adjusted}) = 87.9\%$
 $s = 386.9$ with $38 - 4 = 34$ degrees of freedom

Source	Sum of Squares	df	Mean Square	F-ratio
Regression	40615738	3	1e+7	90.4
Residual	5089749	34	149699	

Variable	Coefficient	s.e. of Coeff	t-ratio
Constant	-540.028	168.2	-3.21
depth	419.141	58.55	7.16
Sed Thickness	257.624	95.53	2.70
Layer	277.504	87.41	3.17

Regression analyses for calibrated age as dependent variable

Dependent variable is: **Cal Age**
 50 total cases of which 9 are missing
 R2 = 83.5% R2(adjusted) = 81.1%
 s = 474.9 with 41 - 6 = 35 degrees of freedom

Source	Sum of Squares	df	Mean Square	F-ratio
Regression	39818218	5	8e+6	35.3
Residual	7894566	35	225559	

Variable	Coefficient	s.e. of Coeff	t-ratio
Constant	-89.5293	598.2	-0.150
depth	559.645	52.33	10.7
is ES	342.229	543.7	0.629
is MRS	-158.141	559.7	-0.283
is SB	-291.435	524.2	-0.556
is JC	-42.9789	621.0	-0.069

Dependent variable is: **Cal Age**
 50 total cases of which 12 are missing
 R2 = 85.6% R2(adjusted) = 84.7%
 s = 434.2 with 38 - 3 = 35 degrees of freedom

Source	Sum of Squares	df	Mean Square	F-ratio
Regression	39106977	2	2e+7	104
Residual	6598511	35	188529	

Variable	Coefficient	s.e. of Coeff	t-ratio
Constant	-278.559	164.5	-1.69
depth	566.188	40.19	14.1
Sed Thickness	171.093	102.7	1.67

Dependent variable is: **Cal Age**
 50 total cases of which 9 are missing
 R2 = 81.6% R2(adjusted) = 80.6%
 s = 481.2 with 41 - 3 = 38 degrees of freedom

Source	Sum of Squares	df	Mean Square	F-ratio
Regression	38914996	2	2e+7	84.0
Residual	8797788	38	231521	

Variable	Coefficient	s.e. of Coeff	t-ratio
Constant	-262.080	151.4	-1.73
depth	407.885	66.05	6.18
Layer	274.773	99.40	2.76

Dependent variable is: **Cal Age**
 50 total cases of which 12 are missing
 R2 = 88.9% R2(adjusted) = 87.9%
 s = 386.9 with 38 - 4 = 34 degrees of freedom

Source	Sum of Squares	df	Mean Square	F-ratio
Regression	40615738	3	1e+7	90.4
Residual	5089749	34	149699	

Variable	Coefficient	s.e. of Coeff	t-ratio
Constant	-540.028	168.2	-3.21
depth	419.141	58.55	7.16
Layer	277.504	87.41	3.17
Sed Thickness	257.624	95.53	2.70

Regression analyses for calibrated age as dependent variable

Dependent variable is: Cal Age
casesselectedaccordingTo ES
48 total cases of which 35 are missing
R2 = 87.1% R2(adjusted) = 85.9%
s = 489.5 with 13 - 2 = 11 degrees of freedom

Source	Sum of Squares	df	Mean Square	F-ratio
Regression	17797099	1	2e+7	74.3
Residual	2635394	11	239581	

Variable	Coefficient	s.e. of Coeff	t-ratio
Constant	167.662	240.7	0.697
depth	579.505	67.24	8.62

Dependent variable is: Cal Age
casesselectedaccordingTo JC
48 total cases of which 45 are missing
R2 = 98.0% R2(adjusted) = 95.9%
s = 179.4 with 3 - 2 = 1 degrees of freedom

Source	Sum of Squares	df	Mean Square	F-ratio
Regression	1538616	1	2e+6	47.8
Residual	32201.0	1	32201.0	

Variable	Coefficient	s.e. of Coeff	t-ratio
Constant	-1023.65	262.2	-3.90
depth	1203.85	174.2	6.91

Dependent variable is: Cal Age
casesselectedaccordingTo SB
48 total cases of which 36 are missing
R2 = 69.9% R2(adjusted) = 66.9%
s = 579.1 with 12 - 2 = 10 degrees of freedom

Source	Sum of Squares	df	Mean Square	F-ratio
Regression	7798588	1	8e+6	23.3
Residual	3353247	10	335325	

Variable	Coefficient	s.e. of Coeff	t-ratio
Constant	-5.85478	380.6	-0.015
depth	455.928	94.54	4.82

Dependent variable is: Cal Age
casesselectedaccordingTo MRS-A
48 total cases of which 38 are missing
R2 = 75.6% R2(adjusted) = 72.5%
s = 289.7 with 10 - 2 = 8 degrees of freedom

Source	Sum of Squares	df	Mean Square	F-ratio
Regression	2075815	1	2e+6	24.7
Residual	671395	8	83924.4	

Variable	Coefficient	s.e. of Coeff	t-ratio
Constant	-289.045	276.2	-1.05
depth	617.458	124.2	4.97

Dependent variable is: Cal Age
casesselectedaccordingTo MRS-B
48 total cases of which 45 are missing
R2 = 96.9% R2(adjusted) = 93.8%
s = 4.614 with 3 - 2 = 1 degrees of freedom

Source	Sum of Squares	df	Mean Square	F-ratio
Regression	669.376	1	669	31.4
Residual	21.2905	1	21.2905	

Variable	Coefficient	s.e. of Coeff	t-ratio
Constant	89.0306	7.666	11.6
depth	35.0459	6.250	5.61

Regression analyses by site for calibrated age as dependent variable

Dependent variable is: depth
 casesselectedaccordingTo
 ES
 45 total cases of which 32 are missing
 R2 = 87.1% R2(adjusted) = 85.9%
 s = 0.7883 with 13 - 2 = 11 degrees of freedom

Source	Sum of Squares	df	Mean Square	F-ratio
Regression	46.1596	1	46.16	74.3
Residual	6.83531	11	0.621392	

Variable	Coefficient	s.e. of Coeff	t-ratio
Constant	0.129284	0.3942	0.328
CalAge	0.001503	0.0002	8.62

Dependent variable is: depth
 casesselectedaccordingTo
 MRS-A
 45 total cases of which 33 are missing
 R2 = 83.1% R2(adjusted) = 81.4%
 s = 0.3693 with 12 - 2 = 10 degrees of freedom

Source	Sum of Squares	df	Mean Square	F-ratio
Regression	6.68555	1	6.6856	49.0
Residual	1.36414	10	0.136414	

Variable	Coefficient	s.e. of Coeff	t-ratio
Constant	0.788739	0.1901	4.15
CalAge	0.001283	0.0002	7.00

Dependent variable is: depth
 casesselectedaccordingTo
 SB
 45 total cases of which 34 are missing
 R2 = 90.3% R2(adjusted) = 89.2%
 s = 0.6308 with 11 - 2 = 9 degrees of freedom

Source	Sum of Squares	df	Mean Square	F-ratio
Regression	33.2667	1	33.27	83.6
Residual	3.58062	9	0.397847	

Variable	Coefficient	s.e. of Coeff	t-ratio
Constant	0.331791	0.3996	0.830
CalAge	0.001842	0.0002	9.14

Dependent variable is: Cal Age
 casesselectedaccordingTo
 ES
 45 total cases of which 32 are missing
 R2 = 87.1% R2(adjusted) = 85.9%
 s = 489.5 with 13 - 2 = 11 degrees of freedom

Source	Sum of Squares	df	Mean Square	F-ratio
Regression	17797099	1	2e+7	74.3
Residual	2635394	11	239581	

Variable	Coefficient	s.e. of Coeff	t-ratio
Constant	167.662	240.7	0.697
depth	579.505	67.24	8.62

Dependent variable is: Cal Age
 casesselectedaccordingTo
 MRS-A
 45 total cases of which 33 are missing
 R2 = 83.1% R2(adjusted) = 81.4%
 s = 262.4 with 12 - 2 = 10 degrees of freedom

Source	Sum of Squares	df	Mean Square	F-ratio
Regression	3373219	1	3e+6	49.0
Residual	688281	10	68828.1	

Variable	Coefficient	s.e. of Coeff	t-ratio
Constant	-365.013	190.5	-1.92
depth	647.340	92.47	7.00

Dependent variable is: Cal Age
 casesselectedaccordingTo
 SB
 45 total cases of which 34 are missing
 R2 = 90.3% R2(adjusted) = 89.2%
 s = 325.3 with 11 - 2 = 9 degrees of freedom

Source	Sum of Squares	df	Mean Square	F-ratio
Regression	8847912	1	9e+6	83.6
Residual	952336	9	105815	

Variable	Coefficient	s.e. of Coeff	t-ratio
Constant	6.91340	213.8	0.032
depth	490.024	53.59	9.14

Regression analyses by site for depth as dependent variable